RMZ

MATERIALS and GEOENVIRONMENT

MATERIALI in GEOOKOLJE

RMZ – M&G, **Vol. 62**, No. 2
pp. 71–146 (2015)

Ljubljana, August 2015

RMZ – Materials and Geoenvironment
RMZ – Materiali in geookolje
ISSN 1408-7073

Old title/Star naslov
Mining and Metallurgy Quarterly/Rudarsko-metalurški zbornik
ISSN 0035-9645, 1952–1997

Published by/Izdajatelj
Faculty of Natural Sciences and Engineering, University of Ljubljana/
Naravoslovnotehniška fakulteta, Univerza v Ljubljani

Associated Publisher/Soizdajatelj
Institute for Mining, Geotechnology and Environment, Ljubljana/
Inštitut za rudarstvo, geotehnologijo in okolje
Velenje Coal Mine/Premogovnik Velenje

Editorial Office/Uredništvo
Secretary/Tajnica Ines Langerholc
Technical Editor/Tehnična urednica Helena Buh
Editor of website/Urednik spletne strani Timotej Verbovšek

Editorial Address/Naslov uredništva
RMZ – Materials and Geoenvironment
Aškerčeva cesta 12, p. p. 312
1001 Ljubljana, Slovenija
Tel.: +386 (0)1 470 45 00
Fax.: +386 (0)1 470 45 60
E-mail: rmz-mg@ntf.uni-lj.si

Linguistic Advisor/Lektor
Jože Gasperič

Design and DTP/Oblikovanje, prelom in priprava za tisk
IDEJA.si

Print/Tisk
Birografika BORI, d. o. o.
Printed in 200 copies./Naklada 200 izvodov.

Published/Izhajanje
4 issues per year/4 številke letno

Partly funded by Ministry of Education, Science and Sport of Republic of Slovenia./Pri financiranju revije sodeluje Ministrstvo za izobraževanje, znanost in šport Republike Slovenije.

Articles published in Journal "RMZ M&G" are indexed in international secondary periodicals and databases:/Članki, objavljeni v periodični publikaciji „RMZ M&G", so indeksirani v mednarodnih sekundarnih virih:
CA SEARCH® – Chemical Abstracts®, METADEX®, GeoRef.

The authors themselves are liable for the contents of the papers./
Za mnenja in podatke v posameznih sestavkih so odgovorni avtorji.

Annual subscription for individuals in Slovenia: 16.69 EUR, for institutions: 22.38 EUR. Annual subscription for the rest of the world: 20 EUR, for institutions: 40 EUR/Letna naročnina za posameznike v Sloveniji: 16,69 EUR, za inštitucije: 33,38 EUR. Letna naročnina za tujino: 20 EUR, inštitucije: 40 EUR.

Current account/Tekoči račun
Nova Ljubljanska banka, d. d., Ljubljana: UJP 01100-6030708186

VAT identification number/Davčna številka
24405388

Online Journal/Elektronska revija
www.rmz-mg.com

Table of Contents

Kazalo

Original scientific papers
Izvirni znanstveni članki

Influence of minor scandium and zirconium additions on the microstructure of Al and Al-5Mg alloy **73**
Vpliv manjših dodatkov skandija in cirkonija na mikrostrukturo Al in zlitine Al-5Mg
Anton Smolej, Boštjan Markoli, Aleš Nagode, Damjan Klobčar

Petrogenesis and functional applications of talcose rocks in Wonu-Apomu and Ilesa areas, southwestern Nigeria **81**
Petrogeneza in uporabna vrednost lojevčevih kamnin na območjih Wonu-Apomu in Ilesa v jugozahodni Nigeriji
Anthony T. Bolarinwa, Morenike A. Adeleye

Idrisi as a tool for slope stability analysis **95**
Idrisi kot orodje za analizo stabilnosti pobočij
Eva Koren, Goran Vižintin

Pore pressure detection and risk assessment of OBL oil field, offshore Niger delta, Nigeria **105**
Ugotavljanje pornega pritiska in ocenitev tveganja v naftnem polju OBL v predobalnem delu Nigrove delte v Nigeriji
Matthew E. Nton, Mosopefoluwa D. Ayeni

Professional papers
Strokovni članki

Evaluation of groundwater occurrences in the precambrian basement complex of Ilorin metropolis, southwestern Nigeria **117**
Ocena virov podtalnice iz predkambrijske podlage območja deželne prestolnice Ilorina v jugozahodni Nigeriji
Anthony T. Bolarinwa, Sulyman Ibrahim

About basalt production and ways to improve basalt product quality **133**
Izkoriščanje bazalta in možnosti izboljšanja kakovosti bazaltnih proizvodov
Soyib Abdurakhmanovich Abdurakhmanov, Rashidova Ra'no, Mamatkarimova Barno Khabibullayevna, Sattarov Laziz Khalmuradovich

Historical Review

More than 90 years have passed since the University Ljubljana in Slovenia was founded in 1919. Technical fields were united in the School of Engineering that included the Geologic and Mining Division, while the Metallurgy Division was established only in 1939. Today, the Departments of Geology, Mining and Geotechnology, Materials and Metallurgy are all part of the Faculty of Natural Sciences and Engineering, University of Ljubljana.

Before World War II, the members of the Mining Section together with the Association of Yugoslav Mining and Metallurgy Engineers began to publish the summaries of their research and studies in their technical periodical Rudarski zbornik (Mining Proceedings). Three volumes of Rudarski zbornik (1937, 1938 and 1939) were published. The War interrupted the publication and it was not until 1952 that the first issue of the new journal Rudarsko-metalurški zbornik – RMZ (Mining and Metallurgy Quarterly) was published by the Division of Mining and Metallurgy, University of Ljubljana. Today, the journal is regularly published quarterly. RMZ – M&G is co-issued and co-financed by the Faculty of Natural Sciences and Engineering Ljubljana, the Institute for Mining, Geotechnology and Environment Ljubljana, and the Velenje Coal Mine. In addition, it is partly funded by the Ministry of Education, Science and Sport of Slovenia.

During the meeting of the Advisory and the Editorial Board on May 22, 1998, Rudarsko-metalurški zbornik was renamed into "RMZ – Materials and Geoenvironment (RMZ – Materiali in Geookolje)" or shortly RMZ – M&G. RMZ – M&G is managed by an advisory and international editorial board and is exchanged with other world-known periodicals. All the papers submitted to the RMZ – M&G undergoes the course of the peer-review process.

RMZ – M&G is the only scientific and professional periodical in Slovenia which has been published in the same form for 60 years. It incorporates the scientific and professional topics on geology, mining, geotechnology, materials and metallurgy. In the year 2013, the Editorial Board decided to modernize the journal's format.

A wide range of topics on geosciences are welcome to be published in the RMZ – Materials and Geoenvironment. Research results in geology, hydrogeology, mining, geotechnology, materials, metallurgy, natural and anthropogenic pollution of environment, biogeochemistry are the proposed fields of work which the journal will handle.

Editor-in-Chief

Zgodovinski pregled

Že več kot 90 let je minilo od ustanovitve Univerze v Ljubljani leta 1919. Tehnične stroke so se združile v Tehniški visoki šoli, ki sta jo sestavljala oddelka za geologijo in rudarstvo, medtem ko je bil oddelek za metalurgijo ustanovljen leta 1939. Danes oddelki za geologijo, rudarstvo in geotehnologijo ter materiale in metalurgijo delujejo v sklopu Naravoslovnotehniške fakultete Univerze v Ljubljani.

Pred 2. svetovno vojno so člani rudarske sekcije skupaj z Združenjem jugoslovanskih inženirjev rudarstva in metalurgije začeli izdajanje povzetkov njihovega raziskovalnega dela v Rudarskem zborniku. Izšli so trije letniki zbornika (1937, 1938 in 1939). Vojna je prekinila izdajanje zbornika vse do leta 1952, ko je izšel prvi letnik nove revije Rudarsko-metalurški zbornik – RMZ v izdaji odsekov za rudarstvo in metalurgijo Univerze v Ljubljani. Danes revija izhaja štirikrat letno. RMZ – M&G izdajajo in financirajo Naravoslovnotehniška fakulteta v Ljubljani, Inštitut za rudarstvo, geotehnologijo in okolje ter Premogovnik Velenje. Prav tako izdajo revije financira Ministrstvo za izobraževanje, znanost in šport.

Na seji izdajateljskega sveta in uredniškega odbora je bilo 22. maja 1998 sklenjeno, da se Rudarsko-metalurški zbornik preimenuje v RMZ – Materiali in geookolje (RMZ – Materials and Geoenvironment) ali skrajšano RMZ – M&G. Revijo RMZ – M&G upravljata izdajateljski svet in mednarodni uredniški odbor. Revija je vključena v mednarodno izmenjavo svetovno znanih publikacij. Vsi članki so podvrženi recenzijskemu postopku.

RMZ – M&G je edina strokovno-znanstvena revija v Sloveniji, ki izhaja v nespremenjeni obliki že 60 let. Združuje področja geologije, rudarstva, geotehnologije, materialov in metalurgije. Uredniški odbor je leta 2013 sklenil, da posodobi obliko revije.

Za objavo v reviji RMZ – Materiali in geookolje so dobrodošli tudi prispevki s širokega področja geoznanosti, kot so: geologija, hidrologija, rudarstvo, geotehnologija, materiali, metalurgija, onesnaževanje okolja in biokemija.

Glavni urednik

Original scientific paper

Received: April 12, 2015
Accepted: July 2, 2015

Influence of minor scandium and zirconium additions on the microstructure of Al and Al-5Mg alloy

Vpliv manjših dodatkov skandija in cirkonija na mikrostrukturo Al in zlitine Al-5Mg

Anton Smolej[1,*], Boštjan Markoli[1], Aleš Nagode[1], Damjan Klobčar[2]

[1]University of Ljubljana, Faculty of Natural Science and Engineering, Department of Materials and Metallurgy, Aškerčeva cesta 12, 1000 Ljubljana, Slovenia

[2]University of Ljubljana, Faculty of Mechanical Engineering, Aškerčeva cesta 6, 1000 Ljubljana, Slovenia

*Corresponding author. E-mail: anton_smolej@t-2.net

Abstract

The article describes the effect of varying minor scandium and zirconium quantities on the grain refinement of the as-cast alloys Al-Sc, Al-Sc-Zr, and Al-5Mg-Sc-Zr, as well as the distribution of either element in the phases formed during the solidification, homogenisation annealing, and ageing of these alloys. Scandium and zirconium in the Al-Sc-Zr and Al-5Mg-Sc-Zr alloys are present in three metallographic formations: in the solid solution of the aluminium matrix, as primary particles $Al_3(Sc, Zr)$, and as dispersive precipitates. The primary particles $Al_3(Sc, Zr)$, sized between 5 μm and 10 μm, act as crystallisation nuclei during the solidification of the alloys. As the EDS SEM analysis indicates, the primary particles are not homogeneous: the scandium and zirconium contents decrease from centre to edge. Another manifestation of scandium and zirconium in the Al-Sc-Zr and Al-5Mg-Sc-Zr alloys takes the form of secondary precipitates. These precipitates exist in the as-cast, homogenised, and aged alloys. Their sizes range from 5 nm to 60 nm in the as-cast alloys, and from 100 nm to 350 nm in the aged ones. The precipitate number density decreases with the annealing of the alloys.

Key words: aluminium alloys, scandium, zirconium, microstructure

Izvleček

Članek se osredinja na učinek različnih manjših količin skandija in cirkonija na udrobnenje zrn v osnovnih zlitinah Al-Sc, Al-Sc-Zr in Al-5Mg-Sc-Zr in porazdelitev obeh elementov v fazah, ki nastanejo med strjevanjem, homogenizacijskim žarjenjem in staranjem teh zlitin. Skandij in cirkonij v zlitinah Al-Sc-Zr in Al-5Mg-Sc-Zr sta v treh metalografskih oblikah: v trdni raztopini aluminijeve matrice, kot primarni delci $Al_3(Sc, Zr)$ in kot dispergirani izločki. Primarni delci $Al_3(Sc, Zr)$ z velikostjo od 5 μm do 10 μm so kristalizacijske kali med strjevanjem zlitin. Kot je pokazala analiza EDS SEM, primarni delci niso homogeni; vsebnosti skandija in cirkonija se manjšata od sredine k robovom delcev. Drugi način pojavljanja skandija in cirkonija je v obliki sekundarnih izločkov. Izločki se nahajajo v ulitih, homogeniziranih in staranih zlitinah. Velikost izločkov je 5–60 nm v ulitih in 100–350 nm v staranih stanjih zlitin. Gostota izločkov se manjša z žarjenjem zlitin.

Ključne besede: aluminijeve zlitine, skandij, cirkonij, mikrostruktura

Introduction

Scandium (Sc) has a considerable influence on the microstructure and properties of aluminium (Al) and its alloys. There are three main reasons for adding Sc to aluminium alloys (Al-alloys): (i) grain refinement during casting, (ii) precipitation hardening, and (iii) grain structure control [1]. It has been demonstrated that a small Sc addition in Al and Al-alloys produces Al_3Sc precipitates, usually termed dispersoids [1–4]. Al_3Sc dispersoids efficiently impede the movement of grain boundaries, which leads to recrystallisation resistance and to the thermal stability of the crystal grains at higher temperatures [1, 2, 4–6]. Beside the binary Al-Sc alloys, the Sc-containing alloys studied most extensively were the Al-Mg-Sc type alloys [3, 4, 7–9].
The beneficial effects of Sc are enhanced when Sc is added to Al-alloys in combination with zirconium (Zr) [1, 4, 7, 8]. The presence of both elements in the alloy improves its recrystallisation resistance, the stability of its crystal grains during high-temperature annealing, and its mechanical properties [1, 4, 8]. These improvements are due to the formation of very fine and uniformly distributed $Al_3(Sc, Zr)$ precipitates, which pin the grain boundaries [1, 7, 8, 10, 11]. The $Al_3(Sc, Zr)$ precipitates have a core/shell structure with an uneven distribution of Sc and Zr: a Sc-rich core is surrounded by a Zr-rich shell [1, 9, 10–12]. The presence of Zr prompts the grain refinement action at lower concentrations of Sc, starting from the mass fraction of Sc w = 0.18 % [4]. It is for this reason that Sc is introduced into commercial Al-alloys together with Zr [4]. A further advantage of the joint addition of Sc and Zr concerns the superplastic forming of Al-alloys, where a fine-grained and stable microstructure is the basic prerequisite for good superplasticity. Recent researches have shown that the combined additions of Sc and Zr to Al-Mg alloys improve their superplasticity more efficiently than the separate addition of either element does [13–16].
The aim of our experiment was to establish the influence of varying minor Sc and Zr quantities on the cast grain structure and to investigate the distribution of Sc and Zr in the phases formed during the solidification, homogenisation annealing, and ageing of Al and Al-5Mg based alloys.

Materials and methods

The experiments were conducted with Al and Al-5Mg alloys containing either a minor addition of Sc or a combination of Sc and Zr. The designation and chemical composition of each alloy is shown in Table 1. The alloys were prepared by laboratory induction melting, using Al99.99 (w/%), Mg99.8, and the master alloys AlSc2.1, AlZr7.5, and AlTi5B1. Three kilograms of Al were melted in a graphite crucible, while the Mg and the master alloys were added to the molten Al at a temperature of (705±5) °C. The melts were repeatedly cast into a wedge-shaped copper mould, where they cooled to ambient temperature at a rate of ≈ 20 K s^{-1}. The shapes of the cut castings are shown in Figure 1. The microstructures of the alloys were examined in their as-cast, homogenised, and aged states. The as-cast alloys without Mg were homogenised for 24 h at 600 °C and those containing Mg for 4 h at 440 °C, followed by 4 h at 460 °C. After the homogenisation annealing, the alloys were aged for 4 h and 24 h at 400 °C.

Table 1: *The chemical composition of the alloys investigated (in mass fractions, w/%)*

Mark	Alloy	Si	Fe	Mn	Mg	Ti	Zr	Sc	Al
A	Al-0.3Sc	0.006	0.002	0.001	0.00	0.002	0.000	0.24	Bal.
B	Al-0.3Sc-0.15Zr	0.008	0.017	0.001	0.00	0.002	0.147	0.28	Bal.
C	Al-5Mg-0.2Sc	0.022	0.048	0.004	5.14	0.016	0.004	0.21	Bal.
D	Al-5Mg-0.2Sc-0.15Zr	0.007	0.013	0.002	5.16	0.011	0.156	0.18	Bal.
E	Al-5Mg-0.35Sc-0.15Zr	0.007	0.016	0.002	4.72	0.012	0.168	0.35	Bal.

The examination methods were light microscopy, scanning electron microscopy SEM (JEOL JSM – 5610 with an EDS detector), and transmission electron microscopy JEOL 3100 (ISIS EDXS with an acceleration voltage of 200 kV). The metallographic investigations were focused on the grain microstructure, the primary phases with Sc and Zr, and the secondary precipitates. The grain microstructure was established by using Baker's reagent. The average crystal grain size was examined with the linear intercept technique. The Sc and Zr contents in the primary phases were checked by SEM EDS, and in the secondary precipitates by the TEM EDXS analysis. The sizes of the secondary precipitates were measured manually, and their density was assessed by a visual count within a set area of bright field TEM (BF TEM) images.

Results and Discussion

Figure 1 shows the macro- and micro-images of crystal grains in as-cast alloys with varying contents of Sc and Zr. The average sizes of the grains are given in Table 2.

An addition of less than w(Sc) = 0.3 % does not drastically reduce the grain size of these alloys. The size of the crystal grains is unevenly distributed over the cross-sections of the castings. On the other hand, the simultaneous addition of Sc and Zr refines the grain size of the alloys Al-0.3Sc-0.15Zr, Al-5Mg-0.2Sc-0.15Zr, and Al-5Mg-0.35Sc-0.15Zr to 54, 41.5 µm and 33 µm respectively. All these alloys have an equiaxed, nondendritic grain structure, usually with a uniform grain size within each casting. A minor addition of Zr – about w = 0.15 % in the Al-Sc and Al-5Mg-Sc alloys – has an intensive grain refining effect on the as-cast structure in spite of the low Sc content.

Figure 2 shows the backscattered electron images (BSE images) of a nearly 10 µm square particle within a crystal grain of the as-cast alloy Al-0.3Sc-0.15Zr (a, b), and its composition analysis at spot 1 (c). The particle is composed of Al, Sc, and Zr with its uneven distribution. Figure 4 presents the contents of Sc and Zr at various points of the particle as established by the EDS analysis. The concentration of both elements decreases from centre to edge, but the Zr content is higher at all analysed points. The stoichiometric ratio of Al to (Sc + Zr), expressed in average mass fraction (w), is about 3 : 1. The ratio Zr : Sc in the particle varies from 1.5 to approximately 1.9, with a mean value of 1.65.

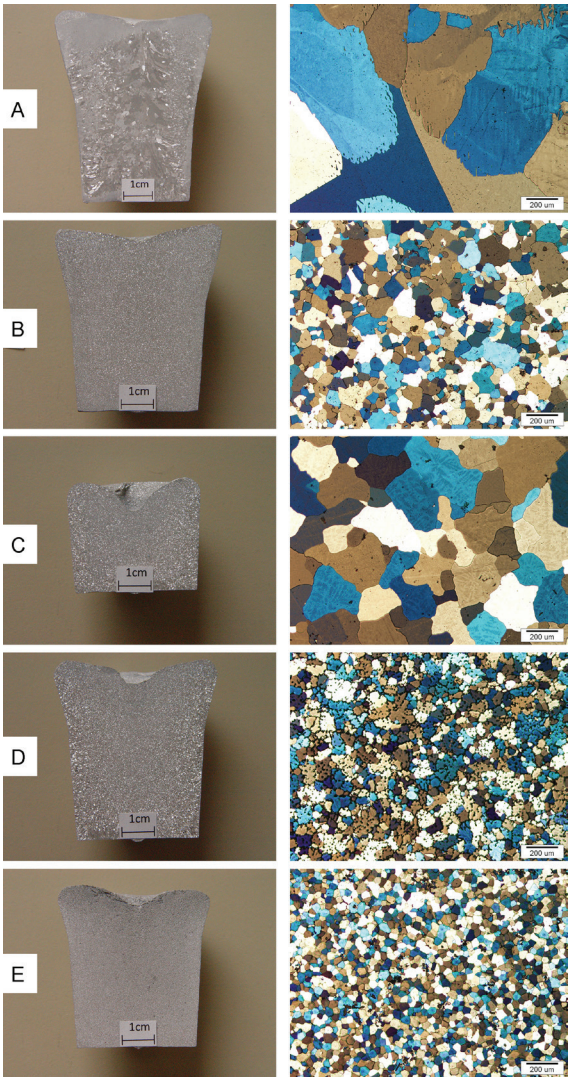

Figure 1: *Macro- and microscopic images of crystal grains in the as-cast A, B, C, D, and E alloys with varying Sc and Zr contents.*

Table 2: *The average grain sizes of the alloys investigated*

Alloy	A	B	C	D	E
Grain size (µm)	295	54	190	41.5	33

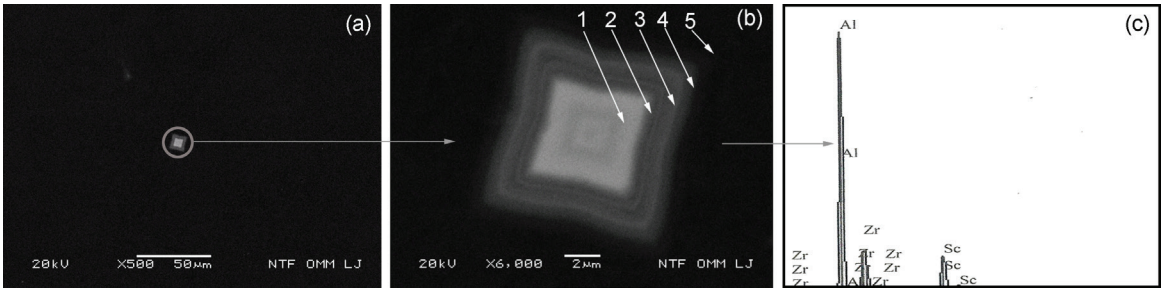

Figure 2: *BSE images of the particle in the as-cast alloy Al-0.3Sc-0.15Zr, with markings of the analysed spots 1–5 (a, b) and a composition analysis of the particle at spot 1 (c).*

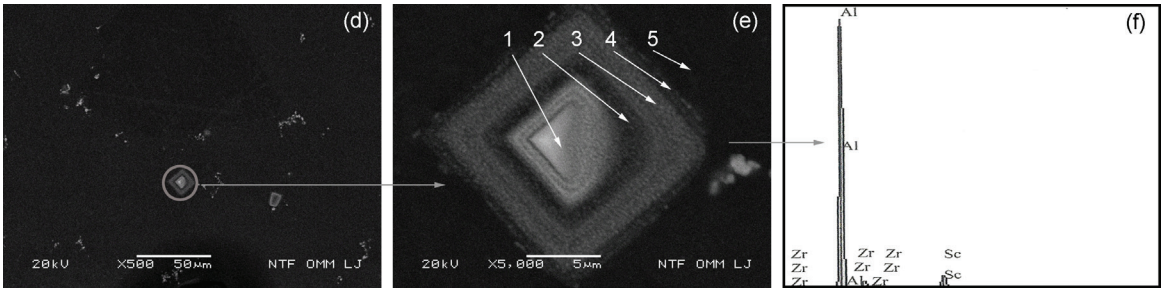

Figure 3: *BSE images of the particle in the homogenised alloy Al-0.3Sc-0.15Zr, with markings of the analysed spots 1–5 (d, e) and a composition analysis of the particle at spot 1 (f).*

Figure 3 shows the BSE images (d, e) of the particle with the composition (c), taken after the homogenisation annealing of the Al-0.3Sc-0.15Zr alloy at 600 °C for 24 h. The concentrations of Sc and Zr are reduced in comparison with the as-cast state of the alloy (Figure 4). The contents of both elements are nearly equal at all analysed spots, decreasing from centre to edge. The decomposition of the particle changes the stoichiometric ratio Al : (Sc + Zr). The contour of the particle does not disappear despite the long-continued homogenisation annealing at a relatively high temperature.

When, on the other hand, Sc and Zr have been added simultaneously, the Al-Sc-Zr and Al-5Mg-Sc-Zr alloys in as-cast, homogenised, and aged states contain not only large particles but also nm-size precipitates. These precipitates, shown in BF TEM and BSE SEM micrographs (Figure 5), consist of Al, Sc and Zr. The average quantitative composition of the precipitate, determined by the EDS TEM analysis, is displayed in Table 3. The average chemical composition of the precipitates in the aged alloy is similar in all states analysed and does not depend on the ageing time. The distribution of Sc and Zr in the precipitates is not evident from the BF TEM

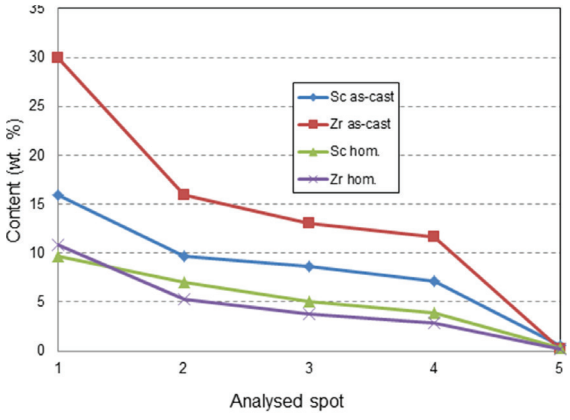

Figure 4: *The Sc and Zr contents in the particles presented in Figures 2 and 3, belonging to the as-cast and homogenised alloy Al-0.3Sc-0.15Zr.*

micrographs. The Al-matrix close to the precipitates does not contain Sc or Zr, and the average stoichiometric ratio Al : (Sc + Zr) in the precipitates is nearly 3 : 1. In addition, the EDS SEM analysis reveals that the bright points in the BSE image (Figure 5h) contain more Sc and Zr than the surrounding Al-matrix does. These results are in agreement with the data found in literature: it has been reported by a number of researchers that dispersive precipitates

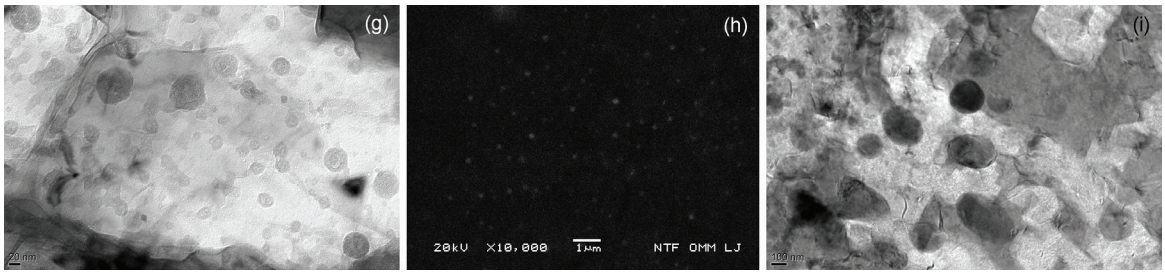

Figure 5: *The BF TEM image of Al_3(Sc, Zr) precipitates in the as-cast alloy Al-0.3Sc-0.15Zr (g); BSE (h) and BF TEM (i) images of Al_3(Sc, Zr) precipitates in the Al-0.3Sc-0.15 Zr alloy, aged for* 4 h *at* 400 °C.

in alloys of the Al-Sc-Zr type consist of Al, Sc, and Zr with random distribution. The chemical formula of the composed precipitates can be noted as Al_3(Sc, Zr) or, more correctly, as $Al_3(Sc_{1-x}, Zr_x)$ [1, 8–10].

The size and distribution of the precipitates in the as-cast and aged alloy Al-0.3Sc-0.15Zr were measured with the help of BF TEM micrographs. The results are shown in Table 4. The smallest precipitates with the highest density are found in the as-cast alloy. The aged alloy, by contrast, contains larger precipitates with a much lower density. While the duration of the ageing time has no considerable influence on their density, longer ageing does slightly increase their size. The size and density of the precipitates in the TEM images are comparable with those in the BSE images.

The microstructures of the quaternary Al-Mg-Sc-Zr (D and E) alloys were investigated in the same way as the Mg-less B alloy. The microstructures of these alloys were found to be very similar to the Al-0.3Sc-0.15Zr (B) alloy, with relatively large primary particles composed of Al, Sc, Zr, and dispersive Al_3(Sc, Zr) precipitates. Figure 6 shows the BSE images of primary particles in the as-cast (j, k) and homogenised (l) Al-5Mg-0.35Sc-0.15Zr (E) alloy. In shape, size, and composition, they equal the particles in the Al-0.3Sc-0.15Zr (B) alloy. The secondary Al_3(Sc, Zr) precipitates are present in D and E alloys – as-cast, homogenised, and aged – and their characteristics are similar to the precipitates in the Mg-less Al-0.3Sc-0.15Zr (B) alloy.

The average grain sizes of the investigated as-cast alloys Al-0.3Sc (A) and Al-5Mg-0.2Sc (C) are 295 μm and 190 μm respectively. Alloys with less than *w*(Sc) = 0.3 % show no grain refinement effect. According to the Al-Sc phase diagram, the eutectic point occurs at approximately

Table 3: *The average composition of the precipitates and of the Al-matrix in the aged Al-0.3Sc-0.15Zr alloy (in mass, w/%, and amount fractions, x/%)*

Place	State	*w*/%			*x*/%		
		Al	Sc	Zr	Al	Sc	Zr
Precipitate	4 h, 400 °C	76.72	14.26	9.02	87.23	9.73	3.03
Precipitate	24 h, 400 °C	73.76	15.01	11.23	85.68	10.46	3.86
Al-matrix	24 h, 400 °C	99.97	0.04	0.01	99.98	0.02	0.00

Table 4: *The average size and density of the precipitates in the as-cast and aged alloy Al-0.3Sc-0.15Zr*

State	Precipitate size	Precipitate density
As-cast	5–60 nm	≈ 320 precipitates/1 μm²
Aged 4 h, 400 °C	100–300 nm	≈ 5–6 precipitates/1 μm²
Aged 24 h, 400 °C	150–350 nm	≈ 6 precipitates/1 μm²

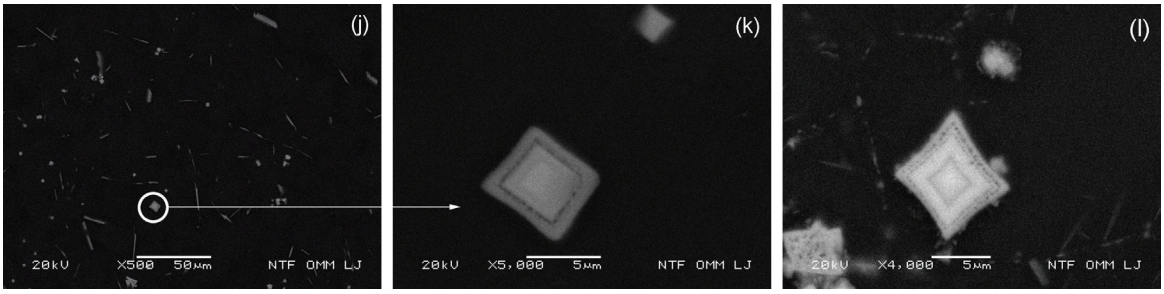

Figure 6: *BSE images of the primary particles in the as-cast (j, k) and homogenised (l) alloy Al-5Mg-0.35Sc-0.15Zr (the E alloy).*

w(Sc) = 0.55 % and at a temperature of 659 °C [1, 4, 6, 17]. The maximum solubility of Sc in Al in the solid state is *w*(Sc) = 0.35 % [4]. When an aluminium melt with a hyper-eutectic content of Sc is slowly cooled, the first phase in the melt will be Al_3Sc [1, 2, 5, 6, 8]. The Al_3Sc phases, fcc with a lattice parameter of 0.4105 µm, act as potential nucleation sites for aluminium crystal grains [5, 6]. The investigated Al-0.3Sc and Al-5Mg-0.25Sc alloys reveal no Al_3Sc particles: this agrees with the data that it is only Sc additions greater than the eutectic composition (*w*(Sc) ≈ 0.55 %) that act as grain refiners of aluminium castings, due to the formation of primary particles during solidification [1, 2, 4–6, 8, 17].

The minimum Sc level required for grain refinement can be reduced by the simultaneous addition of a minor Zr content to the alloys. In the alloys investigated – Al-Sc-Zr and Al-5Mg-Sc-Zr – Sc and Zr are present in three forms: in a solid solution of Al, as primary phases in the form of square or rectangular particles sized between 5 µm and 10 µm, and as fine dispersive precipitates.

The composition of the primary particles is not homogeneous: the Sc and Zr contents decrease from centre to edge. The average ratio Al : (Sc + Zr) is nearly 3 : 1, which is in accordance with the chemical formula $Al_3(Sc, Zr)$ [1, 4]. The $Al_3(Sc, Zr)$ particles are the first to form in the melt, thus serving as effective crystallisation nuclei during the solidification of the residual melt, which results in a fine-grained microstructure. This is demonstrated by the BSE images of the as-cast alloy Al-5Mg-0.35Sc-0.15Zr, which reveal the presence of $Al_3(Sc, Zr)$ particles within some crystal grains (Figure 7). The reason why such particles are not evident in all grains is the variety of their orientation and of their cross-sections, resulting from the preparation of the metallographic samples.

As indicated by the EDS SEM analysis, the Zr content in the centre of the primary particles is higher than the Sc content. On the basis of the Al-Zr and Al-Sc phase diagrams [8, 18–20] as references for the Al-Sc-Zr type alloys, it is believed that Al_3Zr precipitates first form from the melt

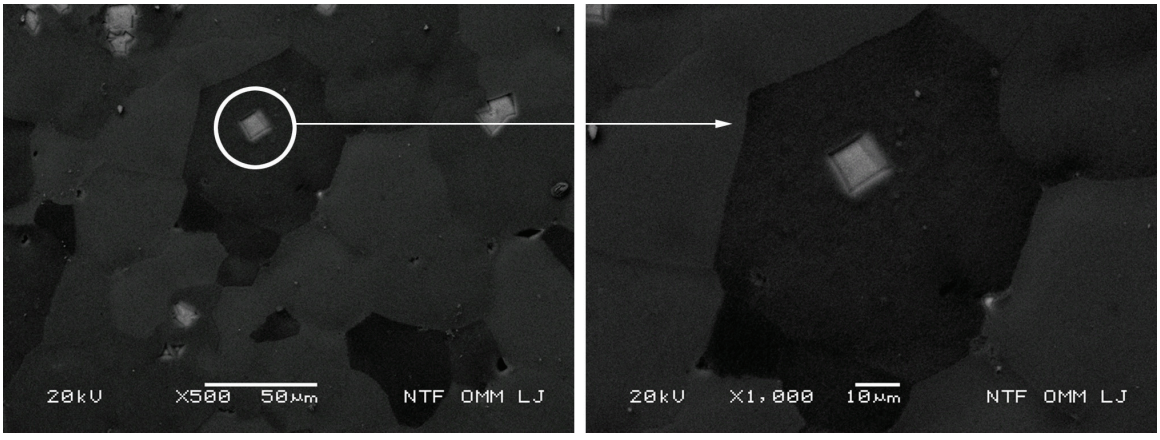

Figure 7: *BSE images of the as-cast alloy Al-5Mg-0.35Sc-0.15Zr containing $Al_3(Sc, Zr)$ particles.*

by peritectic reaction at about w(Zr) = 0.1 %. This is followed by the precipitation of Al_3Sc on the Al_3Zr [4, 8, 21]. The uneven distribution of Sc and Zr in the particles is due to the further diffusion of both elements during the cooling of the alloy after solidification. In the newly formed composed particles Al_3(Sc, Zr), Zr replaces a part of the Sc content required for achieving the critical size of Al_3Sc as a crystallisation nucleus [4, 8]. Thus the addition of about w(Sc) = 0.2 % and w(Zr) = 0.1 % significantly refines the grain sizes of Al and Al-Mg type alloys at a much lower content of the costly Sc [8], and therefore Sc is introduced into commercial aluminium alloys together with Zr [4]. However, the mechanism by which the primary particles containing Sc and Zr are formed in Al and Al-alloys is still not entirely explained.

Another manifestation of Sc and Zr in the Al-Sc-Zr and Al-5Mg-Sc-Zr alloys takes the form of fine secondary precipitates. According to the literature on the subject, these dispersive precipitates have a core/shell structure where the composition of the core differs from that of the surrounding shell. These precipitates, designated as Al_3(Sc, Zr), are coherent with the matrix [1, 8, 10–12]. They consist of a core containing Al and Sc (Al_3Sc) and surrounded by a Zr-rich shell (Al_3Zr) [10]. The distribution of Sc, Zr and Al in the secondary precipitates differs from that in the primary Al_3(Sc, Zr) particles, which is due to the different diffusion rates of Sc and Zr during solidification and in the solid solution [11, 21]. The precipitation in the secondary precipitates starts with the nucleation of nearly pure Al_3Sc, whereas Zr precipitates on Al_3Sc nuclei at a later stage [1]. The Al_3(Sc, Zr) precipitates were found in all three forms of the Al-Sc-Zr and Al-5Mg-Sc-Zr alloys: homogenised, aged, and as-cast. This can be explained with the short incubation period (≈ 102 s) of the Al_3Sc nuclei [8, 21, 22]. Evidently, dispersive Al_3(Sc, Zr) precipitates form in the Al-solid solution even while the castings are still cooling after solidification. These dispersive precipitates are effective in pinning the dislocations and in impeding the movement of high-angle boundaries, thus causing resistance to recrystallisation and improving the thermal stability of the fine-grained microstructure at higher temperatures [7, 8, 10].

Conclusions

The article describes the effect of varying minor scandium and zirconium quantities on the microstructure of the alloys Al-Sc, Al-Sc-Zr, Al-5Mg-Sc, and Al-5Mg-Sc-Zr. The findings of the research include the following:

- Scandium and zirconium are present in the investigated alloys Al-Sc-Zr and Al-5Mg-Sc-Zr in three metallographic formations: (i) in solid solution, (ii) as primary particles Al_3(Sc, Zr), and (iii) as dispersive precipitates.
- There is no grain-refining effect in as-cast alloys Al-Sc and Al-5Mg-Sc with less than w(Sc) = 0.3 %. The addition of about w(Zr) = 0.15 % significantly refines the grain sizes of the Al-0.3Sc and Al-5Mg-0.2Sc alloys.
- The primary particles Al_3(Sc, Zr), sized between 5 μm and 10 μm, act as crystallisation nuclei during the solidification of the alloys. The composition of the primary particles is not homogeneous: the Sc and Zr contents decrease from the centre to the border areas, with the Zr content exceeding that of the Sc. The presence of Mg in the alloys does not alter the formation of primary particles.
- Another manifestation of Sc and Zr in the Al-Sc-Zr and Al-5Mg-Sc-Zr alloys takes the form of secondary precipitates. They are found in as-cast, homogenised and aged alloys. The size of the precipitates ranges from 5 nm to 60 nm in as-cast alloys, and from 100 nm to 350 nm in aged alloys.

Acknowledgements

The authors wish to thank dr. Goran Dražić, Nika Breskvar, Tomaž Martinčič, Božo Skela and Samo Smolej for their help with the experimental work. This study was partly supported by the Slovenian Research Agency (ARRS), Government of the Republic of Slovenia, through Project L2-4183.

References

[1] Röyset, J. (2007): Scandium in aluminium alloys overview: physical metallurgy, properties and applications. *Metallurgical Science and technology*, 25, pp. 11–21.

[2] Röyset, J., Ryum, N. (2005): Kinetics and Mechanisms of precipitation in an Al-0.2 *w*t. % Sc. *Material Science and Engineering A*, 396, pp. 409–422.

[3] Sawtell, R. R., Jensen, C. L. (1990): Mechanical properties and microstructures of Al-Mg-Sc alloys. *Metallurgical Transactions A*, 21 A, pp. 421–430.

[4] Zakharov, V. V. (2003): Effect of scandium on the structure and properties of aluminium alloys. *Metal Science and Heat Treatment*, 45, pp. 246–253.

[5] Blake, N., Hopkins, M. A. (1985): Constitution and age hardening of Al-Sc alloys. *Journal of Material Science*, 20, pp. 2861–2867.

[6] Hyde, K. B., Norman, A. F., Prangnell, P. B. (2001): The effect of cooling rate on the morphology of primary Al_3Sc intermetallic particles in Al-Sc alloys. *Acta Materialia*, 49, pp. 1327–1337.

[7] Peng, Y., Yin, Z., Nie, B., Zhong, L. (2007): Effect of minor Sc and Zr on superplasticity of Al-Mg-Mn alloys. *Transactions of Nonferrous Metals Society of China*, 17, pp. 744–750.

[8] Yin. Z., Pan, Q., Zhang, Y., Jiang, F. (2000): Effect of minor Sc and Zr on the microstructure and mechanical properties of Al-Mg alloys. *Material Science and Engineering A*, 280, pp. 151–155.

[9] Johansen, A., Bauger, Ø., Emburg, J. D., Ryum, N. (2006): Alloy development in the Al-Mg alloy system. Part I, Part II, *Aluminium*, 82, pp. 868–879, pp. 980–985.

[10] Tolley, A., Radmilović, V., Dahmen, U. (2005): Segregation in $Al_3(Sc, Zr)$ precipitates in Al-Sc-Zr alloys. *Scripta Materialia*, 52, pp. 621–625.

[11] Radmilović, V., Tolley, A., Lee, Z., Dahmen, U. (2006): Core-shell structures and precipitation kinetics of $Al_3(Sc, Zr)$ Li_2 intermetallic phase in Al-rich alloy. *MJoM-Metalurgija-Journal of Metallurgy*, 12, pp. 309–314.

[12] Lefebrvre, W., Danoix, F., Hallem, H., Forbord, A., Bostel, A., Mathinsen, K. (2009): Precipitation kinetic of $Al_3(Sc, Zr)$ dispersoits in aluminium. *Journal of Alloys and Compounds*, 470, pp. 107–110.

[13] Lee, S., Utsunomiya, A., Akamatsu, H., Neishi, K., Furukawa, M., Horita, Z., Langdon, T. G. (2002): Influence of scandium and zirconium on stability and superplastic ductilities in ultrafine-grained Al-Mg alloys. *Acta Materialia*, 50, pp. 553–564.

[14] Avtokratova, E., Sitdikov, O., Markushev, M., Mulyukov, R. (2012): Extraordinary high-strain rate superplasticity of severely deformed Al-Mg-Sc-Zr alloy. *Material Science and Engineering A*, 538, pp. 386–390.

[15] Smolej, A., Klobčar, D., Skaza, B., Nagode, A., Slaček, E., Dragojević, V., Smolej, S. (2014): The superplasticity of friction stir processed Al-5Mg alloy with additions of scandium and zirconium. *International Journal of Materials Research (formerly Zeitschrift für Metallkunde)*, 105, pp. 1218–1226.

[16] Smolej, A., Klobčar, D., Skaza, B., Nagode, A., Slaček, E., Dragojević, V., Smolej, S. (2014): Superplasticity of rolled and friction stir processed Al-4.5Mg-0.35Sc-0.15Zr alloy. *Material Science and Engineering A*, 590, pp. 239–245.

[17] Norman, A. F., Prangnell, R. B., McEvan, R. S. (1998): Solidification behaviour of dilute aluminium-scandium alloys. *Acta Materialia*, 46, pp. 5712–5732.

[18] Janghorban, A., Antoni-Zdziobek, A., Lomello-Tafin, M., Antion, C., Mazingue, Th., Pish, A., (2013): Phase equilibria in aluminium rich side of Al-Zr system. *Journal of Thermal Analysis and Calometry*, 14, pp. 1015–1020.

[19] Okomoto. H. (1993): Al-Zr (Aluminium-Zirconium). *Journal of Phase Equilibria*, 14, pp. 259–260.

[20] Murray, J.L. (1998): The Al-Sc (Aluminium-Scandium) system. *Journal of Phase Equilibria*, 19, pp. 380–384.

[21] Song, M., He, Y. H. (2011): Investigation of primary $Al_3(Sc, Zr)$ particles in Al-Sc-Zr alloys. *Material Science and Technology*, 27, pp.431–433.

[22] Blake, N., Hopkins, M. A. (1985): Constitution and age hardening of Al-Sc alloys. *Journal of Materials Science*, 20, pp. 2861–2867.

Original scientific paper

Received: February 20, 2015
Accepted: May 2, 2015

Petrogenesis and functional applications of talcose rocks in Wonu-Apomu and Ilesa areas, southwestern Nigeria

Petrogeneza in uporabna vrednost lojevčevih kamnin na območjih Wonu-Apomu in Ilesa v jugozahodni Nigeriji

Anthony T. Bolarinwa[1,*], Morenike A. Adeleye[1]
[1]University of Ibadan, Department of Geology, Ibadan, Nigeria
*Corresponding author. E-mail: atbola@yahoo.com

Abstract

Petrogenesis and functional applications of the talcose rocks in Wonu-Apomu and Ilesa areas, southwestern Nigeria, were undertaken. Petrographic studies of the talcose rocks showed talc with variable amounts of anthophyllite, and chlorite. X-ray diffraction studies of the talcose rocks further revealed the presence of Al-bearing pyrophyllite (19.0 %) and Cr-bearing clinochlore (14.5 %), which have similar physical characteristics and diffraction peaks with talc and chlorite, respectively thus increasing the intensity of talc and chlorite on the x-ray diffraction charts.

Chemical data of the talcose rocks showed that the Wonu-Apomu samples are more siliceous (ca. 55.62 % SiO_2) than the Ilesa samples with ca. 52.35 %. Trace element data showed higher Cr (> 3 600 µg/g), Ni (> 1 620 µg/g) and Zn (> 160 µg/g) contents in the Ilesa talcose rocks. Petrogenetic indices, including low K, Rb, Rb/Sr (< 0.29), K/Rb (< 49.55), Ni/Co (< 1.05), Ga/Y (< 1.05) and CaO/Al_2O_3 (< 0.72) suggested tholeiitic basalt precursor for the talc bodies. The composition, physical and industrial characteristics of the talc bodies supported functional applications as fillers, filters and absorbents in ceramics, paints, rubber, paper, plastic, roofing materials and textiles.

Key words: talcose rock, mineralogy, geochemistry, petrogenesis, functional applications

Izvleček

Predmet preiskave sta bili določitev petrogenetskih značilnosti in ocena uporabne vrednosti lojevec vsebujočih kamnin s področij Wonu-Apomu in Ilesa v jugozahodni Nigeriji. S petrografskimi preiskavami kamnin so ugotovili razen lojevca še različne deleže antofilita in klorita. Rentgenske difrakcijske preiskave kažejo na prisotnost Al-vsebujočega pirofilita (19,0 %) in Cr-vsebujočega klinoklora (14,5 %), ki imata podobne fizikalne lastnosti in difrakcijske vrhove kot lojevec, iz česar izhaja zvečana intenziteta lojevca in klorita na rentgenskih difrakcijskih diagramih.

Iz podatkov kemijske analize je mogoče sklepati, da vsebujejo vzorci iz Wonu-Apomuja več kremena (povpr. 55,62 % SiO_2) od vzorcev iz Ilese, ki ga imajo povprečno 52,35 %. Analize slednih prvin kažejo v prvih več Cr (> 3 600 µg/g), Ni (> 1 620 µg/g) in Zn (> 160 µg/g) kakor v vzorcih lojevčevih kamnin iz Ilese. Petrogenetski kazalci, med drugim nizek K, Rb, Rb/Sr (< 0,29), K/Rb (< 49,55), Ni/Co (< 1,05), Ga/Y (< 1,05) in CaO/Al_2O_3 (< 0,72), nakazujejo, da je bila izvirna kamnina lojevca tholeiitni bazalt. Glede na sestavo lojevčevih teles in njihove fizikalne ter industrijske značilnosti ugotavljajo, da je mogoče kamnino uporabljati kot polnilo, material za filtre in kot absorbent, v keramiki, izdelavi barvil, gume, papirja, plastičnih snovi, kritine in v tekstilni industriji.

Ključne besede: lojevčeva kamnina, mineralogija, geokemija, petrogeneza, uporabna vrednost

Introduction

Talc bearing rocks and their protolithic amphibolites are common features of the Precambrian schist belts, which are largely confined to the western part of Nigeria (Figure 1). In the Ilesa schist belt of southwestern Nigeria, they occur in localities such as Wonu-Apomu, Ile-Ife, Isaobi near Ilesa, Ikirun and Esa-Oke. Within the Ilesa schist belt, talc bodies are closely associated with mafic and ultramafic bodies, mostly amphibolites and metasedimentary units such as quartzites and pelitic schists [1–7]. Various mineralogical and textural varieties of the talcose rocks have been identified by workers such as [8–10]. The four major mineralogical types according to Elueze and Akin-Ojo [10] are the talcose, tremolitic, chloritic and anthophyllitic varieties. Furthermore, studies on the regional occurrences and comparative industrial applications of various talc occurrences in southwestern Nigeria have also been carried out [10, 11].

Industrial appraisals of various talc bodies from southwestern Nigeria have also been inferred from their textural, mineralogical, chemical and geotechnical attributes [11–18]. Most of these investigations on the amphibolites and various talcose occurrences within the Precambrian basement complex tend to emphasize their field relations, petrological descriptions, mineralogical attributes and aspects of industrial applications, with little effort on the petrogenetic affinity. Mineralogical and chemical data were generated in the present investigation to unravel the petrogenetic affinity and petrochemical trends of the talcose rocks in Wonu-Apomu and Ilesa areas. The functional applications were also evaluated based on physical and thermal characteristics of the talcose bodies.

Location and Geology of study areas

The Wonu-Apomu area is delineated by latitude 7° 15′ and 7° 19′ N and longitude 4° 3′ and 4° 6′ E (Figure 2); while the Ilesa area is defined by latitude 7° 31′ and 7° 38′ N and longitude 4° 38′ and 4° 45′ E (Figure 3). The Precambrian basement complex rocks in Nigeria have been classified into three major groups. These are the ancient migmatite-gneiss-quartzite com-

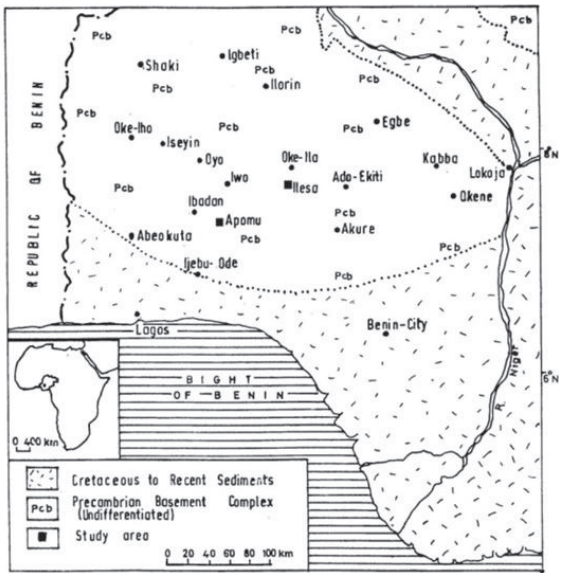

Figure 1: *Map of southwestern Nigeria showing the location of Apomu and Ilesha areas.*

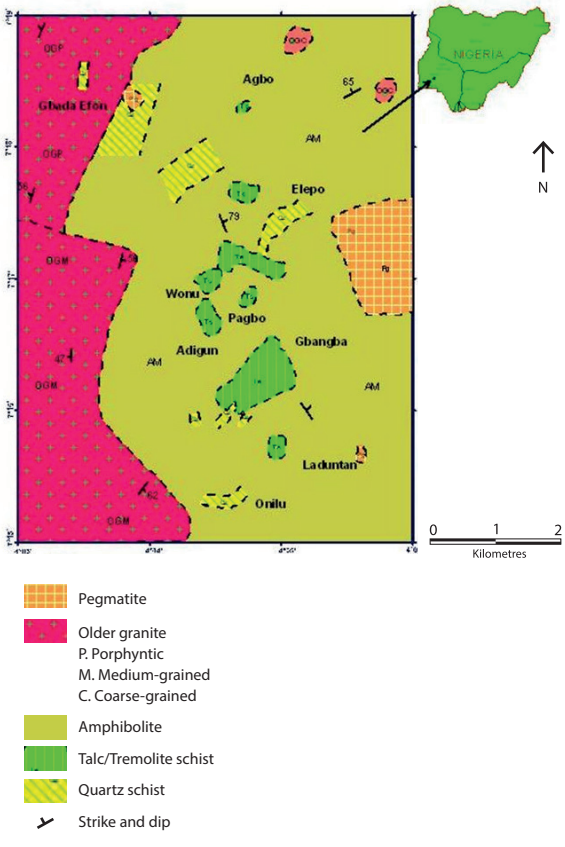

Figure 2: *Geological map of Wonu-Apomu area (modified after Akin-Ojo [9]).*

plex, the schist belts and the Pan African intrusive series (Older Granites). Others minor rocks include unmetamorphosed felsic and mafic intrusives [19].

The Wonu-Apomu and Ilesa areas lie within the schist belts of the basement complex of southwestern Nigeria characterized by migmatites and granitic gneiss, low to medium grade metasedimentary and metavolcanics rocks, notably quartzite and quartz schist, amphibolites and talc schist. Others are porphyritic granite and pegmatites (Figures 2 and 3). Talc schist occurs as narrow, northerly trending, and lens-shaped discontinuous bodies within the amphibolite at Pagbo, Wonu, Baale and Laduntan in the Wonu-Apomu area (Figure 4). In Ilesa area, the talc schists occur within biotite schist and amphibolitic rocks. They contain essentially talc with subordinate amounts of anthophyllite, pyrophyllite and chlorite. Chalcopyrite, pyrite, pyrrhotite and chromite, though intensively

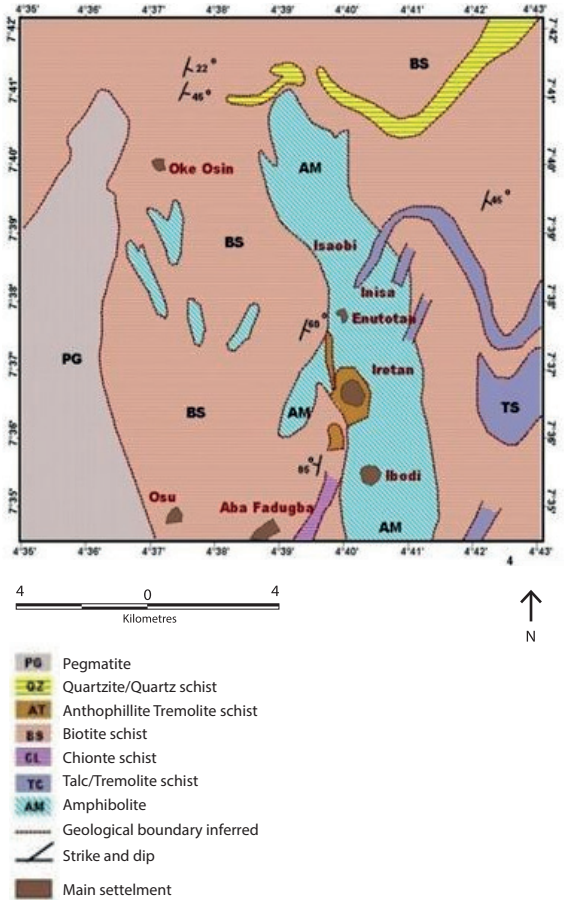

Figure 3: *Geological map of Ilesa area (modified after Kehinde-Phillips [7]).*

Figure 4: *Talc schist outcrop in Wonu-Apomu area.*

altered, are also present in some samples [20]. The mineralogy, feel, colour, texture, area extent, and the degree of weathering of the talcose rocks vary with location. The chlorite content of the talc-schist is reflected in its greenish colour, while the weathering effect is indicated by brownish colouration due to iron oxidation.

Materials and Methods

Forty samples of talc schist were collected from outcrops in Wonu-Apomu and Ilesa areas. The samples were selected for thin sectioning, X-ray diffraction studies and chemical analysis. Thin section of talc-schist and amphibolite samples were prepared and examined under petrographic microscope. X-ray diffraction (XRD) study of the talc schist samples were carried out in order to identify mineral phases that could not be identified with optical characteristics. Ten representative samples were selected from Wonu-Apomu and Ilesa areas. The samples were pulverized, pressed into an aluminium sample holder and analysed using Panalytical X' pert Pro diffractometer. Diffraction peaks obtained in 2θ degrees and nm-values were compared with established standards and interpreted with reference to the Joint Committee on Powder Diffraction Standards, Tables of X-ray powder diffraction patterns [21].

Twenty (20) talc samples were pulverized into fine powder and analysed at the Activation Laboratory in Ontario, Canada using the Inductively Coupled Plasma-Mass Spectrometry (ICP-MS). The ICP-MS technique was used for the determination of major and trace element

composition of the talc bodies, which include SiO_2, Al_2O_3, Fe_2O_3(T), MnO, MgO, CaO, Na_2O, K_2O, TiO_2, P_2O_5, Ba, Sr, Y, Zr, Zn, Rb, Co, Cu, V, Ga, Cr and Ni.

Pellets of raw pulverized talc were produced using a mechanical press. The pellets were dried in an oven set at 105 °C and the natural moisture content (NMC) determined. The pellets were fired in a kiln to temperatures of (950, 1 000, 1 050 and 1 100) °C for 2 h. The loss on ignition (LOI) was determined from the weight difference of the dried and fired samples. The linear shrinkage (LSK) was measured and calculated from the percentage decrease in diameter of the pellets after firing. The water absorption capacity was estimated from percentage weight increase after immersion in water for 24 h. Bleaching test for colour improvement was carried out on 10 samples by soaking 2 g in 5 ml of 1.0 M and 2.0 M HCl for 24 h.

Results and Discussion

Petrography

Thin sections of the talcose rock show flaky aggregates and plates of talc (Figures 5–7). Laths of anthophyllite and chlorite are also observed (Figure 5). Aggregates of prismatic needles and radiating fibres of anthophyllites and pyrophyllite were observed in the thin section of the talc schist. The talc-pyrophyllite-chlorite Wonu-Apomu samples are generally greyish to cream white in colour while the anthophyllite-pyrophyllite-chlorite rich types are brownish to grey. Anthophyllite is pleochroic from colourless to yellowish and green in thin section. Pyrophyllite, anthophyllite, chlorite and clinochlore are commonly present in both talcose bodies. A greenish or brownish tint in colour is observed with increase in chlorite and/or anthophyllite content. The pyrophyllite rich varieties are schistose in texture and cream-white in colour. The talc sample has a strong soapy feel. In thin sections, the talc schists are observed as flaky aggregates and platelets of talc (Figures 5–7). Pyrophyllite ($Al_2Si_4O_{10}\{OH\}_2$) occurs as fibrous aggregates and rosettes around fine-grained matrix of flaky talc. The pyrophyllite crystals have properties similar to those of talc and are observed as foliated masses in the talc schist. Laths of anthophyllite are also present with subordinate chlorite and clinochlore.

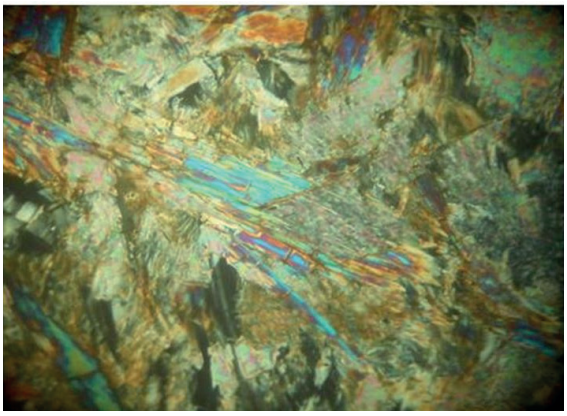

Figure 5: *Photomicrograph of Wonu-Apomu talcose rock showing talc and anthophyllite crystals (40-times, crossed polars).*

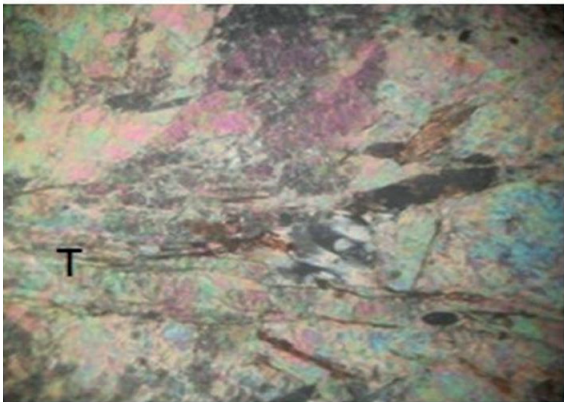

Figure 6: *Photomicrograph of Wonu-Apomu talcose rock showing plates of talc (T) (40-times, crossed polars).*

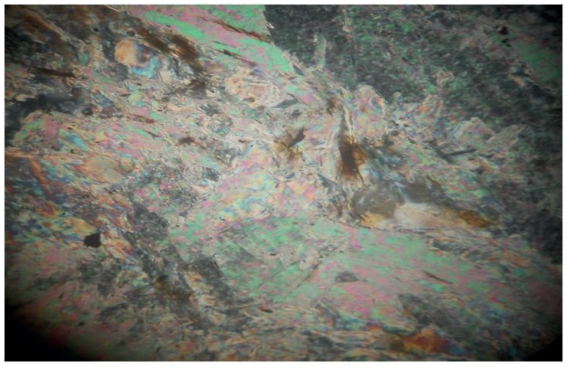

Figure 7: *Photomicrograph showing plates of talc in the Ilesa talcose rock (40-times, crossed polars).*

X-ray diffraction

X-ray diffraction studies revealed the presence of talc, anthophylite and substantial quantity of pyrophyllite and clinochlore (Table 1). Strong peak of pyrophyllite is close to those of talc and anthophyllite. The chromium bearing clinochlore has similar reflection peaks with chlorite. Talc was identified at (9.5, 28.6, 48.8, and 59.4) 2θ values (Figs. 8 and 9). Peaks of pyrophyllite occur closely with those of talc and anthophyllite at (9.5, 19.4 28.9, 29.4) 2θ values. Anthophyllite peaks are recorded at values of 2θ (9.6, 10.7, 19.8, 27.6, 29.1 and 31.2).

Table 1: *Mineral composition (%) of talc schist from Wonu-Apomu and Ilesa areas*

Minerals	1	2	3	4	Mean
Talc	30	32	21	24	26.75
Pyrophyllite	20	20	18	18	19.0
Anthophyllite	21	18	28	22	22.25
Chlorite	14	15	16	20	16.25
Clinochlore	14	14	16	14	14.5
Others	1	1	1	2	1.25
Total	100	100	100	100	100

1–2: Wonu-Apomu Talc-chlorite-anthophyllite schist
3–4: Ilesa Talc-anthophyllite-chlorite schist

Chlorite in association with clinochlore, a chromium-bearing monoclinic chlorite was identified at 2θ values of (6.2, 12.4, 18.6, 25.0 and 31.2). Chlorite is a hydrous silicate of aluminiun, iron and magnesium $(Mg, Fe)_5Al(AlSi_3)\ O_{10}(OH)_9$ while clinochlore with the chemical composition $(Mg, Fe, Al)_6\ (Si,Cr)\ O_{10}\ (OH)_8$ is a monoclinic crystal that is distinctly biaxial and optically positive as observed under the petrological microscope. The average clinochlore composition was about 14 % in each of the ten samples analysed. The total chlorite content (including clinochlore) of the talc schist samples was about 30 %, which was responsible for the greenish colour of most of the samples. The mineralogical data of the whole rock samples, using the peak height ratio showed that they are composed of about 30 % talc, 20 % pyrophyllite, 21 % anthophyllite, 28 % chlorite and 1% unidentified minerals.

Comparative studies of the Ilesa and Wonu-Apomu talc-schist with those of Oke-Ila, Iseyin, Baba-Ode and Erin-Omu (Table 2) showed that the Ilesa and Wonu-Apomu samples are higher in pyrophyllite and anthophyllite but lower in talc and tremolite/actinolite contents. The range values of talc for Ilesa and Wonu-Apomu samples is 21–32 % while those of Oke-Ila is about (58–81 %) and Iseyin (48–59 %) [15].

Table 2: *Comparison of mineral composition (%) of the Ilesa and Apomu talc schist with some other talc bodies in southwestern Nigeria*

Minerals	This study				Oke-Ila			Iseyin (TTSC)			Baba-Ode		Erin-Omu
	1	2	3	4	2 m	3 m	4 m						
Talc	30	32	21	24	58	66	81	59	52	48	24	74	59
Pyrophyllite	20	20	18	18	–	–	–	–	–	–	–	–	–
Anthophyllite	21	18	28	22	–	–	–	–	–	–	9	3	6
Tremolite/ Actinolite	–	–	–	–	18	20	10	28	26	33	48	7	24
Muscovite	–	–	–	–	–	–	–	–	–	–	–	6	2
Chlorite	14	15	16	20	22	12	8	12	21	17	16	–	7
Clinochlore	14	14	16	14	–	–	–	–	–	–	–	–	–
Others	1	1	1	2	2	2	1	1	1	2	1	1	2
Total	100	100	100	100	100	100	100	100	100	100			

1–2: Wonu-Apomu talc-chlorite-anthophyllite schist
3–4: Ilesa talc-anthophyllite-chlorite schist
Oke-Ila: talc-tremolite chlorite schist [15]
TTSC: talc-tremolite schist, Iseyin [14]
Baba-Ode: talc-tremolite chlorite anthophyllite schist [16]
Erin-Omu: talc-tremolite chlorite anthophyllite schist [18]

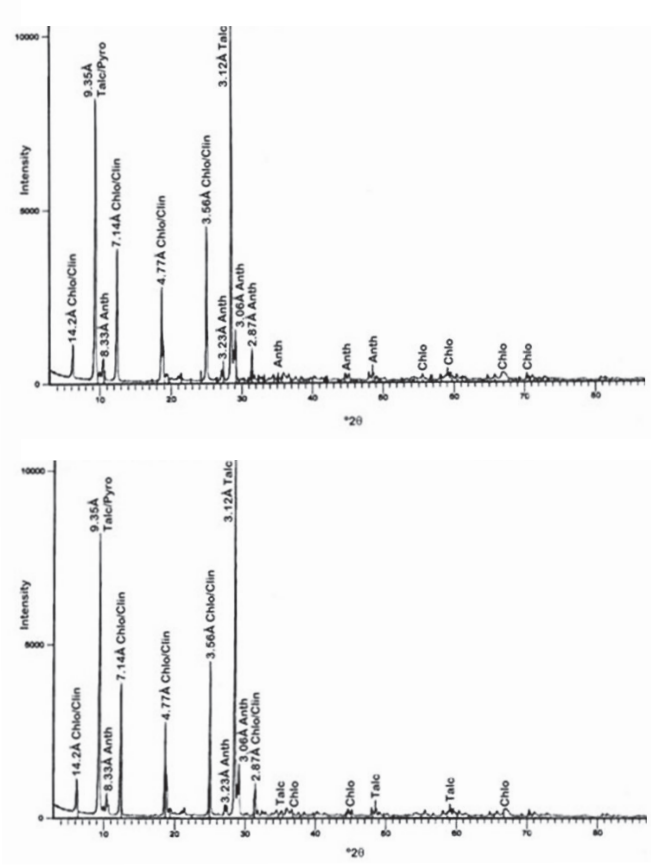

Figure 8: *X-ray diffraction charts of Wonu-Apomu talc - chlorite schists.*
(Anth – Anthophyllite, Chlo – Chlorite, Clin – Clinochlore, Pyro – Pyrophyllite)

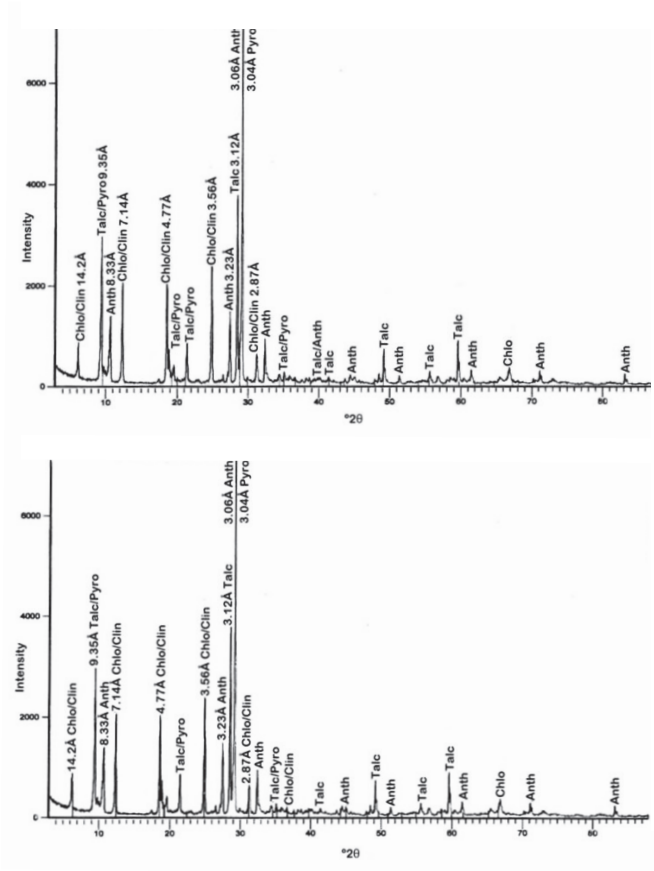

Figure 9: *X-ray diffraction chart of Ilesa talc - pyrophyllite schists.*
(Anth – Anthophyllite, Chlo – Chlorite, Clin – Clinochlore, Pyro – Pyrophyllite)

Table 3: *Major (%) and trace element composition of talc schist of Wonu-Apomu and Ilesa areas*

	1	2	3	4	5	6	7	8	9	10
SiO_2	52.29	51.43	52.23	61.15	61.01	52.42	52.82	52.1	52.24	52.15
Al_2O_3	4.16	4.3	3.62	0.84	0.77	5.2	4.99	5.22	5.3	5.14
$Fe_2O_{3(t)}$	8.34	7.83	8.27	3.94	3.75	9.54	9.26	9.38	9.42	9.33
MnO	0.14	0.13	0.15	0.48	0.05	0.15	0.14	0.14	0.14	0.14
MgO	28.59	27.89	29.18	30.04	30.06	26.54	26.67	26.03	26.46	26.02
CaO	2.7	3.17	2.59	0.06	0.05	1.39	1.34	1.38	1.31	1.38
Na_2O	0.04	0.01	0.11	0.03	0.03	0.08	0.07	0.01	0.01	0.01
K_2O	0.06	0.05	0.11	0.01	0.02	0.03	0.01	0.08	0.06	0.01
TiO_2	0.19	0.20	0.187	0.2	0.02	0.09	0.1	0.1	0.11	0.11
P_2O_5	0.03	0.03	0.03	0.01	0.01	0.03	0.02	0.03	0.03	0.03
LOI	4.42	4.65	4.21	4.81	4.79	5.22	5.24	5.33	5.27	5.1
Total	100.96	99.7	100.59	101.57	100.56	100.69	100.66	99.8	100.41	99.42
Trace element (µg/g)										
Ba	32	30	37	9	10	15	14	18	15	15
Co	69	69	70	71	73	72	70	69	70	69
Cr	1880	1820	1870	1030	1190	3770	3720	3640	3670	3610
Cu	70	60	70	10	10	20	10	10	10	10
Ga	7	6	5	2	2	8	8	8	8	8
Ni	1110	1080	1150	1670	1750	1710	1650	1620	1650	1640
Rb	29	6	4	3	2	2	3	2	2	2
Sr	10	12	9	2	2	4	3	4	4	4
V	78	80	67	5	5	48	46	45	48	45
Y	34	25	33	2	2	10	10	11	11	11
Zr	17	14	13	8	8	20	11	15	17	18
Zn	50	60	60	40	70	220	170	160	170	190
K/Rb	0.002	0.007	0.0021	0.003	0.008	0.013	0.003	0.033	0.025	0.004
Rb/Sr	2.9	0.5	0.44	1.5	1	0.5	1	0.5	0.5	0.5
K/Ba	0.002	0.001	0.0002	0.001	0.002	0.002	0.001	0.004	0.003	0.001
Ga/Y	0.2	0.24	0.152	1	1	0.8	0.8	0.727	0.727	0.727
Rb/Y	0.85	0.24	0.12	1.5	1	0.2	0.3	0.182	0.182	0.182
Na/K	0.6	0.178	9.83	2.675	1.337	2.38	6.25	0.111	1.042	0.892
Ba/Rb	1.1	5.0	9.25	3.0	5.0	7.5	4.66	9.0	7.5	7.5

1–5: Wonu-Apomu samples
6–10: Ilesa samples

Baba-Ode and Erin-Omu talc contents are ca. 49 % and 59 % respectively. Chlorite, on the other hand, is 14–20 % for Ilesa and Wonu-Apomu, while those of Oke-Ila and Iseyin are (18–22 %) and (12–22 %) respectively. It must be noted that pyrophyllite and anthophyllite, which occur prominently in the Ilesa and Wonu-Apomu samples are absent in the Iseyin and Oke-Ila samples.

Anthophyllite, an orthorhombic amphibole is a major constituent in the Ilesa and the Apomu talc-schist while tremolite, a monoclinic amphibole, which is one of the major constituents in the Oke-Ila, Iseyin, Baba-Ode and Erin-Omu talc-schist are absent in the Wonu-Apomu and Ilesa samples (Table 2). Anthophyllite is stable only at low temperatures. When heated to about 400 °C, it may alter to a monoclinic amphibole, such as, tremolite. The heat for the conversion of the anthophyllite to tremolite in the areas where they occur could have been provided by the granitic intrusives around the talc bodies.

Geochemistry

Chemical data show that the talcose rocks of the study areas are highly siliceous with an average value of 55.62 % and 52.35 % SiO_2 for Wonu-Apomu and Ilesa samples, respectively (Table 3). Also magnesia contents ranges between 27.89–30.06 % and 26.02–26.67 % for the Wonu-Apomu and Ilesa talcose samples. Alumina (0.77–4.3 %), Fe_2O_3 (3.75–8.345 %) and CaO (0.05–3.17 %) contents of Wonu-Apomu talcose rock show lower values and a wider range within samples when compared to the Ilesa samples with 4.99–5.55 %, 9.26–9.54 % and 1.31–1.39 % for Al_2O_3, Fe_2O_3 and CaO contents, respectively. Some samples from Wonu-Apomu, however, exhibit high silica (> 61 %) and magnesia contents (> 30 %), but correspondingly low Al_2O_3 (< 2 %), $Fe_2O_{3(t)}$ (< 4 %), CaO (0.05 %) and MnO contents (Table 4). These samples are higher in talc content than others (Tables 2, 3 and 4). The abundances of SiO_2, MgO, Al_2O_3, $Fe_2O_{3(t)}$ and CaO between Wonu-Apomu and Ilesa samples invariably reflect subtle mineralogical differences between samples. The MnO, Na_2O, K_2O, TiO_2 and P_2O_5 concentrations are generally low (< 0.05 %) and are not strikingly varied within samples. The loss on ignition (LOI) does not generally exceed 5.4 %.

As observed from Tables 3 and 4, Ilesa talcose samples are enhanced in Cr (> 3 600 μg/g), Ni (> 1 620 μg/g) and Zn(> 160 μg/g), while Wonu-Apomu indicated an average concentrations of 1 558 μg/g, 1 353 μg/g and 56 μg/g for Cr, Ni and Zn, respectively. Other trace elements such as Ba, Co, Cu, Ga, Rb, Sr, V, Y and Zr are generally low and do not show any marked trend. The talcose rock showed SiO_2 enrichment, probably due to the effect of chemical weathering. Hydrothermal alteration accompanied by serpentinization of the tholeiitic protoliths was reflected in high MgO (26.34–29.15 %) and $Fe_2O_{3(t)}$ (6.43–9.39 %) contents of the talcose rocks. The relative chemical mobility of Na, Ca and K during secondary alteration processes is largely displayed by strong depletions of these Na, Ca and K oxides in the talcose samples relative to the protolith amphibolites (Table 5) [22].

The Ba (24 μg/g), Sr (7 μg/g) and Rb (9 μg/g) concentrations in the talcose rocks are generally low compared to the amphibolites within the area (Table 5). This trend is also due to their chemical instability during secondary alteration processes. On the other hand, Cr (3 684 μg/g) and Ni (1 654 μg/g) contents, as a result of their chemical immobility even under hydrothermal alteration, which commonly produce talc, serpentine and chlorite from mafic and ultramafic rocks showed distinctive chemical enrichment trends in the talcose rocks. The values for Co (ca. 70 μg/g) remain unchanged in both the talcose rock and the amphibolites (Table 4). These could serve as exploration guide for basemetals and platinum group elements (PGE) in the area.

Functional potentials of the talc bodies

The physical and industrial properties of the talcose body include determination of natural moisture content (NMC), loss on ignition (LOI), linear shrinkage (LSK), water absorption capacity (WAC), firing colour and pH. Results obtained from these tests (Table 6) served as basis for the evaluation of functional potentials of the talc bodies. The results showed that the NMC ranged from 5.00 % to 6.55 %.

Table 4: *Average chemical composition of Wonu-Apomu and Ilesa talcose rocks compared with other talcose rocks elsewhere in Nigeria*

	Wonu-Apomu		Ilesa		Iseyin (TTCS)		SW Nigeria (TTAS)	
	Mean	Range	Mean	Range	Mean	Range	Mean	Range
SiO_2	55.62	51.23–61.15	52.35	52.15–52.82	54.70	53.61–55.35	55.01	46.82–55.37
Al_2O_3	2.74	0.77–4.3	5.17	4.99–5.3	3.54	1.86–4.84	2.52	1.19–2.86
$Fe_2O_{3(t)}$	6.43	3.75–8.34	9.39	9.26–9.54	6.50	5.75–7.25	4.50	3.20–4.50
MnO	0.19	0.05–0.48	0.14	0.14–0.15	0.16	0.10–0.25	0.05	0.004–0.13
MgO	29.15	27.89–30.06	26.34	26.02–26.67	27.20	22.06–30.38	30.04	29.13–32.04
CaO	1.71	0.05–3.17	1.36	1.31–1.39	4.43	2.76–5.32	1.50	0.41–4.47
Na_2O	0.04	0.01–0.11	0.05	0.01–0.08	0.22	0.16–0.32	0.01	0.01–0.02
K_2O	0.03	0.01–0.11	0.04	0.01–0.08	0.03	0.01–0.06	0.02	0.01–0.02
TiO_2	0.16	0.02–0.2	0.10	0.09–0.11	Nd	Nd	Nd	Nd
P_2O_5	0.02	0.01–0.03	0.03	0.02–0.03	0.02	0.02–0.3	0.06	0.05–0.13
LOI	4.58	4.21–4.81	5.23	5.1–5.33	2.99	1.82–4.88	6.00	3.60–5.41
Total	100.68		100.2		99.86		99.71	
Trace element (µg/g)								
Ba	24	9–37	15	14–18	Nd	Nd	Nd	Nd
Co	70	69–73	70	69–70	71	52–80	Nd	Nd
Cr	1558	1030–1880	3684	3610–3770	826	806–897	2000	Nd
Cu	44	10–70	12	10–20	Nd	Nd	Nd	Nd
Ga	4	2–7	8	8	Nd	Nd	Nd	Nd
Ni	1352	1080–1750	1654	1620–1710	1278	1034–1702	1500	Nd
Rb	9	2–29	2	2–3	Nd	Nd	Nd	Nd
Sr	7	2–12	4	3–4	Nd	Nd	Nd	Nd
V	47	5–80	46	45–48	Nd	Nd	Nd	Nd
Y	19	2–34	11	10–11	Nd	Nd	Nd	Nd
Zr	12	8–17	16	11–20	Nd	Nd	Nd	Nd
Zn	56	40–70	182	160–220	69	58–82	Nd	Nd
K/Rb	0.004	0.001–0.008	0.0155	0.003–0.033	Nd	Nd	Nd	Nd
Rb/Sr	1.27	0.44–2.9	0.6	0.5–1.0	Nd	Nd	Nd	Nd
K/Ba	0.011	0.001–0.002	0.002	0.004–0.006	Nd	Nd	Nd	Nd
Ga/Y	0.52	0.15–1.0	0.756	0.727–0.8	Nd	Nd	Nd	Nd
Rb/Y	0.74	0.24–1.5	0.21	0.182–0.3	Nd	Nd	Nd	Nd
Na/K	2.92	0.18–9.83	2.136	0.111–6.25	Nd	Nd	Nd	Nd
Ba/Rb	4.67	1.10–9.25	7.23	4.66–9.00	Nd	Nd	Nd	Nd

Nd: Not determined
TTCS: Talc-tremolite schist, Iseyin [14]
TTAS: Talc-tremolite/actinolite schist, SW Nigeria [13]

Table 5: *Comparison of the major (%) and trace element (%) composition of the amphibolites and the talcose rocks in Wonu-Apomu and Ilesa areas*

	*Amphibolite				Talcose rocks			
	Wonu-Apomu		Ilesa		Wonu-Apomu		Ilesa	
	Mean	Range	Mean	Range	Mean	Range	Mean	Range
SiO_2	48.91	44.79–50.62	47.27	44.86–49.10	55.62	51.23–61.15	52.35	52.15–52.82
Al_2O_3	15.11	14.01–16.41	17.29	15.20–20.22	2.74	0.77–4.3	5.17	4.99–5.3
$Fe_2O_{3(t)}$	13.31	12.27–14.62	12.44	11.56–13.34	6.43	3.75–8.34	9.39	9.26–9.54
MnO	0.13	0.07–0.23	0.11	0.08–0.14	0.19	0.05–0.48	0.14	0.14–0.15
MgO	9.84	8.08–12.15	9.52	7.85–11.16	29.15	27.89–30.06	26.34	26.02–26.67
CaO	9.33	8.72–10.00	9.50	8.11–10.55	1.71	0.05–3.17	1.36	1.31–1.39
Na_2O	1.52	1.13–1.88	1.87	1.28–2.72	0.04	0.01–0.11	0.05	0.01–0.08
K_2O	0.73	0.46–0.99	0.732	0.55–0.85	0.03	0.01–0.11	0.04	0.01–0.08
TiO_2	0.05	0.25–0.88	0.61	0.39–0.86	0.16	0.02–0.2	0.10	0.09–0.11
P_2O_5	0.03	0.01–0.05	0.03	0.02–0.05	0.02	0.01–0.03	0.03	0.02–0.03
LOI	0.31	0.25–0.35	1.46	0.24–0.35	4.58	4.21–4.81	5.23	5.1–5.33
Total	99.69		99.86		100.68		100.20	
Trace elements (µg/g)								
Ba	184	86–350	137	88–231	24	9–37	15	14–18
Sr	123	106–143	122	106–145	7	2–12	4	3–4
Rb	33	26–40	34	27–46	9	2–29	2	2–3
Cr	79	58–92	63	45–94	1 558	1 030–1 880	3 684	3 610–3 770
Co	71	40–85	62	48–82	70	69–73	70	69–70
Ni	64	24–98	57	25–85	1 352	1 080–175	1 654	1 620–1 710
Zr	55	48–62	56	46–66	12	8–17	16	11–20
Y	37	26–45	37	25–45	19	2–34	11	10–11

* Wonu-Apomu and Ilesa amphibolites [29]

The LOI ranged between 4.21 % and 5.27 %. The LSK values are generally low (2.33–4.40 %). The WAC ranged from 8.05 % to 10.00 % while the pH of the slurry produced from the talcose rock ranged between 8.00 and 8.35 indicating alkalinity (Tables 6 and 7). The pH values and the LOI compare favourably with those of talc bodies from Erin-Omu, Iseyin, Oke-Ila and Baba-Ode (Table 7) all in southwestern Nigeria [15, 16, 18]. On the other hand the WAC is lower than those of the Erin-Omu and Baba-Ode samples and comparable to that of Oke-Ila but higher than that of Iseyin (Table 7). The variation in the mineralogical compositions and textures of the talcose rocks from one area to the other is reflected in the results of the firing tests presented. Generally, the results are comparable to other similar talc bodies within the schist belts of south-western Nigeria as reported by Durotoye and Ige [11]. The colour of the raw talcose pellets changes from green, brown, grey or cream to shades of red, yellow and cream after firing (Table 6). Bleaching of the talcose rocks yielded white to off-white coloured samples with increasing concentration of the HCl acid used.

Based on the foregoing the talc bodies of Wonu-Apomu and Ilesha areas are assessed

as viable industrial raw materials in coloured ceramics including insulation ceramics [23]. They could also function as filler and extender in paints [24], paper, roofing materials and textiles after screening to remove gritty particles, which are mainly quartz [25–27]. The talc bodies could be used to improve the stability and rigidity of plastic goods at high temperatures based on the specifications of Noble [28]. It must be noted that pyrophyllite is commonly used for the same purpose as talc. The high content of trace elements in the talc bodies, notably Cr, Ni, Co, Cu, V and Zn would not permit utilization for pharmaceutical purposes. Also, chemical data are not within the specifications of the American Society for Testing of Materials [29] for the manufacture of powder, creams and soaps. However, the bleaching test suggested that they could serve as absorbents for oil, grease and other chemicals.

Conclusions

Talcose rocks from Wonu-Apomu and Ilesa areas contain talc, pyrophyllite, anthophyllite and chlorite (clinochlore). Comparative studies of these talc bodies with those of Erin-Omu, Iseyin, Oke-Ila and Baba-Ode showed that the former is higher in pyrophyllite, anthophyllite and chlorite (clinochlore) but lower in talc and lack tremolite/actinolite contents.

Chemical data for the talcose rock showed that they are siliceous. Petrochemical trends of the major and trace element data of the talcose rocks reflected some subtle relationships to the amphibolites in the areas. Trace elements concentrations of the talcose rocks indicated enrichments in Cr, Ni, Cu, V and Zn relative to the amphibolites within the area. Petrogenetic indices suggest tholeiitic basalt precursor for the talc bodies [29].

Table 6: *Industrial properties of Wonu-Apomu and Ilesa talcose rocks*

	1	2	3	4	5	6	7	8	9	10
NMC	5.20	5.35	5.20	6.20	6.55	5.00	5.26	5.10	5.44	5.00
LOI	4.42	4.65	4.21	4.81	4.79	5.22	5.24	5.33	5.27	5.10
LSK	4.40	3.83	4.27	2.40	2.33	2.54	3.60	3.38	3.42	3.33
WAC	8.54	8.33	8.05	9.48	10.00	8.05	8.40	8.55	8.40	8.35
Raw colour	Brown	Brown	Green	Cream	Cream	Brown	Green	Brown	Brown	Brown
Fired colour	Red	Red	Yellow	White	White	Red	Yellow	Red	Red	Red
pH	8.35	8.30	8.33	8.00	8.10	8.30	8.26	8.34	8.30	8.25

NMC – Natural moisture content (%)
LOI – Loss on ignition (%)
LSK – Linear shrinkage (%)
WAC – Water absorption capacity (%)

Table 7: *Result of physical and industrial test on Wonu-Apomu and Ilesha talcose rocks compared to similar rock types in SW Nigeria*

	This study	Erin-Omu	Iseyin	Oke-Ila	Baba-Ode
NMC	5.00–6.55	Nd	Nd	7.50–8.90	Nd
LOI	4.21–5.27	2.87–4.11	1.45–6.03	3.75–5.28	4.25–4.41
LSK	2.33–4.40	1.01–1.81	0.25–2.0	2.45–3.50	1.01–1.52
WAC	8.05–10.00	13.25–16.25	6.96–11.65	4.21–5.80	15.14–18.25
pH	8.00–8.35	8.01–8.21	Nd	7.5–9.5	8.01–8.21

This study – Wonu-Apomu and Ilesa areas
NMC – Natural moisture content (%)
LOI – Loss on ignition (%)
LSK – Linear shrinkage (%)
WAC – Water absorption capacity (%)

The Wonu-Apomu and Ilesa talc bodies possess requisite mineralogical, chemical and industrial specifications for use as raw materials in the manufacture of ceramics, paints, rubber, paper, textile, plastic, roofing materials and textiles. They can also be used as absorbent. However, they might not be appropriate for use in the pharmaceutical, powder, creams and soaps manufacturing industries without rigorous beneficiation, which might not be economical.

Acknowledgements

The authors would like to thank Mr. Wale Aromolaran for his assistance and Mr. Aikhiero Ata for preparing the thin sections. The comments and suggestions of the anonymous reviewers are appreciated.

References

[1] De Swardt, A. M. J. (1953): The geology of the county around Ilesa. *Geological Survey of Nigeria. Bulletin,* 23, 54 p.

[2] Olade, M. A., Elueze, A. A. (1979): Petrochemistry of the Ilesa amphibolites and Precambrian crustal evolution in the Pan-African domain of southwestern Nigeria. *Precambrian Research*, 8, pp. 303–318.

[3] Ajayi, T. R. (1980): On the geochemistry and origin of amphibolites in Ife-Ilesa area, southwestern Nigeria. *Journal of Mining and Geology,* 17(2), pp. 177–196.

[4] Elueze, A. A. (1982): Mineralogy and chemical nature of meta-ultamafites in Nigerian schist belt. *Journal of Mining and Geology,* 19(2), pp. 21–29.

[5] Elueze, A. A. (1988): Geology of the Precambrian schist belt of Ilesa area, southwestern Nigeria. In: Oluyide, P.O. (Ed); *Precambrian Geology of Nigeria*, Geological Survey of Nigeria, pp. 77–82.

[6] Ige, O. A., Asubiojo, O. I. (1991): Trace element geochemistry and petrogenesis of some metaultramafites in Apomu and Ife-Ilesha area of southwestern Nigeria. *Chemical Geology*, 91, pp. 19–32.

[7] Kehinde-Phillips, O. O. (1991): *Compositional variations in lateritic profiles over mafic and ultramafic rock units of Ilesa schist belt, southwestern Nigeria.* Unpublished Ph.D. Thesis, University of Ibadan, Ibadan, Nigeria. 201 p.

[8] Elueze, A. A. (1981): Petrographic studies of metabasic rocks and meta-ultramafites in relations to mineralization in Nigerian schist belt. *Journal of Mining and Geology,* 18(1), pp. 31–36.

[9] Akin-Ojo, O. A. (1992): *Compositional and industrial studies of talc bodies in the Precambrian domain of southwestern Nigeria*. Unpublished Ph.D. Thesis, University of Ibadan, Ibadan, Nigeria, 215 p.

[10] Elueze, A. A., Akin-Ojo, O. A. (1993): Functional characteristis of talc bodies in southwestern Nigeria. *Mineral Wealth*, 85, pp. 7–14.

[11] Durotoye, M. A., Ige, O. A. (1991): An inventory of talc deposits in Nigeria and its industrial application potentials. *Journal of Mining and Geology,* 27(2), pp. 27–31.

[12] Ige, O. A. (1985): Mineralogical and industrial properties of some Wonu Apomu talcs, western Nigeria. *Nigerian Journal of Science,* 19, pp. 121–130.

[13] Elueze, A. A., Ogunniyi, S. O. (1985): Appraisal of talc bodies of the Ilesa district, southwestern Nigeria, and their potential for industrial applications. *Natural Resources and Development,* 21, pp. 26–34.

[14] Elueze, A. A., Awonaiya, F. A. (1989): Investigation of talc bodies in Iseyin area, southwestern Nigeria, in relation to their application as industrial raw materials. *Journal of Mining and Geology,* 25(1&2), pp. 217–225.

[15] Bolarinwa, A. T. (2001): Compositional and industrial evaluation of talc bodies of Oke-Ila area, Ilesa schist belt, southwestern Nigeria. *Mineral Wealth,* 118, pp. 48–52.

[16] Okunlola, O. A., Ogedengbe, O., Ojutalayo, A. (2002): Compositional features and industrial appraisal of the Baba-Ode talc occurrence, southwestern Nigeria. *Global Journal of Geological Sciences,* 1(1), pp. 63–72.

[17] Adeola, A. J. (2006): *Compositional and industrial characteristics of talc bodies and associated rocks in Odogbe-Okolom area, Egbe-Isanlu schist belt, southwestern Nigeria.* Unpublished M. Sc. Project, Department of Geology, University of Ibadan, Ibadan, Nigeria, 88 p.

[18] Okunlola, O. A., Anikulapo, F. A. (2006): Compositional characteristics and industrial qualities of talcose rock in Erin Omu area, southwestern Nigeria. *Journal of Mining and Geology,* 42(2), pp. 105–112.

[19] Oyawoye, M. O. (1984): The geology of the Nigerian basement complex. *Journal of Mining and Geology,* 1, pp. 87–102.

[20] Adeleye, M. A. (2009): *Petrogenetic studies of talc and amphibolites in Wonu-Apomu and Ilesa areas, southwestern Nigeria.* Unpublished M.Sc. Project, Department of Geology, University of Ibadan, 87 p.

[21] JCPDS, (1974): Selected powder diffraction data for minerals 1st edition, (Ed. L.G. Berry), Joint Committee on Powder Diffraction Standards, Philadelphia, 833 p.

[22] Mitchel, L. (1975). Ceramic raw materials. In Leford J. (ed). *Industrial minerals and rocks,* American institute of mining and Metallurgical and Petroleum Engineers, New York, 33 p.

[23] National Paint and Coating Association (1975): *Industrial specification for the paint industry*, New York, 25 p.

[24] Payne, H. F. (1954): *Organic coating technology*. John Wiley, New York, 2, 725 p.

[25] Severinghus, N. (1975): Fillers, filters and absorbents. In: Letond, J.S (ed) *Industrial minerals and rocks,* New York, 125 p.

[26] American Textile Manufacturer Institute (1975): *Industrial specification for raw materials in the textile industry*, 54 p.

[27] Noble, P. (1988): *Marketing guide to the paper and pulp industry*. Fairfteld, N. J, 148 p.

[28] American Society For Testing of Materials (1988): *Handbook of construction materials*, 45 p.

[29] Bolarinwa, A. T., Adeleye, M. A. (2015): Nature and origin of the Amphibolites in the Precambrian Basement Complex of Iseyin and Ilesha schist belts southwestern Nigeria. *Journal of Geography and Geology*, 7(2) pp. 6–17.

Original scientific paper

Received: April 5, 2015
Accepted: April 20, 2015

Idrisi as a tool for slope stability analysis

Idrisi kot orodje za analizo stabilnosti pobočij

Eva Koren[1], **Goran Vižintin**[2,*]

[1]Rečica ob Savinji 60, 3332 Rečica ob Savinji, Slovenia

[2]University of Ljubljana, Faculty of Natural Sciences and Engineering, Aškerčeva cesta 12, 1000 Ljubljana, Slovenia

*Corresponding author. E-mail: goran.vizintin@ntf.uni-lj.si

Abstract

For the entire area of municipality of Krško the analysis of slope stability has been done. The analysis is based on publicly available geological data (MOP, Ministry of environment, ARSO – Slovenian Environment Agency etc.) and engineering – geological rock classification. Based on this a map of slope stability was produced. As a result the map is showing the maximum slope angles where the landslides start to appear.

Key words: municipality of Krško, GIS, slope stability analysis, stability map, stability classes, applied geology

Izvleček

Za območje občine Krško je bila s programom IDRISI izdelana analiza stabilnosti pobočij. Analiza je temeljila na osnovi javno dostopnih geoloških podatkov (MOP, Ministrstvo za okolje, ARSO – Agencija Republike Slovenije za okolje itd.) in inženirsko-geološke klasifikacije kamnin. Na osnovi te analize je bila izdelana karta stabilnosti pobočij, ki kot rezultat prikazuje mejne naklonske kote, pri katerih se začnejo pojavljati plazovi.

Ključne besede: občina Krško, stabilnostna analiza, GIS, stabilnostna analiza pobočij, karta stabilnosti, razredi stabilnosti, aplikativna geologija

Introduction

Long-term impact of exogenous factors such as surface weathering, river and stream erosion, and groundwater flow, cause changes on the surface of the terrain and weaken the rock strength. Such action can cause a kind of balance collapse between the gravity and the inner strength of rock. These two reasons are the main factors for development of the landslides. GIS – Geographical Information System is designed to work with databases or, for integration, observation, analyses, processing and plotting of spatially oriented data, as well [1].
Litostratigraphic geological units of the researched area are for this basic outline summarized in a condensed form after the Basic Geological Map (OGK) – sheet Zagreb [2] and sheet Novo Mesto [3, 4], with corresponding explanatory notes. The oldest rocks in this area belong to Middle Triassic – Anisian.

Triassic - T

Anisian T_2^1 – In the time of sedimentation in the Anisian stage a dolomite formed, with intercalations of bedded limestones. Dolomite is mostly of dim grey color, occasionally bedded and generally massive. Sometimes it is also brecciaed. There are no fossil remains in the dolomite. It lies concordantly on the Lower Triassic (Scythian) beds, and its age can be determined only by its stratigraphic position. It can be found north of Krško.

Ladinian T_2^2 – Above the Anisian dolomite in the Krško hills between the Sava valley and Bučka, and northwest of Krško, lies indurated massive, rarely thick-bedded dolomite with cherts. This dolomite is lightly grey, coarse-grained and changes into dolomitized limestone. As it is partly porous, it resembles the Cordevolian dolomite. In its upper part are present layers and lenses of black chert. In this dolomite one can also find lenses of green and violet tuff with interlayers of silicified tuff and cherts.

Late Triassic T_3 – Upper Triassic Dolomite can be found in the Gorjanci hills, south of Čatež. Lightly grey massive and sometimes thick-bedded dolomite prevails, with layers of dolomitized limestones. Upward it changes into bedded and lightly weakly bedded white and lightly grey coarse-grained dolomite with chert layers and lenses.

Cretaceous - K

Late Cretaceous K_2 – Upper Cretaceous beds lie mostly trangressively on Middle and Upper Triassic dolomites. On the surface they outcrop in the vicinity of Krško and Gorjanci hills, south of Krška vas and Boršt. Elsewhere they are mostly eroded or present as small erosional patches. Lithologically they are developed as a typical flysch, as an alternation of sandstones, marls, siltstones, calcarenites or marly limestones with layers of cherts and chaotical breccias.

Miocene - M

M_2^2 *(Tortonian)* – Middle Miocene Tortonian sediments appear south of Brežice and Čatež in the area of Mrzla vas in the Gorjanci hills. From a lithological point of view the sediments are very diverse. In the lower parts one can find breccias, loosely consolidated conglomerates, and above yellow and white marly limestone. Some beds of porous lithotamnian limestone also appear, which changes into a sandy and marly limestone and marl. The latter contains thin beds of sandstone.

M_3^1 *(Sarmatian)* – In the area of Libna, Krška vas and Gazice Upper Miocene beds outcrop at the surface, consisting mostly of marl and clayey marl.

Pliocene - Pl

Pl_1^1 *(Early Pontian)* – Early Pliocene rocks outcrop at the terrace near Brežice. They are developed as a grey massive clayey marl and marlstone. Above it are continuously sedimented the Late Pontian (Pl_1^2) sand, sandy clay and sandy marl.

Plio-quarternary (Pl,Q)

A vast part of the studied area is build of Plio-Quaternary sediments (Pliocene/Pleistocene). In the lower part of these beds one can find grey and brown loam with quartz pebbles. On this base a 100 m thick sand and gravel terrace has been deposited. The terrace is covered by sandy clays, sand, silt and clayey gravel.

Quarternary (Q) – a, $a_{1, 2, 3}$

The complete basin is covered by fluvial gravel terrace of the Sava river. The thickness of this terrace is estimated to be 12 m in average (from 7 m to 20 m). It consists of sand and gravel of various granulation, and pebbles are mostly carbonate. After deposition, the river has incised fluvial terraces (a_1 to a_3) and drained oxbows. The latter are more abundant in the vicinity of villages Brege and Skopice. They are filled by organogenic clays and silts, and the environment is mostly marshy. Sandy and gravel terrace is sometimes covered by lentoid beds of silty and clayey sands. Their thickness varies from some decimeters to several meters.

Tectonics

The complete Krško basin is a young tectonic syncline depression, filled by Quaternary fluvial sediments. The subsidence of this area has started already in the Miocene and has intensely continued in Late Pliocene. The subsidence also took place in the Middle Pleistocene (neotectonics) and is active in the present time.

The syncline belongs to Zagorje Tertiary basin and forms its southeastern part. The syncline axis lies in the SW–NE direction. The northern boundary of the syncline is represented by the horst of Krško hills and the anticlyne of Bohor and Orlica, and the southern limb by the horst of Gorjanci hills. In the base of Krško syncline, below the Tertiary clastic sediments, the Middle and Upper Triassic limestones and dolomites appear. These rocks are intensely deformed and fractured.

Background and methods

For the purpose of stability analysis the rocks have been classified in the appropriate slope classes according to the Table 1. The results of classifications process, which was made on the basis of indication in Table 1, are presented in Table 2. As can be seen from Table 2 a strongly conservative approach has been selected. Decision on conservative approach is based on relatively small scale lithologic information [2–4] and in lack of information of rainfall impact on the rock stability [5–7]. As it is very well known, significant impact on rock and slope stability is attributed to rainfall [5, 6]. Unfortunately the impact is strongly depending on the type of rainfall duration, moisture content in soils and rocks, vegetation, seismic risk etc. Many of parameters mentioned before can't be directly included in topical analyses due to lack of knowledge on their impact on the rock formation [7], so to avoid them, only slope and lithological information with conservative transition approach to engineering geology information were selected.

The basic data for the rock slopes stability map were derived from geological data and DMR map – (Digital Terrain Model) with a cell size of 25 m × 25 m (Figure 1). Based on the DMR data the map of terrain slopes has been done (Figure 2). The creation of slopes map was completely made by Idrisi program using Slope function inside the Surface Analysis (Figure 3). The slopes map is only the first step in a way to the final rock slopes stability map.

Table 1: *Inclination angles depending on the rocks type* [8, 9]

Classification	Name	Inclination classes	Stable inclinations
rocks	igneous and metamorphic	rock	above 50°
	carbonates	rock	to 50°
	clastites	soil	
		rock	
soft rocks	tertiary sediments	soil	
		rock	
soil	gravely soils (*gravel fill*)		to 40°
	mixed soils (*clay and gravel fill*)	prevailing clay	
		prevailing gravel	
	lake, marsh and marine sediments		to 12°

Table 2: *Inclination angles derived from geology map*

Rock description	Age	Slope (°)
Alluvial deposits	al	15
Alluvial deposits: mostly sand to clay	al	10
Alluvial deposits: gravel to clay	a	15
Limestone, breccia	K2	50
Limestone and dolomite, breccia and conglomerate	Ol2	50
Limestone, limestone breccia, silicified limestone, chert with parts of dolomite	J1+2	50
Limestone, silicified limestone, chert	J3	50
Limestone and dolomite with chert, marl, shale and tuff	T22	40
Limestone marls, sandstone, sand and conglomerate	2M31, 2	35
Limestone and sandstone	1, M31	35
White limestone	M22	50
Breccia, conglomerate, shell, claystone, marl, limestone and chert	K2	40
Dolomite with layers of mica mudstone, sandstone, shale and shaley limestone	T1	44
Dolomite, marly limestone, mica shale and sandstone	T1	40
Dolomite, limestone, shale, chert and tuff	T2	35
Clay	j	10
Clay and loam with pieces of chert	Pl, Q	10
Clay and clay with gravels	Pl, Q	10
Clay, gravel	sg	15
Shale, calcarenite and limestone breccia	K14, 5	35
Clay and sandy marl with inlays of sand and sandstone	M32	35
Shale, limestone with chert, calcarenite and tuffs	T22	35
Shale, limestone with chert, marl and limestone breccia	K1, 2	35
Terra rossa	ts	10
Quartz sand	Pl 3	35
Marl, marly limestone, limestone and sandy marl	M22	35
Marl, marly limestone, limestone and sandy marl	M31	35
Marl, marly clay, send, conglomerates	Pl11	10
Sea clay	Ol2	10
Limestone	M22	50
Massive limestone, partially dolomite	T31	50
Massive limestone and dolomite marl	T21	50
Massive granulated dolomite	T31	50
Massive granulated dolomite	T32+3	50
Soft clayey marl	M32	20

Rock description	Age	Slope (°)
Shale, quartz sandstone and conglomerate	C, P	40
The lowest terrace: gravel, sand, clay	a1	15
Organic and bioclastic limestone, sandstones, lime and clayey marl	2, M22	40
Sand	M, Pl	30
Sand and gravel with a few inserts of clay and sandy marl	Pl1	30
Sand, sandstone, sandy clay, sandy marl and shale with coal	Ol, M	20
Sand, sandy marl and clay	Pl12	15
Composite limestone	T32+3	50
Limestone, marly limestone with chert	J, K	50
Dolomite with chert	T32+3	50
Slope debris	s	35
Massive dolomite	T21	50
Gravel, sand and clay	Pl, Q	15
Red and greenish sandstone, siltstone, and conglomerate, claystone	P22	40
River sediments in gravel terraces and erosion remnants - mostly felsic gravel	Pl, Q	35
Brown and green marl, sandy marl, marly limestone and grey or red limestone with inserts of breccia	K2	35
Weathered brown clay	Pl, Q	10
Mine works	10	
Grey to black partially stratified limestone	K11	50
Grey marl	M32	40
Grey marl and sandy marl	M31	40
Grey marl, white and brown sandy marl, sandstone and quartz sand	M22	40
Grey stratified and white grained dolomite	T2+3	50
Grey stratified dolomite, tuff, limestone, dolomite breccia and conglomerate	T22	40
Grey clay	g	10
Grey and brown clay	Pl, Q	10
Stratified limestone with chert	T31	50
Well rounded conglomerate	pr	35
Diabase and tuff	bb	25
Below micritic limestone and hard marl, up clayey marl	M31	40
Gravel and sand of middle river terrace	a2	35
Light grey densely stratified limestone	J1,2	50
Light grey massive dolomite and dolomite with chert	T2,3	50
Light grey stratified limestone	J1+2	50
Light grey stratified and massive dolomite with limestone inclusions	T21	50
Conglomerate of first river terrace	t	50

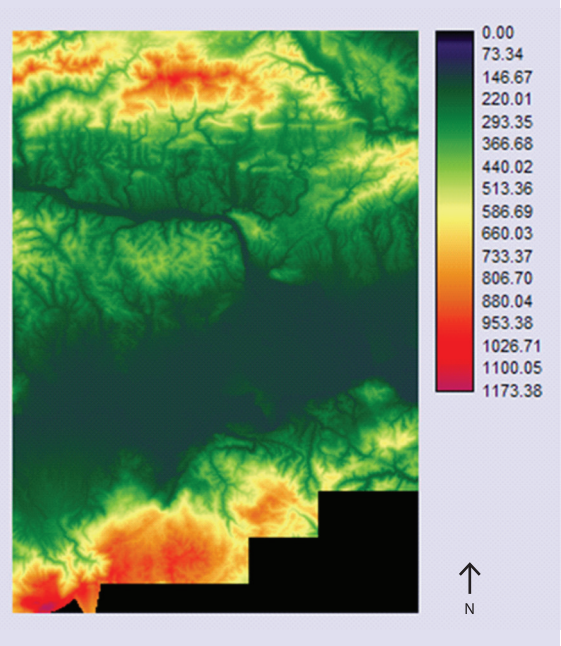

Figure 1: *Map of digital elevation model municipality of Krško Unit: [m. o. s. l.].*

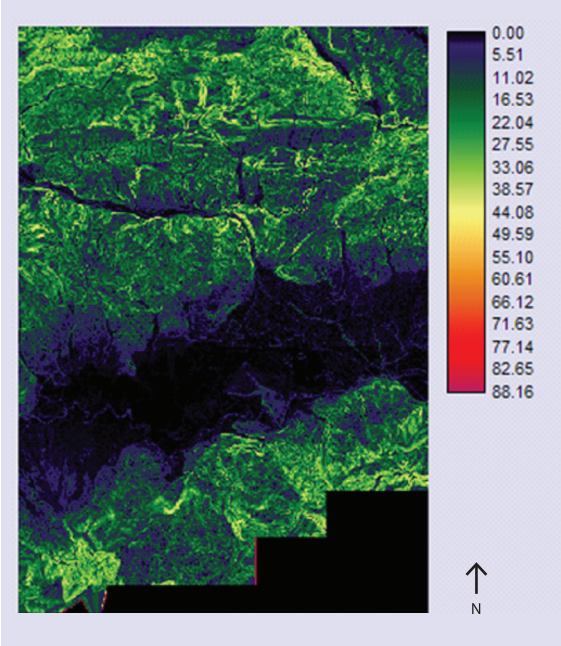

Figure 2: *Map of slopes.*

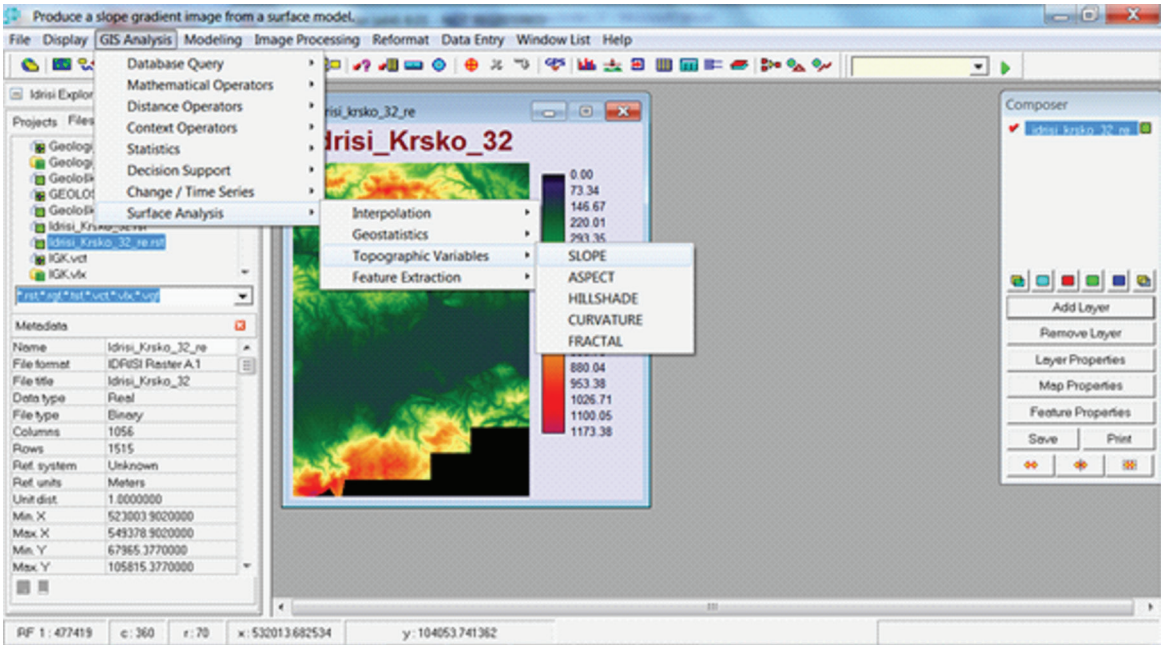

Figure 3: *Demonstration of the operation Idrisi – Taiga.*

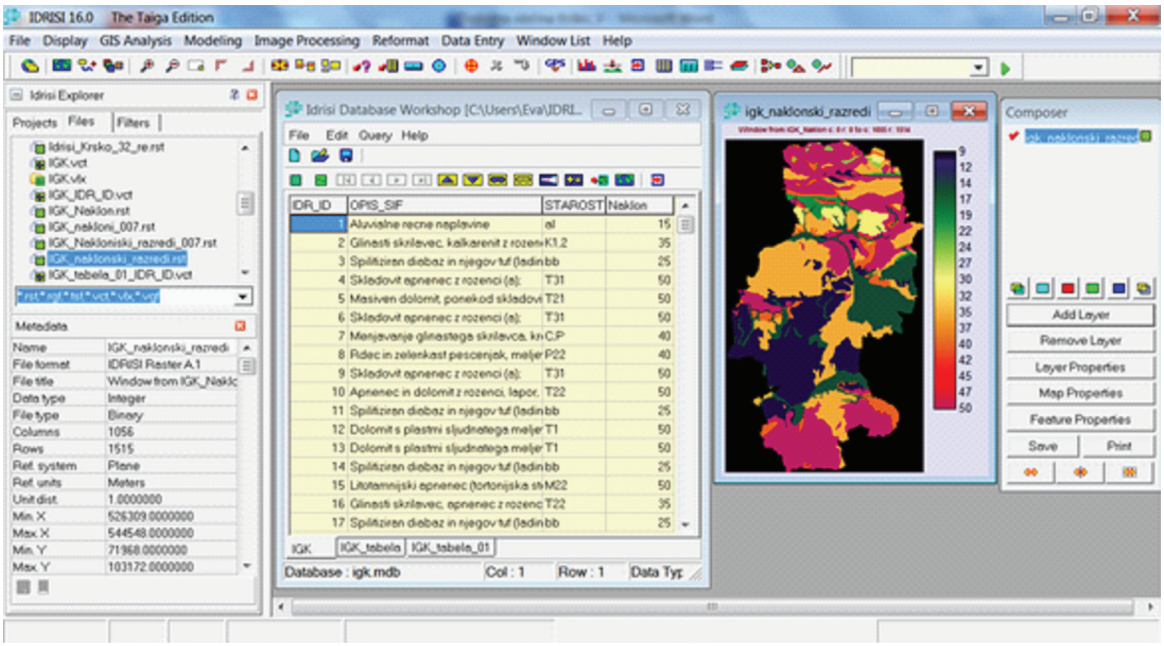

Figure 4: *Transformation of geological information into the rocks' maximum allowable inclinations.*

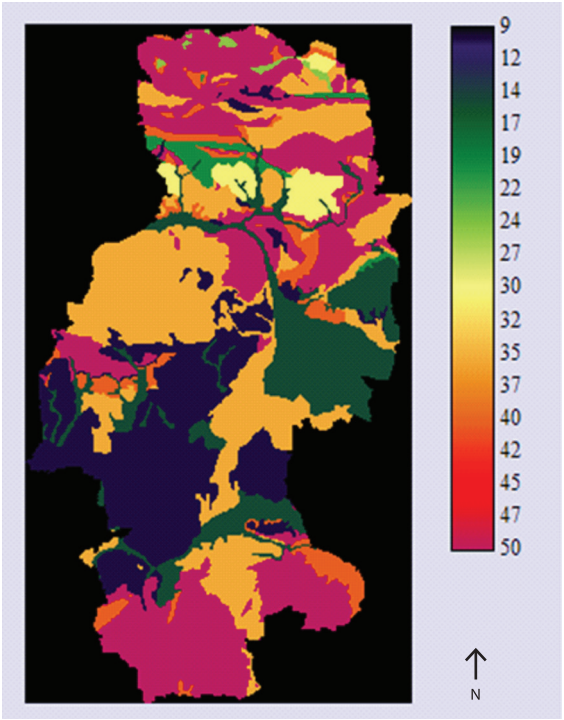

Figure 5: *Map of Maximum rock slope stability. Unit: [Degrees]*

The second step was based on the geological data described before. In this step the geological information was transformed to the rocks maximum allowable inclinations. As a result of this transformation (Figure 4) a Map of maximum rock slope stability was made (Figure 5).

Discussion and results

The first two maps were needed for the further rock stability analysis. The combination of data derived from Map of slopes (Figure 2) and Map of maximum rock slope stability (Figure 5) using Idrisi image calculator was made (Figure 6). The process can be described with the equation (1):

$$RS = \frac{Slopes}{Max.\ rock\ stability} \quad (1)$$

To do the final map of stability (Figure 7) it was necessary to obtain the so called normalized values of relative slopes (Equation 2).

$$norm.\ value = 1 - \frac{Slopes}{Max.\ rock\ stability} \quad (2)$$

And finally using a Reclass command (Figure 8) 4 classes of stability were defined. The first: very stable (1–0.8), second: stable (0.8–0.5), third: conditionally stable (0.5–0) and the fourth: unstable with the values below 0.

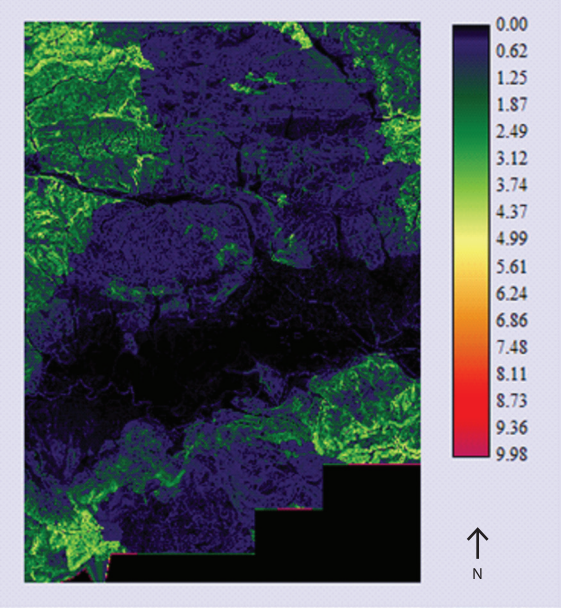

Figure 6: *Map of the relative slopes.*

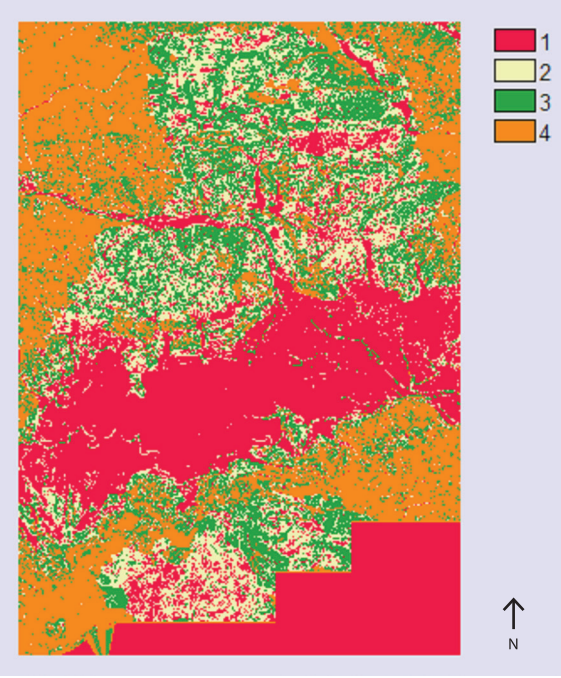

Figure 7: *Final stability map.*

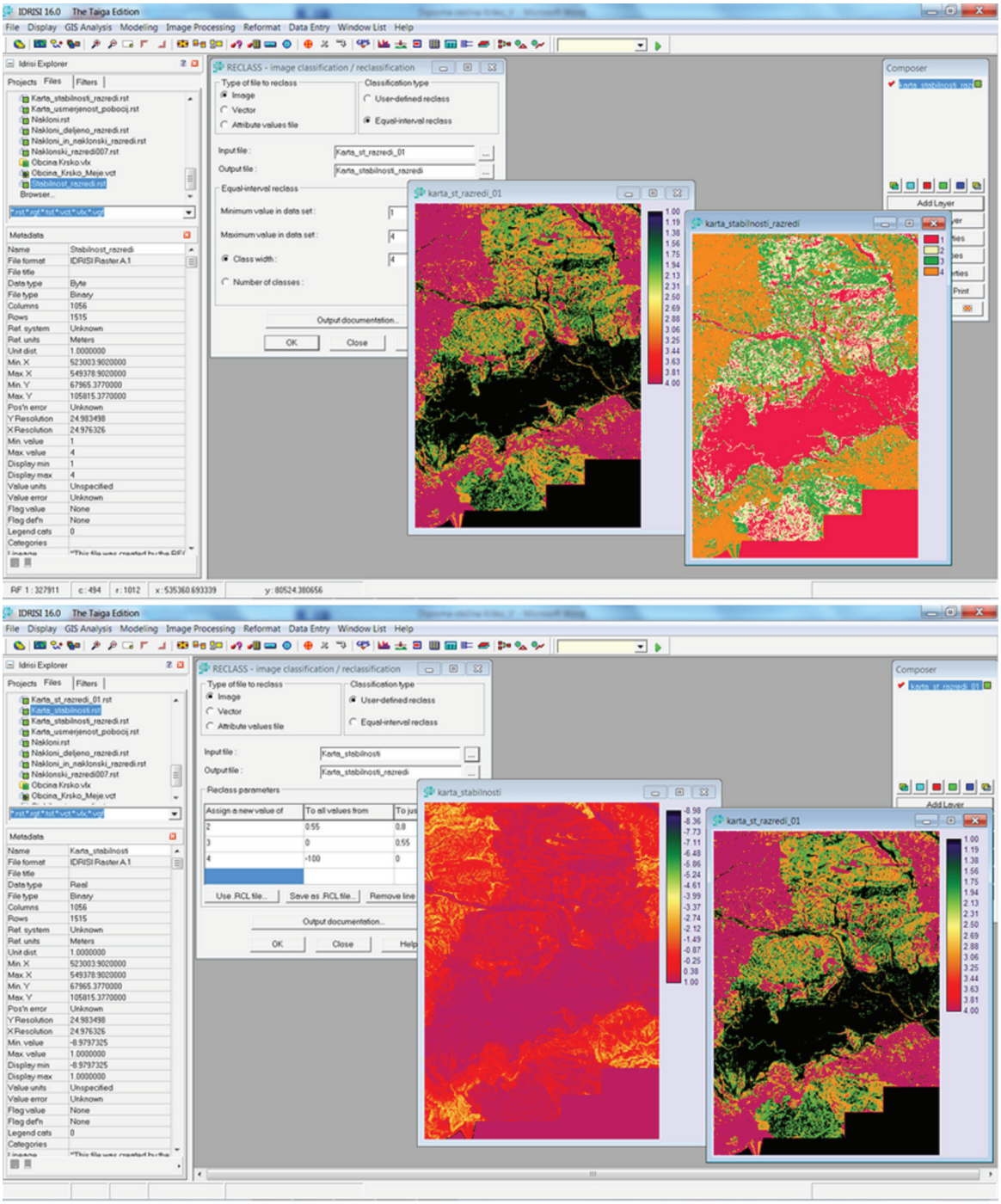

Figure 8: *View works by Idrisi- eat (making maps stability, maps stability classes and final maps stability with four classes).*

Conclusion

For the entire area of municipality of Krško an analysis of stability has been done using Idrisi GIS. Generally available public geological and topographical data were used for analyzing and processing described maps. It needs to be emphasized that during the process the data on intensity of rainfall were not included due to their absence on a smaller scale.

Because of the fact, that rainfall precipitations were not included in the process of slope stability analysis, the demands of stability were placed higher as they would be. Considering these facts the classes of stability were made on the more conservative approach than they would be in case the data on intensity of rainfall precipitations were available.

Analyses and maps like these presented are generally helpful especially for urbanists for creation of urban plans. At the same time they are very helpful for prediction of landslide occurrence especially in the populated areas in the period of heavy rainfall.

References

[1] Burrough, P., Mcdonnell, R. (1998): *Principles of Geographical Information Systems*, Oxford, 352 p.

[2] Šikić, K., Basch, O., Šimunić, A. (1979): Osnovna geološka karta M 1:100.000. *Tumač za list Zagreb*, ZGZ Beograd, arhiv GeoZS, HGEM.

[3] Pleničar, M., Premru, U., Herak, M. (1975): Osnovna geološka karta M 1:100.000. *List Novo Mesto*, 1977, ZGZ Beograd, arhiv GeoZS, HGEM.

[4] Pleničar, M. Premru, U. (1977): Osnovna geološka karta M 1:100.000. *Tolmač za list Novo Mesto*, ZGZ Beograd, arhiv GeoZS, HGEM.

[5] Raj, M., Sengupta, A. (2014): Rain-triggered slope failure of the railway embankment at Malda, India. *Acta Geotechnica*, 10.1007/s11440-014-0345-9.

[6] Zhang, G., Qian, Y., Wang, Z., Zhao, B. (2014): Analysis of Rainfall Infiltration Law in Unsaturated Soil Slope. *The Scientific World Journal*, 10.1155/2014/567250, pp. 1–7.

[7] Huang, C., Lo, C., Jang, J., Hwu, L. (2008): Internal soil moisture response to rainfall-induced slope failures and debris discharge. *Engineering Geology*, 10.1016/j.enggeo.2008.04.009, pp. 134–145.

[8] Ribičič, M. (1997): *Skrtipta tehnična geologija I*, Naravoslovnotehniška fakulteta, Univerza v Ljubljani.

[9] Ribičič, M. (2002): *Inženirska geologija skripta I*, Naravoslovnotehniška fakulteta, Univerza v Ljubljani.

Original scientific paper

Received: May 8, 2014
Accepted: December 22, 2014

Pore pressure detection and risk assessment of OBL oil field, offshore Niger delta, Nigeria

Ugotavljanje pornega pritiska in ocenitev tveganja v naftnem polju OBL v predobalnem delu Nigrove delte v Nigeriji

Matthew E. Nton*, Mosopefoluwa D. Ayeni
University of Ibadan, Department of Geology, Nigeria
*Corresponding author. E-mail: matthew.nton@mail.ui.edu.ng; ntonme@yahoo.com

Abstract

The Niger Delta is a prolific petroleum sedimentary basin in the Gulf of Guinea and is posed with a major challenge of overpressure development in many of its fields. Integrated study, utilising 3D seismic data and well logs from four wells, namely; OBL_1, OBL_2, OBL_4 and OBL_5 was carried out in the offshore Niger Delta. The study aims at evaluation of structural influences on pressure development, detection of overpressure zones and consequently examining the risk involved in drilling. Log signatures show decrease in density log values and corresponding increase in sonic log readings in wells OBL_1, OBL_2 and OBL_4. Well OBL_5, reveals increase density log values but decrease sonic log readings. Two regional and few minor faults observed to penetrate the overpressure zones were mapped out and integrated with the surfaces of the tops of the over pressured zones to generate three stratigraphic zones. Aside from under compaction mechanism, the regional faults penetrating the surfaces generated across the overpressure intervals could have influenced pressure development in the wells.

Key words: pore pressure, risk assessment, Niger Delta

Izvleček

Za vrsto naftnih polj v bogatem naftnem območju delte reke Nigra v Gvinejskem zalivu je značilen pojav visokih pritiskov. Na predobalnem delu Nigrove delte so izvedli kompleksno raziskavo na osnovi tridimenzionalne seizmike in karotažnih podatkov iz štirih vrtin, in sicer OBL_1, OBL_2, OBL_4 in OBL_5. Namen je bil oceniti vplive geološke zgradbe na razvijanje pritiskov, ugotoviti prostorsko porazdelitev pritiska in določiti stopnjo tveganja pri globinskem vrtanju. Karotažni podatki pričajo o manjšanju gostote in s tem povezanim naraščanjem zvočnih karotažnih meritev v vrtinah OBL_1, OBL_2 in OBL_4. Nasprotno so v vrtini OBL_5 ugotovili naraščanje vrednosti gostotnih in zmanjševanje zvočnih karotažnih meritev. Dva regionalna in nekaj manjših prelomov, ki potekajo čez pasove visokih pritiskov, so kartirali in povezali s podatki iz teh pasov ter opredelili tri stratigrafske cone. Ugotovili so, da utegnejo vplivati na razvijanje visokih pritiskov v vrtinah razen mehanizma kompakcije tudi regionalni prelomi, ki potekajo čez intervale pod visokim pritiskom.

Ključne besede: porni pritisk, ocena tveganja, Nigrova delta

Introduction

Drilling in an overpressure zone without taking precautionary measures can pose serious challenges. Hydrocarbon within the pore structures of sedimentary rocks tend to migrate from high pressured zones to relatively low pressured zones of a basin. However, if the formation is isolated or laterally sealed by impermeable clay or shale bed, such that pressure cannot be dissipated through connected pores to regions of low pressure, the formation remains under abnormally high pressure [1].

High pore pressure fluids are encountered worldwide in formations ranging in ages from Paleozoic to Cenozoic era and may be encountered in shale-sand sequences and/ or carbonate-evaporite sections at depths ranging from a few 100 m below the earth's surface to depths exceeding 6 100 m [2]. Therefore as exploration and exploitation of hydrocarbon move into deeper water environment, pore pressure analysis has become an important asset in the team's planning process [3].

Pore pressure analysis serves as a useful tool in many areas. In exploration, it is useful for detecting presence of hydrocarbon seals, mapping of hydrocarbon pathways, analysing trap configuration and for basin modelling. It also serves as a great tool in drilling as it helps in understanding mechanisms and influences of overpressure development on hydrocarbon accumulation [4]. For example; almost half of the gas production in the South Louisiana (Tertiary) in USA has been from a 600 m thick interval around the top of abnormal pressure zone [5]. Authors [6–8] established that the best zone to look for gas accumulation is in the over pressure region and in the formations above such area. In line with this assertion, it becomes necessary to critically examine pore pressure analysis as an integral procedure in exploration.

Like most petroliferous sedimentary basins in the world, the Niger Delta basin is posed with the challenge of overpressure development in most of its oil fields [9]. This study therefore attempts to evaluate the influence of structures on pore pressure development, detection of over pressure zones as well as examine drilling risks in the Niger Delta Basin, Nigeria.

Study area and regional geology setting

The study area, OBL field, lies between Latitudes 4° N–6° N and Longitudes 4° E–9° E in the south western offshore region of Niger Delta, Nigeria (Figure 1) and falls within the Chevron Nigeria Limited Concession. The base map showing location of study wells is shown on Figure 2.

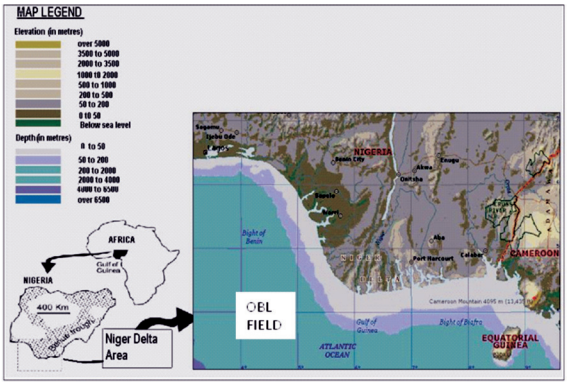

Figure 1: *Location map of the study area.* [Modified from 33, 34]

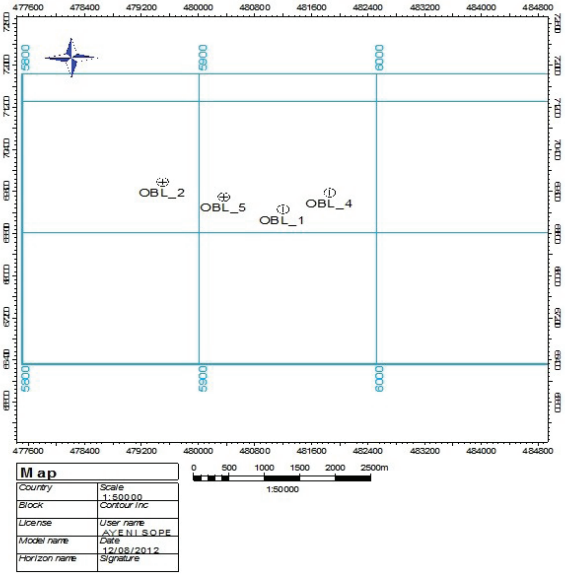

Figure 2: *Base map of the study area produced using Petrel software.*

In the Niger Delta, clastic wedges were deposited along the failed arm of a triple junction system. Originally, the Delta was formed during the break-up of the South American and African plates during the Late Jurassic [10, 11].

The two rift arms that followed the southwestern and southeastern coasts of Nigeria and Cameroon developed into the passive continental margin of West Africa; whereas, the third failed arm formed the Benue Trough which is located under the Gulf of Guinea, offshore Nigeria. After an early history of rift filling in the Mesozoic, the clastic wedge steadily prograded into the Gulf of Guinea during the Tertiary as drainage expanded into the African craton with consequent subsidence of the passive margin.

These upward- coarsening strata, offlapping the continental margin (Niger Delta), have been divided into three diachronous lithostratigraphic units, namely from oldest to youngest; the Akata, Agbada and Benin Formations (Figure 3; [12, 13]). The Akata Formation is the oldest of the units and comprised mainly marine shales which range in age from Eocene to Recent. The Agbada Formation overlies the Akata Formation and made up of alternating deltaic sandstones with shale. Its age ranges from Eocene to Recent. The Benin Formation is the youngest in the lithostratigraphic succession, and comprises sandstone, grits, claystone and streaks of lignite. Its age ranges from Oligocene to Recent.

The Niger Delta is subtly disturbed at the surface but the subsurface is affected by large scale synsedimentary features such as growth faults, rollover anticlines and diapirs [13, 14]. The structural style, both on regional and on field scale, can be explained on the basis of influence of the ratio of sedimentation to subsidence rates. The different types of structures are namely, simple non-faulted anticline rollover structures, faulted rollover anticline with multiple growth faults or anticline faults and complicated collapse crest structures [15]. Others are sub-parallel growth fault (k-block structures) and structural closures along the back of major growth faults (Figure 4)

Continental-margin collapse structures exert control on depositional and stratigraphic patterns within the Niger Delta clastic wedge (Figure 4). At the largest scale, these structures extend laterally along depositional strike nearly across the entire Niger Delta (hundreds of kilometers), defining ''mega structures'' [15] and associated ''depobelts'' that are tens of kilometers wide perpendicular to the shoreline [13, 16].

Six regional depobelts were deposited during the 25 million years from early Miocene to present. Depobelts tend to become finer-grained, laterally away from areas of most rapid delta progradation and basin ward away from areas of most rapid growth fault development [13].

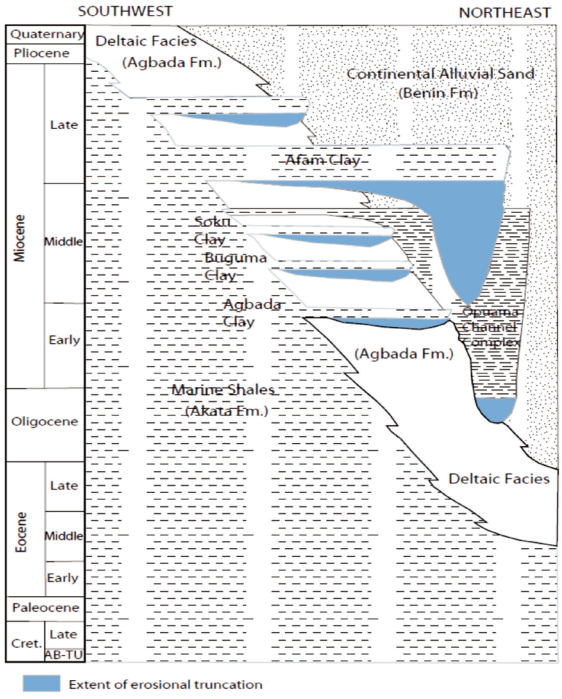

Figure 3: *Stratigraphic columns of the three formations in the Niger Delta [13].*

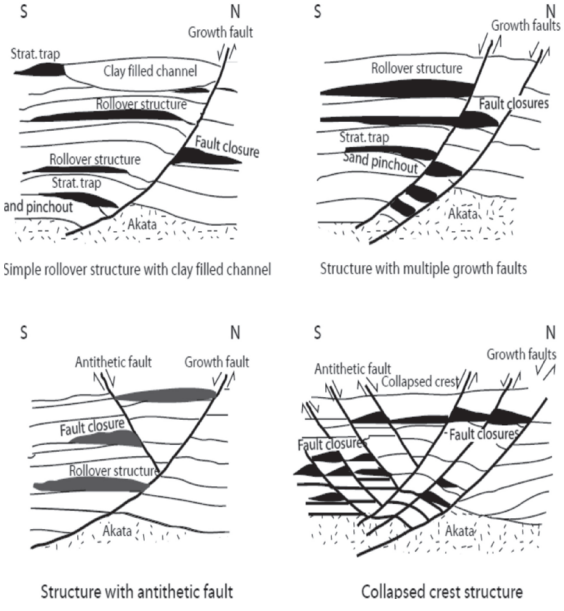

Figure 4: *Examples of Niger Delta oil field structures and associated trap types [13, 14].*

Smaller-scale faults and associated structural deformation accommodating collapse of depobelts tend to be more complex near the progradational axis of the delta than at its margins. This pattern of deposition continues still today, with extensional development of growth faults on the modern shelf and slope and compressional uplift near the toe of the slope [17, 18].

Materials and methods of study

Data Acquisition

The data set utilized in this study were acquired from Chevron Nigeria Limited, Lagos, Nigeria and comprised 3-D seismic volume in SEG-Y format and well logs in LAS format. Four wells namely, OBL_1, OBL_2, OBL_4 and OBL_5 with relative positions across 2D seismic survey as shown in Figure 2 were used. The composite logs utilized include among others; gamma ray, sonic, density and resistivity logs. The 3-D seismic volume on the other hand covers in-lines and cross lines ranges of 5 800 to 6200 and 1480 to 1700 respectively.

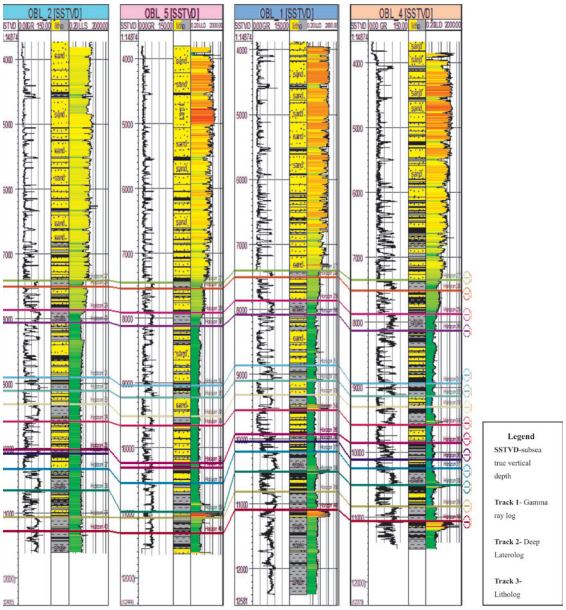

Figure 5: *Seismic and fault interpretations of the study area.*

Methods of Study

The methods of study entailed analysis of the data set by integration of petrel software with well logs and 3D seismic volume for stratigraphic and seismic interpretations. Lithology delineation and well correlation were done by observing gamma ray log signatures across the four wells. Similarly, readings on density and sonic logs were observed for overburden assessment and delineation of overpressure intervals respectively. Major and minor faults were picked at intervals of 10 on in lines and reflected on the cross lines across the planes on the seismic section (Figure 5). Synthetic seismogram was generated across the study wells and was utilized in seismic-well tie; thus, enhancing picking of seismic horizons across seismic section for generation of time structural contour maps.

Results and discussion

Lithology Identification and Well Correlation

In lithology identification across wells OBL 1, OBL 2, OBL 4 and OBL 5; increase and decrease from the baseline on gamma ray log were interpreted as shale and sand intervals respectively. The four wells located within the study area penetrated two distinct lithological zones; as depicted by the litholog on the second track of the wells (Figure 6). Zones with yellow and dotted patterns indicate sand unit, while zones with black and dash-line patterns indicate shale units.

Zone one (1) lies between 0 m and 1 676 m (0–5 500 ft) and is composed predominantly of sand unit. Based on the blocky signature of the gamma ray log and the predominantly sandy lithology, the zone could be inferred to be the Benin Formation [19]. Zone two (2) extends from 1 676 m (5 500 ft) to about 3 505 m (11 500 ft) which can be further delineated into upper and lower sections as reported by Doust and Omatsola [13]. The upper section (1 676 m (5 500 ft) to 2 286 m (7 500 ft)) shows thicker sand intervals compared to the alternating shale laminae which may be indicative of the upper Agbada paralic sequence based on the concept of [13]. The lower section on the other hand (2 286 m

(7 500 ft) to 3 505 m (11 500 ft)) has thicker shale units which increases with depth compared with the alternating sands. This zone characterised the Lower Agbada paralic sequence and is an indication of gradation into deeper portion of the basin [14]. It is assumed that the Akata Formation was not penetrated by the wells, probably due to its overpressured nature [20]; however, seismic section of the study area covers this zone (Figure 5).

From Figure 5, seismic reflection patterns between 0 ms and 1 350 ms two-way travel time; shows low amplitude, parallel and discontinuous types. Based on regional studies and seismic reflection patterns observed within this interval; the zone could be inferred to be the Benin Formation [19, 21]. Similarly, reflection patterns at interval between 1 350 ms and 2 800 ms two-way travel time shows high amplitude, parallel continuous reflection and fault zones which are diagnostic of Agbada Formation (Figure 5). Below this depth, chaotic reflections are observable which is inferred to be the Akata Formation (Figure 5).

Based on the relative positions of the wells on the base map on Figure 2, the wells were correlated in the order, OBL-2, OBL-5, OBL-1 and OBL-4 as shown on the well section in Figure 6. These wells seem to have some units with good correlations, based on the lithologies and similar log motifs, which may be indicative of similar depositional processes and environment [22].

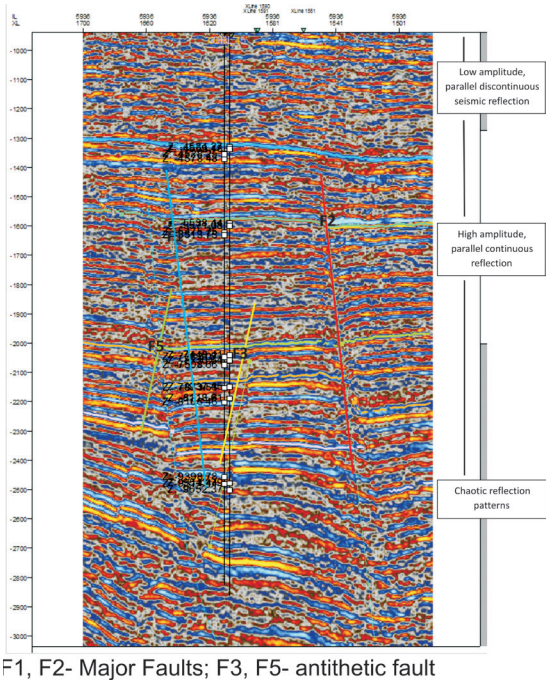

F1, F2- Major Faults; F3, F5- antithetic fault

Figure 6: *Lithology identification and well correlation.*

Detection of Overpressure Zones

Overpressure detection is based on the premise that pore pressure affects compaction-dependent geophysical properties like bulk density, velocity and porosity. An overpressured interval displays geophysical characters different from a hydrostatic reservoir such as decrease in density log values and increase in sonic log values [3]. Burst [6] established that the principal reason for this abnormality in velocity and density logs readings in shale units is attributed to the presence of trapped interstitial water in pore spaces of shale layers which could not escape before being sealed. Consequently, the trapped fluids within the pore spaces of the shale unit inevitably begin to support overburden pressure which slows down the mechanical process of compaction by increase in pore pressure which consequently resist further compaction [23]. Log signatures show decrease in density log values and corresponding increase in sonic log readings at delineated overpressure intervals of (42.57 m, 84.43 m, 34.75 m, 30.02 m, 58.81 m, 63.95 m, 75.50 m, 119.86 m, 93.56 m) in well OBL_1, (152.4 m, 31.12 m, 25.14 m, 25.67 m, 146.74 m) in OBL_2 and (35.84 m, 61.08 m, 21.28 m) in OBL_4 (Figures 7–9). Based on the findings of authors [6, 23], incomplete dewatering and compaction could have occurred in the sediments within the delineated overpressure intervals, resulting in slight increases in sonic log values and consequent reduction in density log readings at these intervals. However, density and sonic log readings in well OBL_5 reveal hydrostatic pressure condition as log readings show no deviation from normal, thus indicating a normal compaction trend (Figure 10). This view corroborates the findings of [24]. The intervals, depth to top and base of these overpressure zones in the study wells are shown on Table 1.

Arising from regional study, predominantly sandy lithology and depth of delineated overpressure zone in well OBL 4 (1 597.82 m (5 239 ft) to 1 619.10 m (5 311.68 ft), Figure 11)); the mechanisms or causes of overpressure development at such a relatively shallow depth may

not necessarily be due to under compaction. Tissot and Welte [25] established that the generation of biogenic gas by anaerobic bacteria which occurs during diagenesis at depths ranging from a few hundredths of metres to about 1 500 m or more in sedimentary rocks could be a possible cause of overpressure. However, the pressure posed by these sources may be short-lived. Gas generation at shallow depth could be the possible cause of overpressure observed at such a shallow depth in OBL_4. Similar observations have been made in the Gulf of Mexico, where a major cause of overpressure was formerly attributed to under compaction. A detailed study by Hunt [26] has shown convincing evidence that generation of gas by decomposition of organic matter from freshly deposited mud could be a major cause of overpressure development.

Risk Assessment

Influence of Faults on Overpressure Development

As aids to structural studies, two major faults and some minor faults picked at intervals of 10 across the seismic planes were mapped. The observed faults penetrate all the overpressure zones delineated. The major faults F1 and F2, show sub-parallel relationship and extend up to 70 % across the breadth of the region as shown on the structural time maps and 3D grids on Figures 11–16. Fault F3, an antithetic fault, extends to about 25 % across the map and lie discordantly against faults F1 and F2 (Figures 13–16).

Four surfaces, representing the tops of overpressure zones across wells OBL 1, OBL 2 and OBL 4 were mapped out (Figures 11, 13, 15 and 16) and observed to be penetrated by the regional, antithetic and synthetic faults. The colour legend indicates increasing depth from the top (red) to the base (purple).

Surface map 1 represents the top of overpressure zone1, delineated at depth of about 1 676 m (5498.7 ft) (Figure 11). The influence of the antithetic and synthetic faults at this depth seems to be unnoticed, compared with zones at greater depth. This could be interpreted to be the base and top of Benin and Agbada Formations. Such structures have been reported by Doust and Omatsola [13].

Table 1: *Depth to Top and Base of Overpressure interval in OBL_1, OBL_2 & OBL_4*

Well Name	Overpressure Zone (OVZ)	Top (m)	Base (m)	Thickness (m)
OBL_1	OVZ 1	884.49	927.06	42.57
	OVZ 2	1 379.66	1 464.09	84.43
	OVZ 3	1 674.70	1 709.45	34.75
	OVZ 4	2 256.04	2 286.06	30.02
	OVZ 5	2 464.64	2 523.44	58.81
	OVZ 6	2 644.48	2 708.43	63.95
	OVZ 7	2 775.95	2 851.44	75.50
	OVZ 8	2 911.83	3 031.69	119.86
	OVZ 9	3 212.33	3 305.89	93.56
OBL_2	OVZ 1	762.00	914.40	152.4
	OVZ 2	1 372.44	11 403.56	31.12
	OVZ 3	1 911.21	1 936.39	25.14
	OVZ 4	2 260.26	2 285.93	25.67
	OVZ 5	2 398.26	2 539.00	140.74
OBL_4	OVZ 1	1 356.91	1 392.75	35.84
	OVZ 2	1 460.39	1 521.47	61.08
	OVZ 3	1 597.82	1 619.10	21.28

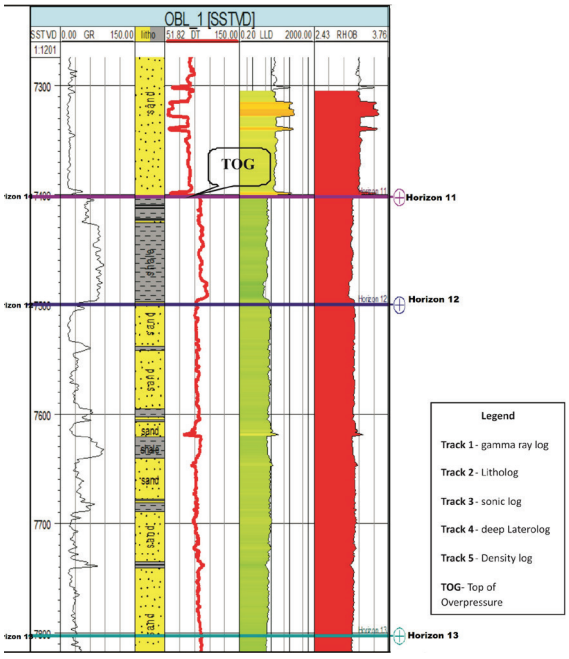

Figure 7: *Depth to top and base of overpressure interval in OBL_1 at depth* 2 256.04 m *to* 2 286.06 m.

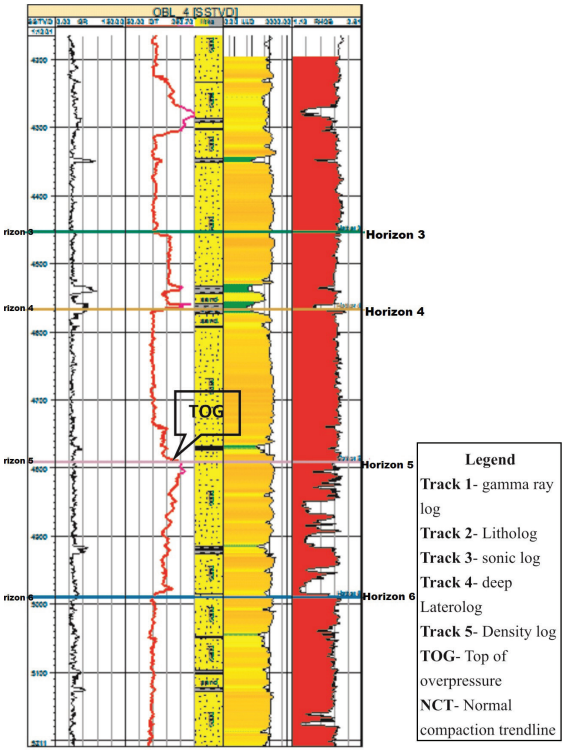

Figure 9: *Depth to top and base of overpressure interval in OBL_4 at depth* 1 597.82 m *to* 1 619.10 m.

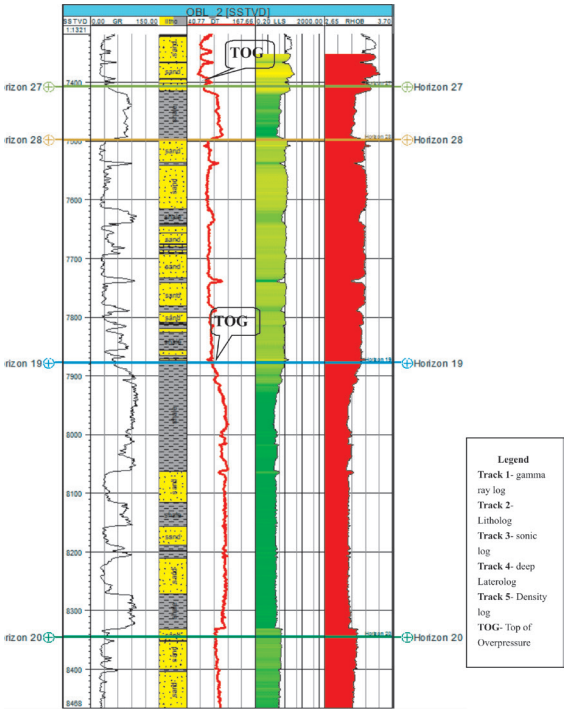

Figure 8: *Depth to top and base of overpressure intervals in OBL_2 at depths of* 2 260.22 m *to* 2 285.93 m *and* 2 398.26 m *to* 2 539.00 m.

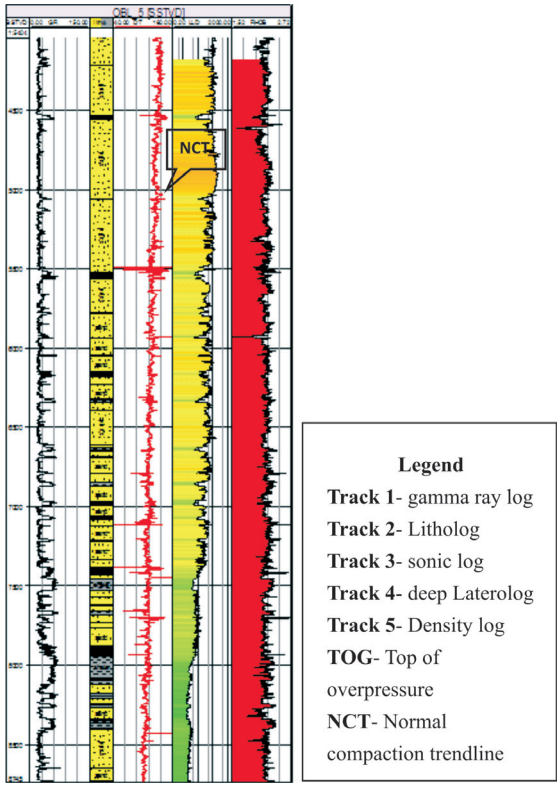

Figure 10: *Hydrostatic pressure condition in OBL-5.*

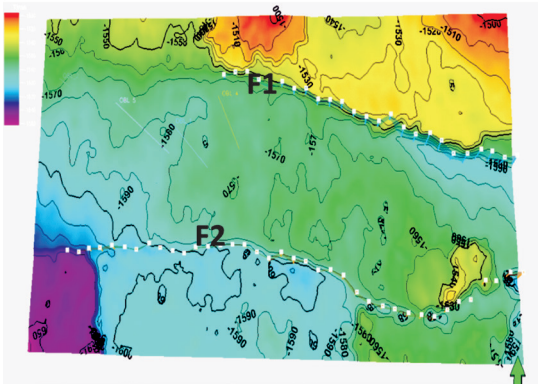

Figure 11: *Time structure map 1 - Top of overpressure zone1 above the faults at depth of about* 1 676 m.

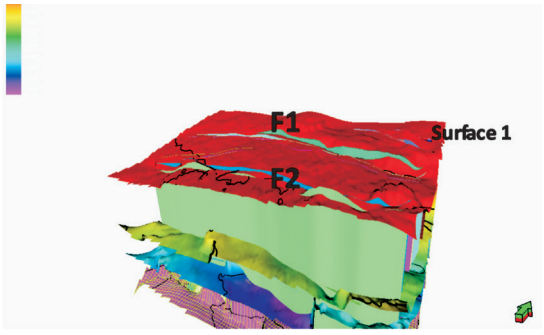

Figure 12: *3D grid showing geometry of faults and position of surface 1 across the faults.*

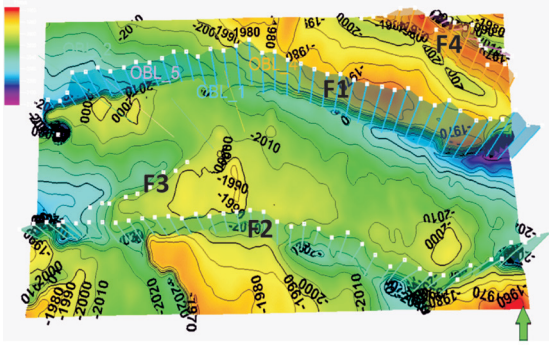

Figure 13: *Time structural map 2 - Top of over pressure zone 2 across the fault at depth of about* 2 257.54 m.

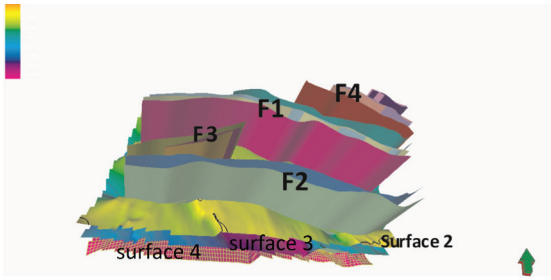

Figure 14: *3D grid showing geometry of faults and positions of surfaces 2, 3 and 4 across the faults.*

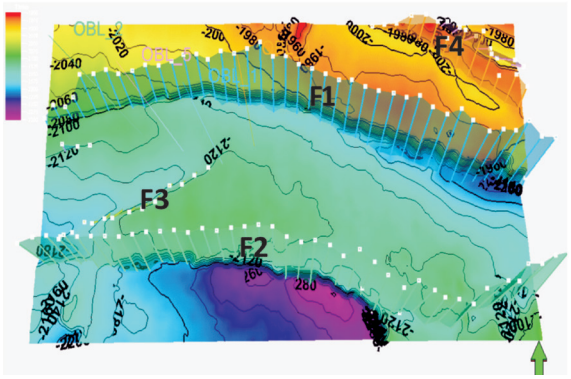

Figure 15: *Time structure map 3-Top of overpressure zone 3 across the fault at depth of about* 2 400.95 m.

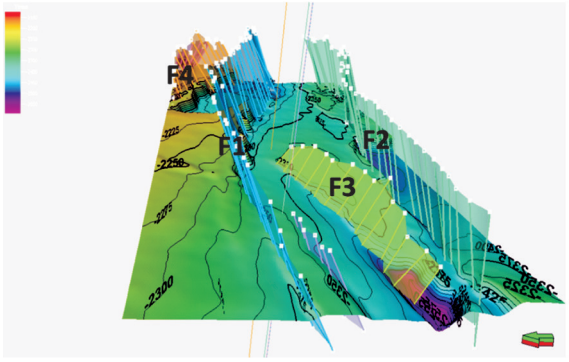

Figure 16: *Time structural map 4 - Top of over pressure zone 4 across the fault at depth of about* 2 744.73 m.

Surface maps 2 and 3 represent tops of overpressure zones 2 and 3, delineated at depths of about 2 257.54 m (7 406.63 ft) and 2 400.95 m (7 877.13 ft) respectively (Figures 13 and 15). These zones are penetrated more deeply by the regional growth faults, antithetic and synthetic faults; indicating that they have penetrated the Agbada Formation. The antithetic fault F3, plays a significant role in trapping of hydrocarbon within the reservoir especially, around the fault assisted closure as depicted by contour values of 2 010 to 1 990 on surface map 2 (Figure 13); as most of the wells were sunk around this closure.

Similarly, surface map 4, represents overpressure zone 4, delineated at depth 2 744.73 m (9 005.02 ft). The map shows a massively faulted zone penetrated by the regional growth faults F1& F2, antithetic fault F3 and synthetic faults F4 (Figure 16). This zone most probably represents the lower portion of the Agbada Formation because of its proximity to the over pressured Akata shale. Tuttle [20] proposed

the top of Akata shale as the most pressurized zone in the Niger Delta. It implies that pressure regime would be higher in this zone due to its proximity to Akata Formation than zones in shallower depths. Weber [28] reported the occurrence of overpressure in some sand units isolated by faults in the Gulf of Guinea. Similar occurrence may be observed in sand reservoirs in well OBL 1, at depth greater than 2 895 m (9 500 ft), which seem to be isolated due to the intense influence of the major, antithetic and synthetic faults; thus resulting in high pore pressure. There is need for caution when drilling such zones. Of all the wells sunk around the antithetic fault F3, all indicate overpressure interval except in OBL 5 well (Figure 10). The reason for this in OBL_5 may be due to the dissipation of pressure through the faults to shallower reservoirs up dip.

Faults are known to possess capacity for overpressure development where sealing units are present [9]. Studies have shown that the sealing ability of a fault is dependent on presence of over 25 % shale/clay smears along the fault [28]. Generally, the soft over pressured Akata shale in the Niger Delta basin rises up to fill the fault zones, thus enhancing the sealing capability of faults [28]. Apart from under compaction, overpressure development in wells OBL 1, OBL 2 and OBL 4 may also be attributed to sealing faults.

Summary and recommendations

Bore hole logs comprising gamma ray, density and sonic logs in four wells offshore western Niger Delta, Nigeria were integrated with 3D-Seismic section for pore pressure detection and structural studies. At the upper sections of the wells, high sand: shale ratio was delineated while at the deeper sections shale ratio increased. Two regional, antithetic and synthetic faults characterized the study area. They are observed to penetrate beyond the four overpressure intervals represented as surfaces and stratigraphic zones; thus showing the magnitude and influence of these faults in overpressure development within the study area. Of the four wells analysed, wells OBL_1, OBL_2 and OBL 4 showed overpressure intervals, while none is evident in well OBL_5. Owing to the relative positions of the wells across the regional fault and the rate of sedimentation in the Niger Delta, sealing faults that penetrated the basin could have also influenced overpressure development in the study wells.

Arising from pressure conditions in wells OBL_1, OBL_2 and OBL_4; evaluation of pore pressure development, well bore stability, formation strength and related uncertainties should be carried out prior to drilling other wells in the study area. It is suggested that a standard drilling, well design and well operation program should be aimed at ensuring safety of lives, environment and cost effectiveness [29]. As part of the assessment and releases for oil mining lease in developed nations, Canada precisely; pore pressure prognosis and formation strength assessment are important criteria that must be met [30].

Faults play an important role in hydrocarbon accumulation in the Niger Delta basin; as many of the hydrocarbon reservoirs within this basin are structurally controlled [19]. However, there may be some risk involved in drilling through the overpressure zones, penetrated by the regional faults F1, F2 and other minor faults. These faults may serve as conduits for pressure communication from deeper formations to shallower depths especially in gas -charged zones, thereby posing problems when a shallow formation is being drilled. Often times when this happens, the reservoir may not be encountered at all leading to loss of capital. Sometimes, wells may be re-cemented, to drill later or completely abandoned as reported by Mohamad [31] and O'Connor [32]. Fault gouges around the fault zones may cave-in into the well bore during drilling, thereby causing the drill string to get stuck due to the instability or incompetent nature of lithologies around the fault zones.

It is recommended therefore, that evaluation of pore pressure development, well bore stability, formation strength and related uncertainties should be carried out. Comprehensive studies on regional sealing potential of the faults across the basin would help reduce drilling risk and in planning of drilling activities.

Acknowledgements

The authors are grateful to Chevron Nigeria Limited for provision of data set for this study. We appreciate the invaluable assistance of Schlumberger Nigeria limited, in the provision of Petrel software for data interpretation. Many thanks to the anonymous reviewers for useful suggestions and criticisms that have improved the quality of this paper.

References

[1] Bradley, J. S. (1975): Abnormal formation pressure. *American Association of Petroleum Geologists Bulletin*, 59, pp. 957–973.

[2] Petroconsultants (1996): *Petroleum exploration and production database*: Houston, Texas, Petroconsultants. Inc. P.O Box 740619, Houston Tx 77274–0619.

[3] Roger, Y. A., Taylor, L. (2005): *Five things your pore pressure analyst won't tell you*. AADE National Technical Conference and Exhibition.

[4] Satinder, C., Alan, H. (2006): *Velocity determination for pore pressure prediction*. CSEG Recorder, April 2006.

[5] Leach, W. G., (1994): *Distribution of hydrocarbons in abnormal pressure in South Louisiana, U.S.A.* In: Fertl, W. H., Chapman, R. E. and Hotz, R. F.(eds) ; Studies in abnormal pressures, Elservier, 452 p.

[6] Burst, J. F. (1969): Diagenesis of Gulf Coast clayey sediments and its possible relation to petroleum migration. *American Association of Petroleum Geologists Bulletin*, 53, pp. 73–93.

[7] Dow, W. G. (1984): Oil source beds and oil prospect definition in the Upper Tertiary of the Gulf Coast. *Gulf Coast Assoc. Geol. Soc. Trans.*, XXXIV, pp. 329–339.

[8] Fertl, W. H., Chapman, R. E., Hotz, R. F. (1994): *Studies in abnormal pressure*. Elsevier, 453 p.

[9] Swabrick, R., O'Connor, S., Pindar, B., Lucas, O., Odesanya, F., Adedayo, A., Nwankwoagu, K., Edwards, A., Heller, J., Kelly, P. (2011): *Niger Delta pressure study-improved safety and exploration opportunities in deep water acreage*. 29th Annual International Conference & Exhibition of the Nigerian Association of Petroleum Geologists (NAPE), Book of Abstracts.

[10] Burke, K. (1972): Longshore drift, submarine canyons, and submarine fans in development of Niger Delta. *Bull. AAPG*, 56, pp. 1975–1983.

[11] Whiteman, A. (1982): *Nigeria: Its Petroleum Geology, Resources and Potential*. London, Graham and Trotman, Vols. 1 & 2, 394 p.

[12] Short, K. C., Stauble, A. J. (1967): Outline of Geology of Niger Delta. *American Association of Petroleum Geologists Bulletin*, 51, pp. 761–779.

[13] Doust, H., Omatsola, M. E. (1990): Niger Delta, In: Edwards J. D. and Santogrossi, P. A. (eds.), Divergent / Passive margin basins, AAPG. Memoir 48, Tulsa, *American Association of Petroleum Geologists*, pp. 239–248.

[14] Stacher, P. (1995): *Present understanding of the Niger Delta hydrocarbon habitat*. In: M. N. Oti and G. Postma (*eds*.), Geology of Deltas: Rotterdam, A. A. Balkema, pp. 257–267.

[15] Evamy, B. D., Haremboure, J., Kamerling, P., Knaap, W. A., Molloy, F. A., Rowlands, P. H. (1978): Hydrocarbon habitat of Tertiary Niger Delta. *Bull. American Association of Petroleum Geologists*, 62, pp. 277–298.

[16] Knox, G. J., Omatsola , M. E. (1989): *Development of the Cenozoic Niger Delta in terms of the escalator regression model and impact on hydrocarbon distribution*. In: W. J. M van der Linden; S. A. P. L. Cloetingh., J. P. K. Kaasschieter., W. J. E. van der Graff, J. Vandenberghe., J. van der Graff., J. Vandenberghe. and J. A. M. van der Gun (eds), KNGMGG Symposium on Coastal lowland Geology and Geotechnology, Proceedings: Dordrecht, The Netherlands, Kluwer Academic Publishers, pp. 181–202.

[17] Armentrout, J. M., Kanschat, K. A., Meisling, K., Tsakma, J. J., Antrim, L., Mconnell, D. R. (2000): *Neogene turbidite systems of the Gulf of Guinea continental margin slope, offshore Nigeria*. In: Bouma, A. H. and Stone, C. G. (eds). Fine grained Turbidite Systems. American Association of Petroleum Geologists Memoir 72 and SEPM, Special Publication, 68, pp. 93–108.

[18] Hooper, R. J., Fitzsimmons, R. J., Grant, N., Vendeville, B. C. (2002): The role of deformation in controlling depositional patterns in the South Central Niger Delta, West Africa. *Journal of Structural Geology*, 24, pp. 847–859.

[19] Weber, K. J. (1971): Sedimentological aspects of oilfields in Niger Delta. *Geologie en Mijnbouw*, 50 (3), pp. 559–576

[20] Tuttle, M. L. W., Charpentier, R. R., Brownfield, M. E. (1999): *The Niger Delta Petroleum System: Niger Delta Province, Nigeria, Cameroon, and Equatorial Guinea, Africa.* U.S. Department of the Interior, U.S. Geological Survey. Open-File Report 99-50-H.

[21] Orife J. M., Avbovbo, A. A, (1982): Stratigraphy and the unconformity traps in Niger Delta. *AAPG Memoir*, 32, 256 p.

[22] Sam, B. (2006): *Principles of Sedimentology and Stratigraphy*. 4th Edition, Prentice Hall, 663 p.

[23] Dutta, N. C., Borland, W. H., Leaney, S. W., Meehan, R., Nutt, L. W. (2002): *Pore pressure ahead of the bit: An integrated approach*. In: Alan R. Huffman and Glenn Bowers (Eds.), Pressure regimes in sedimentary basins and their prediction. AAPG Publication.

[24] Bowers, G. L. (2002): Detecting high overpressure. *The Leading Edge*, 21, 2, pp. 174–177.

[25] Tissot, B. P., Welte, D. H. (1984): *Petroleum Formation and Occurrence.* Springer-Verlag, Berlin, 518 p.

[26] Hunt, J. M., Whelan, J. K., Eglinton, L. B., Cathles, L. M. (1994): Gas generation—a major cause of deep Gulf Coast overpressures. *Oil and Gas Journal*, 92 (29), pp. 59–63

[27] Hart, B. S., Flemings, P. B., Desphande, A. (1995): Porosity and pressure: Role of compaction disequilibrium in the development of geopressures in a Gulf Coast Pleistocene Basin. *Geology*, 23, pp 45–48

[28] Weber, K. J., Daukoru, E. M. (1975): *Petroleum Geology of the Niger Delta*. Proceedings of the Ninth World Petroleum Congress, Volume 2, Geology: London, Applied Science Publishers Ltd, pp. 210–221.

[29] Alun, W. (1991): *Mud Logging Hand Book*. Englewood Cliffs, NJ: Prentice Hall, 531 p.

[30] Norsk SokkelS Konkuaranseposisson Standard (1998): Drilling and well completion operations D-010 Rev. 2, December 1998 Norsk standard, pp. 1–55.

[31] Mohamad, H., Jaini, N., Tajuddin., M. R. (2006): *Drilling of deep seated reservoir in high pressure regime in the North Malay Basin*. Petroleum Geology Conference and Exhibition, Book of Abstracts, Kualar Lumpur, Malaysia.

[32] O'Connor, S., Swabrick, R., Hoesni, J., Lahann, R. (2011): *Deep pore pressure prediction in challenging areas, Malay Basin, SE Asia.* Proceedings of Indonesia Petroleum Association, 35th Annual Convention and Exhibition

[33] Owoyemi, A. O. D. (2004): *The sequence stratigraphy of Niger Delta, Delta field, offshore Nigeria*. Unpublished M.S. Thesis: Texas A&M University, 88 p.

[34] Microsoft Encarta (2006): Reference Library Premium, DVD-ROM.

Professional paper

Received: January 30, 2015
Accepted: May 2, 2015

Evaluation of groundwater occurrences in the precambrian basement complex of Ilorin metropolis, southwestern Nigeria

Ocena virov podtalnice iz predkambrijske podlage območja deželne prestolnice Ilorina v jugozahodni Nigeriji

Anthony T. Bolarinwa[1,*], Sulyman Ibrahim[1]
[1]University of Ibadan, Department of Geology, Ibadan, Nigeria
*Corresponding author. E-mail: atbola@yahoo.com

Abstract

Surface water from the Asa and Agba dams, which hitherto supply water to Ilorin metropolis is inadequate, hence the need to supplement with water from boreholes. Forty two boreholes drilled into migmatites, granite gneiss and quartzite in Ilorin area were evaluated. Borehole data showed varied overburden thickness (1.00 m to 36.00 m). The static water level (SWL) contour map showed a radial groundwater flow pattern trending in the NE–SW and NW–SE directions, which is consistent with the structural trends in the area. Estimated yields of the boreholes ranged from 0.30 l/s to 2.75 l/s. Pumping/recovery test of four selected boreholes showed increase in productivity from granite gneiss (transmissivity, T = 11.42 m^3/d; permeability, K = 4.94 × 10^{-1} m/d) through migmatites (T = 13.4 m^3/d; K = 6.93 × 10^{-1} m/d) to quartzites (T = 17.56 m^3/d; K = 9.54 × 10^{-1} m/d). The groundwater occurrence in the area is adjudged to be moderately high. Strong correlation coefficients (+0.99) exist between Vertical Electrical Sounding (VES) and borehole log indicating that the success of borehole in the area depends strongly on production of VES report. Based on this study, minimum borehole depth of 33 m is recommended for the area.

Key words: groundwater, basement complex, borehole yield, aquifer, Ilorin

Izvleček

Površinska voda iz zajezitev Asa in Agba ne zadostuje potrebam deželne prestolnice Ilorina, zato iščejo dodatne vodne vire z vrtanjem. Na območju Ilorina so izvrtali dvainštirideset vrtin v migmatitih, granitnem gnajsu in kvarcitu. Debelina prevrtanega preperinskega pokrova je med 1 m in 36 m. Iz razporeda plastnic na karti statične gladine podtalnice je videti, da gre za radialni vzorec tečenja podtalnice v smereh NE–SW in NW–SE, kar tudi ustreza geološki zgradbi območja. Ocenjene izdatnosti vrtin so med 0,30 l/s in 2,75 l/s. Črpalni preizkusi v štirih izbranih vrtinah pričajo o naraščanju izdatnosti od granitnega gnajsa (prevodnost, T = 11,42 m^3/d; prepustnost, K = 4,94 × 10^{-1} m/d) prek migmatitov (T = 13.4 m^3/d; K = 6.93 × 10^{-1} m/d) do kvarcitov (T = 17,56 m^3/d; K = 9,54 × 10^{-1} m/d). Vire podtalnice na preiskovanem območju so ocenili za zmerno izdatne. Visoki korelacijski koeficient (+0,99) med rezultati vertikalne električne karotaže (VES) in karotažnih profilov vrtin priča o močni povezavi uspešnosti vrtin od opravljene vertikalne električne karotaže. Iz raziskave izhaja, da je na tem območju priporočljiva minimalna globina vrtanja 33 m.

Ključne besede: podtalnica, kamnine podlage, izdatnost vrtine, vodonosnik, območje Ilorina

Introduction

Rapid population growth, due to rural-urban migration resulted in increase in the number of commercial and industrial activities in Ilorin area. This population growth in turn is responsible for the rapid increase in water demand and persistent water shortage in the area. Water supply from Asa and Agba dams could no longer meet the water demand of the populace contrary to the report of Oluyide [1], which stated that Ilorin area has excess water and that boreholes are unnecessary. As a result of water inadequacy, the State Government decided to look for additional and sustainable water sources that can supplement water supply from the existing dams through the introduction of various water supply schemes. These water supply schemes include drilling of numerous boreholes. However, as laudable as this policy seems, it was not supported by adequate geological and hydrogeological baseline data, which include information on the degree of weathering and fracturing of the crystalline basement rocks and hence, the high number of low yield and outright unproductive wells reported in the area. Alao [2] investigated the occurrence of lateritic brick-clay within the weathered profiles at Okelele/Dada of Ilorin Local Government area. It is believed in this study that the occurrence of such interstitial clay in large quantity within the weathered basement could result in low yields.

Other published works on the groundwater situations of the Ilorin area include those of Oyegun [3] who identified water resources, development and management strategies in Kwara State, including Ilorin, based on a few borehole data, which is grossly inadequate to generalize the groundwater situation of the study area. Olasehinde [4] and Olasehinde and Taiwo [5] compared the geological and geophysical exploration methods for groundwater in the basement complex of the study area. They were able to establish positive relationship between the two exploration techniques. Offodile [6] studied the groundwater occurrence in basement complex of Nigeria with reference to Pampo, a village in the southern outskirts of the study area. The study was based on pumping test of a single borehole. A single borehole is considered inadequate to study the groundwater potential of such a large area.

The objectives of this study were to determine the hydrogeological characteristics of the rock units within Ilorin metropolis, to evaluate the influence of geology on the groundwater flow and development in the area, to assess the groundwater occurrence with a view to determine whether the groundwater of Ilorin metropolis could serve as additional and sustainable water supply sources.

The Study Area

Ilorin area lies between longitude 4° 30' E–4° 37' E and latitude 8° 26' N–8° 33' N (Figure 1). It covers an approximate area of 200 km^2. The sampling areas include Agbo-Oba in the west, Airport in the southwest, Sobi Hill in the northwest, Oyun in the northeast, Tanke and Fate in the east. The study area is underlain by the Precambrian basement rocks, which comprise of migmatite, granite gneiss and quartzite. The area falls between semi arid in the north and sub-humid in the south. It is characterized by two main seasons: Wet season – (March – Mid October) and Dry season – (Mid October – March). Rainfall is moderate with annual average of 1 250 mm. Humidity is relatively low. It is about 50 % between June and August. The annual mean temperature is 27 °C.

The area is well drained by various streams and their tributaries. The distributaries show dendritic drainage pattern. The main rivers are Asa and Agba Rivers, while minor rivers include Oyun and Aluko rivers. The terrain is undulating and dissected by rivers and streams. The highest altitude is about 1 200 m above sea level corresponding to the top of Sobi Hill (migmatite), while along major streams the altitude is about 250 m above sea level. The vegetation cover is basically Guinea savannah with ruminant tropical forest.

Geology and Hydrogeology of the Area

The Ilorin area is part of the Precambrian basement complex of southwestern Nigeria (Figure 1). The main rock types that characterize the geology of the area are migmatite-gneiss, granite gneiss and quartzite (Figure 2). Intrusions of pegmatite, dolerite dykes and quartz veins cut across the major rock units in the area. The migmatite-gneiss

complex is presumably the oldest rock in the basement complex of Nigeria [7]. It is the most abundant and the most widespread in the study area. It is foliated and jointed. The migmatite is closely associated with quartzite in the southeastern part. Granite gneiss extends from the eastern to the southeastern part. Mineral components of the migmatite and granite gneiss are mainly microline, quartz, plagioclase, biotite and muscovite. The constituent quartz and few mica grains in the quartzite of the area are recrystallised with interlocking mosaic textures. Other rock types include pegmatite and quartz veins within the migmatite and the granite gneiss. They are of few millimeters to about a metre. They are concordant or discordant unmetamorphosed rock bodies cutting across foliation planes in the gneisses.

These crystalline basement rocks are generally older than 500 million years and contain negligible amount of groundwater when not weathered or fractured. However, significant aquifers may develop within those areas with thick weathered overburden and most importantly, fractured bedrock [8]. Annor and Olasehinde [9] noted that the basement complex of Ilorin area has varied weathered horizons as well as fractured rocks. The fractured rocks represent the deeper aquifers, which are overlain by shallow porous lateritic soil cover. Although, these rocks have low groundwater content, places abound where there are thick weathered, gritty overburden and fractures which aid groundwater accumulations. Areas with high clay contents are usually characterised by low permeability and poor aquifer conditions. Pegmatite and quartz vein filled fractures in the migmatite and quartzite of Ilorin metropolis are generally NS and NW–SE while those in the granite gneiss are NS and NE–SW (Figure 2).

Methodology

Collection of hydrogeological data from 42 boreholes within the three main rock types, namely migmatite, granite gneiss and quartzite in Ilorin metropolis were undertaken. Thirty seven (37) of the boreholes were sited within migmatite, four (4) within granite gneiss and one (1) within quartzite. The hydrogeological data were collected in November 2005 when the boreholes were completed. Location and elevation of each of the borehole above sea level was measured with Geographical Positioning System (GPS) equipment [10]. The static groundwater level in the boreholes was determined using dipper water level indicator. Computation of static water level, above sea level (SWL_{asl}) from static water level, below ground level (SWL_{bgl}) and elevation above sea level (E_{asl}) were carried out.

Depths to basement, depth to the overburden and basement aquifers, as well as, aquifer thickness were extracted from borehole log reports. Also, Vertical Electrical Sounding (VES) data on depth-to-basement were taken to facilitate comparison

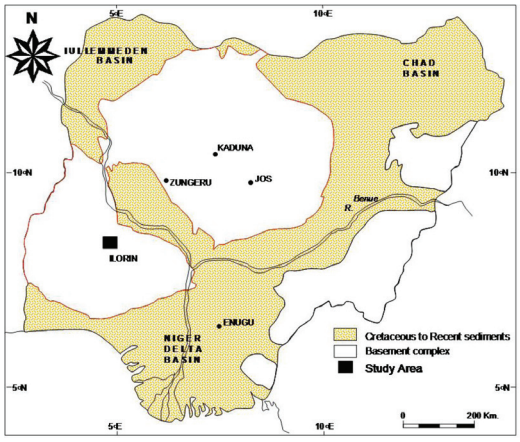

Figure 1: *Generalised geological map of Nigeria showing the location of Ilorin area.*

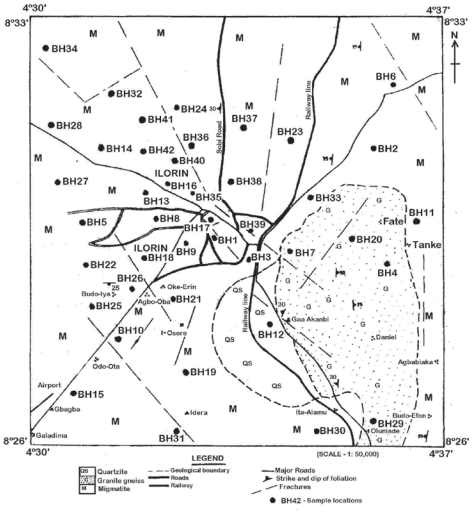

QS - Quartzite
G - Granite gneiss
M - Migmatite

LEGEND
Geological boundary
Roads
Railwa

Major Roads
Strike and dip of foliation
Fractures
BH 42 - Sample locations

Figure 2: *Geological and structural map of Ilorin area showing borehole locations (BH1-BH42) .*

with borehole log. Yields from selected boreholes were estimated. Correlation of the borehole parameters with estimated yields and Vertical Electrical Sounding (VES) report with borehole-logs were carried out. Computation of aquifer parameters [Transmissivity (T) and Permeability (K)] from constant pumping/recovery test was carried out, for 8 h, using 1HP submersible pump. The static water levels (above sea level) (SWL_{asl}) for the 42 boreholes were computed and used to produce *SWL* contour map which was used to determine the groundwater flow direction in the study area. The pumping and recovery test data are presented in supplementary Tables S1–S8 and Figures S1–S10.

Results and Discussion

The borehole data are presented in Table 1 with the summary in Table 2. The geological and structural map of the area is presented in Figure 2. Summary of the pumping and recovery tests are presented in Table 3. Results of correlations of the borehole parameters are presented in Table 4. Other details are presented as supplementary Tables and Figures.

The depth of boreholes in the study area ranged between 19.50 m and 67.60 m with mean value of 33.59 m (Table 1). Borehole productivity in the area is not strictly a function of the total depth drilled as reflected in some deep boreholes (> 30 m) with low yield (BH15, 23, 28 and 30), and some shallow boreholes (< 30 m) with high yield (BH 13, 25, and 36) (Table 1). However, it is recommended that the depth of borehole to be drilled in the area must not be less than 33.00 m so that the borehole can penetrate the fractured basement and to create sufficient space for water accumulation within the hole. The *SWL* contour map showed a radial groundwater flow direction in the study area (Figure 3). It is multidirectional, trending in the NE-SW and NW-SE directions. This is consistent with the structural trends in the area (Figure 2).

Depth to basement varies between 1.00 m and 36.0 m with a mean value of 12.23 m (Tables 1 and 2). Borehole log report shows that twenty four of the forty two boreholes have overburden thickness of less than 10 m (Table 1). The overburden is characterized by lateritic and clayey formations which constitute an aquitard. Aquifer thickness is between 3.00 m and 30.00 m with a mean value of 12.03 m (Table 2). Most of the aquifers occurred in the saprolite of the weathered zone and the fractured basement. However, in the northwestern part of Ilorin metropolis around Okelele and Dada area (BH 35 and BH 38), reasonable amount of groundwater occur within the thick overburden on highly fractured migmatite. Estimated yield (Tables 1 and 2) ranged between 0.30 l/s and 2.75 l/s. This determines how successful a borehole is, and showed the maximum rate a borehole can sustain reasonable drawdown in the study area. The average value of 1.60 l/s; suggested a high groundwater potential for the study area. This is in agreement with the yield of 1.5–20 l/s obtained by Offodile [6] for aquifers in some crystalline basement rocks in Nigeria.

Results of the Pumping/Recovery tests (Table 3) showed transmissivity (T) values between 9.11 m^3/d and 17.56 m^2/d, averaging 13.43 m^3/d, and permeability (K) values between 4.52×10^{-1} m/d and 9.54×10^{-1} m/d with mean value of 6.65×10^{-1} m/d. Generally, the pumping/recovery test of the four (4) selected boreholes showed increase in borehole productivity from granite gneiss (T = 11.42 m^3/d; $K = 4.94 \times 10^{-1}$ m/d) through migmatites (T = 13.4 m^3/d; $K = 6.93 \times 10^{-1}$ m/d) to quartzite (T = 17.56 m^3/d; $K = 9.54 \times 10^{-1}$ m/d). The highest values of T (17.56 m^3/d) and K (9.54×10^{-1}m/d) occurred in the borehole drilled through quartzite reflecting the highly fractured nature of the metasediment, while the lowest values (T = 9.11 m^3/d and $K = 5.35 \times 10^{-1}$ m/d) are obtained in boreholes within the granite gneiss (Table 3). It can therefore be said that borehole productivity increases from granite gneiss through migmatite to quartzite in the study area. However, value for storativity could not be obtained due to lack of observation wells to be used for the pumping / recovery tests.

Borehole parameters are correlated in order to obtain baseline data and relationships, which can serve as a guide to borehole site and drill depth recommendations that could be applied in related basement areas. Correlation results (Table 4) showed very high positive values for Yield/T (0.96), and moderately high positive value for Yield/Aquifer thickness (0.50). These showed very strong and strong dependence of yield on

transmissivity and aquifer thickness respectively. However, for Yield/Total depth and Yield/depth to basement, the correlation values are low (0.26 and 0.28 respectively). This indicated weak dependence of yield on the two parameters. Yield/*SWL* gave an extremely low correlation value of +0.004, which suggested borehole yield does not depend on *SWL* in the area. Correlation of VES data with Borehole-logs also gave a very high positive value of 0.99. This confirmed that the VES results obtained from the area are very reliable and can be used for borehole location.

Table 1: *Borehole Data of Ilorin metropolis (Source: Field Survey, 2005)*

BH No.	Borehole location	$SWL_{(bgl)}$	$SWL_{(asl)}$	BH depth	Depth to basement (m)		Depth to aquifer	Aquifer thickness	Estimated yield
		(m)	(m)	(m)	BH Log	VES	(m)	(m)	(l/s)
BH 1	Ikokoro street	9.50	290.50	46.60	5.00	6.50	15.00	30.00	2.00
BH 2	Sango Area	8.20	301.80	34.60	19.00	22.50	22.00	9.00	1.50
BH 3	Union Bank	11.50	288.10	53.60	2.00	5.00	39.00	12.00	2.20
BH 4	Tanke	5.00	305.00	46.60	15.00	16.00	15.00	21.00	1.50
BH 5	Ilt Kewu	8.00	312.00	37.60	9.00	10.00	12.00	21.00	1.80
BH 6	Oyun	7.40	307.60	37.60	9.00	10.00	9.00	22.00	1.90
BH 7	Golf Club	16.90	295.10	67.60	3.00	6.00	42.00	5.00	2.40
BH 8	Pakata	6.30	323.70	26.00	9.00	10.00	9.00	6.00	0.30
BH 9	Ile Seriki	7.60	317.40	27.60	8.00	12.00	11.00	16.00	1.50
BH 10	Olorunshogo	5.90	304.00	21.00	15.00	16.00	15.00	8.00	1.30
BH 11	Tanke Iledu	5.90	299.10	36.00	15.00	17.00	15.00	18.00	1.75
BH 12	Gaa Akanbi	4.30	325.70	33.00	3.00	5.00	33.00	12.00	2.70
BH 13	Alore Primary School	5.30	319.70	27.00	18.90	33.00	21.00	9.00	2.00
BH 14	Ile Oloje	7.20	303.80	26.25	24.00	21.00	18.00	10.00	1.50
BH 15	Airport	5.00	357.00	34.00	24.00	28.00	25.00	4.00	1.25
BH 16	Ile Iya Balogun	7.30	316.70	32.00	6.00	9.00	6.00	15.00	1.50
BH 17	Ile Jimba	4.50	313.50	26.00	6.00	8.00	6.00	12.00	1.90
BH 18	Ode Alfa Nda	7.90	315.10	38.20	18.00	22.00	18.00	12.00	2.00
BH 19	Parliament Village	6.00	339.00	21.50	6.00	7.00	6.00	7.00	1.30
BH 20	Kitibi's residence	5.40	326.6	30.00	15.00	17.50	20.00	15.00	2.10
BH 21	C.A.C. Taiwo road	6.25	303.75	33.00	15.00	16.00	15.00	8.00	2.00
BH 22	Ojatuntun	5.00	300.25	30.75	1.00	1.50	3.00	27.00	2.75
BH 23	Railway station	11.30	239.70	38.00	3.00	4.00	3.00	15.00	1.00
BH 24	Akerebiata	5.80	300.20	29.00	12.00	14.00	12.00	12.00	1.95
BH 25	Baboko/Eruda	7.50	297.50	26.00	15.00	16.00	15.00	12.00	1.80
BH 26	Agbo-Oba	7.00	293.00	19.50	6.00	6.50	6.00	15.00	1.80
BH 27	Popo Giwa	4.00	326.00	21.00	6.00	7.50	12.00	9.00	1.50
BH 28	FGC, Ogigi	6.00	343.00	40.00	7.00	9.00	10.00	6.00	1.00
BH 29	Olunlade	3.00	337.00	38.00	10.00	12.50	20.00	17.00	1.35
BH 30	Ita Alamu	8.00	329.00	40.00	8.50	10.00	10.00	3.00	0.40
BH 31	Idera	4.00	303.00	31.00	7.00	9.00	12.00	6.50	1.25
BH 32	Oloje Housing Estate	4.00	316.00	31.00	5.00	6.00	6.00	18.00	2.00
BH 33	G.S.S. Ilorin	6.80	293.20	22.00	6.00	8.50	6.00	3.00	0.35
BH 34	Oko Olowo Garage	8.00	321.00	33.00	7.00	8.00	10.00	8.00	1.40
BH 35	Okelele	5.30	319.70	27.00	18.00	19.00	21.00	9.00	1.50
BH 36	Banni area	5.75	318.25	24.00	9.00	10.00	9.00	9.00	1.90
BH 37	Gaa Osibi	7.00	329.00	33.00	8.50	10.00	15.00	5.00	1.45
BH 38	Dada	6.00	324.00	29.00	27.00	28.00	23.00	12.00	1.60
BH 39	Ita Kudimo	6.00	298.00	32.00	7.00	8.00	22.00	6.00	1.20
BH 40	Ile Ikare Okelele	9.00	324.00	39.00	36.00	38.00	24.00	12.00	1.50
BH 41	Ile Gbongbon Okelele	7.00	328.00	33.00	33.00	34.00	18.00	15.00	1.30
BH 42	Ile Oniponmo Okelele	8.00	322.00	39.00	24.00	26.00	24.00	12.00	1.60

$SWL_{(bgl)}$ - Static Water Level $_{(below\ ground\ level)}$, BH – Borehole,
$SWL_{(asl)}$ - Static Water Level $_{(above\ sea\ level)}$, VES – Vertical Electrical Sounding

Table 2: *Summary of Borehole data of Ilorin metropolis*

	$SWL_{(bgl)}$	$SWL_{(asl)}$	BH depth	Depth to basement (m)		Depth to aquifer	Aquifer thickness	Estimated yield
	(m)	(m)	(m)	BH Log	VES	(m)	(m)	(l/s)
Minimum	3.00	288.50	19.50	1.00	1.50	3.00	3.00	0.30
Maximum	16.90	357.00	67.60	36.00	38.00	42.00	30.00	2.75
Mean	6.80	313.84	33.59	12.23	14.15	15.86	12.03	1.60
Standard deviation	2.66	15.63	9.99	8.06	8.30	11.39	6.43	0.52

$SWL_{(bgl)}$ - Static Water Level (below ground level), BH – Borehole,
$SWL_{(asl)}$ - Static Water Level $_{(above\ sea\ level)}$, VES – Vertical Electrical Sounding

Table 3: *Summary of the results of constant-rate pumping and recovery tests*

Pumping recovery test No.	BH No.	Rock type	*T*-value from PT (m^3/d)	*T*-value from RT (m^3/d)	Average *T* (m^3/d)	*K*-value from PT ($\times 10^{-1}$ m/d)	*K*-value from RT ($\times 10^{-1}$ m/d)	Average *K* ($\times 10^{-1}$ m/d)
1	BH 29	Granite gneiss	8.99	9.24	9.11	5.28	5.43	5.35
2	BH 4	Granite gneiss	13.07	14.38	13.72	4.35	4.7	4.5
3	BH 10	Migmatite	11.48	16.21	13.84	6.37	9.00	7.68
4	BH 24	Migmatite	11.39	14.54	12.96	5.42	6.92	6.17
5	BH 12	Quartzite	16.37	18.75	17.56	9.09	10.00	9.54
		Minimum	8.99	9.24	9.11	4.35	4.70	4.52
		Maximum	16.37	18.75	17.56	9.09	10.00	9.50
		Mean	12.26	14.62	13.43	6.10	7.21	6.65

BH = Borehole, PT = Pumping test, RT = Recovery test, *T* = Transmissivity, *K* = Permeability

Table 4: *Table of correlation of borehole data from Ilorin metropolis*

S/No	Parameter Correlated	Coefficient of correlation	Implications
1	Yield/Total depth	0.26	Yield weakly depends on the total depth.
2	Yield/Aquifer Thickness	0.50	Yield moderately depends on aquifer thickness.
3	Yield/Depth to basement (Overburden thickness)	0.28	Yield weakly depends on overburden thickness.
4	Yield/SWL	0.004	Yield is almost independent of static water level.
5	Yield/Transmissivity	0.96	Yield depends strongly on transmissivity of aquifer.
6	Borehole log/VES	0.99	Detection of subsurface structures strongly depends on VES.

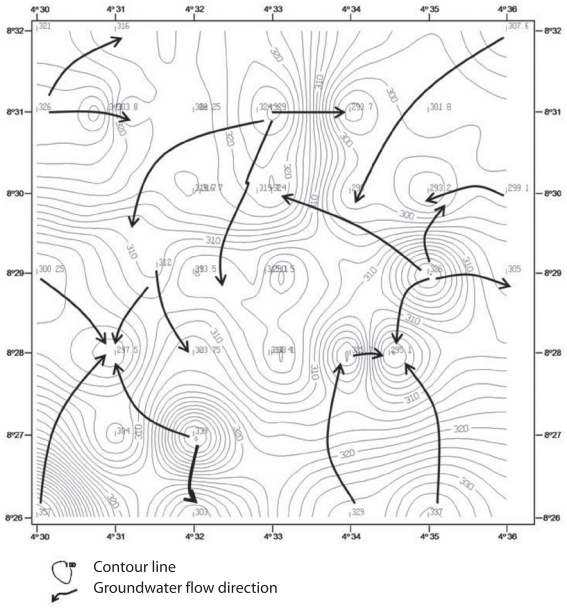

Figure 3: *Static Water Level (SWL) above sea level Contour map of the Study Area showing the groundwater flow direction.*

Conclusions

Groundwater occurred in the weathered and fractured zones of the basement rocks underlying Ilorin metropolis. The groundwater flow direction is generally radial and multidimentional, trending mainly in the NE–SW and NW–SE directions, which is consistent with the fracture pattern in the area. Borehole productivity increases from granite gneiss through migmatite to quartzite. It can be concluded that the groundwater potential of Ilorin metropolis is moderately high, judging from the values of the aquifer parameters, transmissivity (*T*), permeability (*K*) and yield, which are consistent with data of good aquifers in the crystalline basement complex of Nigeria.

Observation wells should be used during pumping test in order to determine average storativity of the aquifers. Further studies should involve pumping of borehole water for several days to reach equilibrium. This would permit assessment of the groundwater using specific capacity rather than aquifer parameters. The groundwater of Ilorin area can be harnessed through boreholes to support the existing dams however, computation of safe yield is necessary for proper groundwater planning, development and management.

Acknowledgements

The authors acknowledged the support of the Director, Kwara State UNICEF (WES) Project for the permission granted to undertake the study. Mr. M. A. Oyeyipo (H. O. D, Water Supply Department), Mr. S. O. Aina (UNICEF, WES Project, Ilorin) and Professor P. I. Olasehinde (Department of Geology, Federal University of Technology, Minna, are also appreciated for making some of the reference materials used in this work available. Comments and suggestions of the anonymous reviewers are appreciated.

References

[1] Oluyide, P. O., Nwajide, C. S., Oni, A. O. (1998): *The Geology of Ilorin Area.* Nigerian Geological Survey Agency (N. G. S. A.), Bulletin 42, Explanation of the 1:250,000 sheet 50 (Ilorin), 84 p.

[2] Alao, W. A., Hussein, A. Y., Olatunde, S. O. (1982): *Geological investigations on brick-clay deposits at Okelele/Dada, Ilorin Local Government Area, Kwara State.* Unpublished report. Geological Survey of Nigeria (GSN), 10 p.

[3] Oyegun, R. O. (1983): *Water Resources in Kwara State, Nigeria.* Occasional paper, Kwara State Water Corporation. Matanmi Printing and Publishing Company Ltd, 73 p.

[4] Olasehinde, P. I. (1999): An Integrated geological and Geophysical exploration techniques for groundwater in the basement complex of West Central Nigeria. *Water Resources*, *Journal of Nigerian Association of Hydrogeologists,* 11, pp. 46–49.

[5] Olasehinde, P. I., Taiwo, K. A. (2000): A correlation of Schlumberger Array Geoelectrical Log with borehole Lithologic Log in the southwestern part of the Nigeria basement complex terrain. Water Resources, *Journal of Nigerian Association of Hydrogeologists,* 11, pp. 55–61.

[6] Offodile, M. E. (2002): *Groundwater study and Development in Nigeria*, 2nd Edition. Mencon Geology and Engineering Services Ltd, 453 p.

[7] Oyawoye, M. O. (1972): The basement Complex of Nigeria. In T. F. J. Dessauvagie and A. J. Whiteman, Eds., *African Geology,* University of Ibadan Press, pp. 67–97.

[8] Wright, E. P., Burgess, W. G. (1992): *The hydrogeology of crystalline basement aquifers in Africa*. Special Publication No. 66, Geographical Society, London, pp. 1–20.

[9] Annor, A. E., Olasehinde, P. I. (1996): Vegetational Niche as a Remote sensor for subsurface aquifer: A geological-geophysical study in Jere Area, Central Nigeria. *Water Resources, Journal of Nigerian Association of Hydrogeologists,* 7(1&2), pp. 26–30.

[10] Burrough, P. A. (1986): *Principles of Geographical Information Systems for Land Resource Assessment.* Clarendon Press, Oxford, U. K.

Supplementary Material

Tables S1–S8 and Figures S1–S10.

Table S1: *Pumping Test of Borehole (BH 29) and (BH 4) in granite gneiss of Ilorin metropolis*

Borehole (BH 29) in granite gneiss				Borehole (BH 4) in granite gneiss			
Time (min)	**Water level (Draw- down, S) (m)**	**Time (min)**	**Water level (Draw- down, S) (m)**	**Time (min)**	**Water level (Draw- down, S) (m)**	**Time (min)**	**Water level (Draw- down, S) (m)**
1	3.105	85	6.040	1	5.205	85	8.099
2	3.230	90	6.115	2	5.352	90	8.199
3	3.271	100	6.175	3	5.484	100	8.225
4	3.271	110	6.263	4	5.610	110	8.360
5	3.472	120	6.324	5	5.785	120	8.451
6	3.575	130	6.410	6	5.812	130	8.525
7	3.652	140	6.505	7	5.903	140	8.580
8	3.794	150	6.613	8	5.981	150	8.642
9	3.839	160	6.721	9	6.091	160	8.795
10	4.030	170	6.800	10	6.180	170	8.805
12	4.030	180	6.901	12	6.297	180	8.875
14	4.176	190	6.984	14	6.365	190	8.993
16	4.275	200	7.072	16	6.444	200	9.192
18	4.340	210	7.183	18	6.540	210	9.275
20	4.455	230	7.254	20	6.641	230	9.388
22	4.596	250	7.331	22	6.721	250	9.465
24	4.663	270	7.430	24	6.782	270	9.530
26	4.701	290	7.531	26	6.884	290	9.622
28	4.877	310	7.610	28	6.992	310	9.720
30	4.945	330	7.699	30	7.100	330	9.801
35	5.076	350	7.792	35	7.203	350	9.890
40	5.170	370	7.881	40	7.298	370	9.967
45	5.293	390	7.979	45	7.406	390	10.065
50	5.384	410	8.067	50	7.492	410	10.184
55	5.455	430	8.157	55	7.585	430	10.275
60	5.531	450	8.247	60	7.665	450	10.351
65	5.620	470	8.325	65	7.763	470	10.415
70	5.735	490	8.413	70	7.822	490	10.487
75	5.845			75	7.901		
80	5.957			80	7.985		

Location: Borehole (BH 29) Olunlade
SWL: = 3.00 m
Average pumping rate (*Q*) = 1.28 l/s
Type of Pump: 1 HP

Borehole (BH 4) location: Tanke
SWL (Static Water Level) = 5.00 m
Average Pumping Rare (*Q*) = 1.82 l/s
Pumping Duration = 490 mins
Type of Pump = 1 HP Submersible

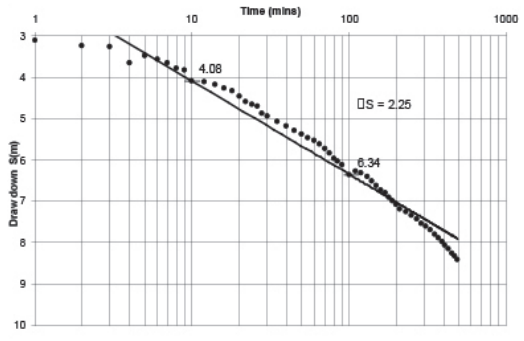

Figure S1: *Pumping Test curve of borehole (BH 29) in granite gneiss of Ilorin metropolis.*

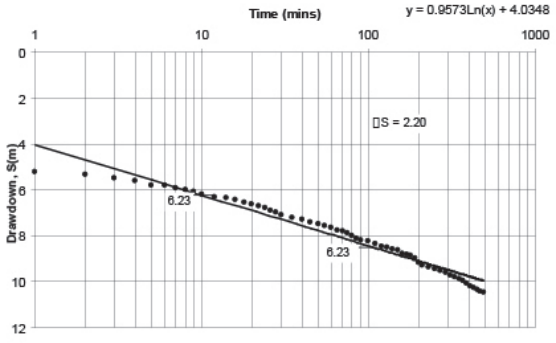

Figure S2: *Pumping Test Curve of Borehole (BH 4) in granite gneiss of Ilorin metropolis.*

Table S2: *Recovery Tests of Borehole (BH 29) in granite gneiss of Ilorin metropolis.*

t' (min)	*R.W.L* (m)	S' *(RWL-SWL)* (m)	t (490 + t') (min)	t/t'	t' (min)	*RWL* (m)	S' *(RWL-SWL)* (m)	t (490 + t') (min)	t/t'
1	8.263	5.263	491	491.00	85	4.677	1.635	575	6.76
2	8.111	5.111	492	246.00	90	4.635	1.635	580	6.44
3	7.966	4.966	493	164.33	100	4.594	1.594	590	5.90
4	7.810	4.810	494	123.50	110	4.559	1.559	600	5.45
5	7.656	4.656	495	99.00	120	4.519	1.519	610	5.08
6	7.506	4.506	496	82.66	130	4.439	1.439	620	4.76
7	7.357	4.357	497	71.00	140	4.404	1.404	630	4.50
8	7.207	4.207	498	62.25	150	4.372	1.372	640	4.26
9	7.058	4.058	499	55.44	160	4.379	1.379	650	4.06
10	6.907	3.907	500	50.00	170	4.307	1.307	660	3.88
12	6.761	3.761	502	41.83	180	4.277	1.277	670	3.72
14	6.746	3.746	504	36.00	190	4.245	1.245	680	3.57
16	6.601	3.601	506	31.62	200	4.214	1.214	690	3.45
18	6.455	3.455	508	28.22	210	4.181	1.281	700	3.33
20	6.303	4.303	510	25.50	230	4.146	1.246	720	3.13
22	6.163	3.163	512	23.27	250	4.114	1.114	740	2.96
24	6.017	3.017	514	21.41	270	4.083	1.083	760	2.81
26	5.872	2.872	516	19.84	290	4.053	1.053	780	2.68
28	5.352	2.742	518	18.50	310	4.018	1.018	800	2.58
30	5.607	2.607	520	17.33	330	3.984	0.984	820	2.48
35	5.472	2.472	525	15.00	350	3.950	0.950	840	2.40
40	5.352	2.352	530	13.25	370	3.911	0.911	860	2.32
45	5.242	2.242	535	11.88	390	3.871	0.871	880	2.25
50	5.143	2.143	540	10.80	410	3.876	0.876	900	2.19
55	5.053	2.053	545	9.90	430	3.875	0.874	920	2.13
60	4.968	1.968	550	9.16	450	3.874	0.874	940	2.08
65	4.898	1.898	555	8.53	470	3.874	0.874	960	2.04
70	4.836	1.836	560	8.00	490	3.874	0.874	980	2.00
75	4.773	1.773	565	7.53					
80	4.7231	1.723	570	7.13					

SWL = 3.00 m
Time of pumping = 490 min
Borehole location: Olunlade
Average pumping rate (*Q*) = 1.28 l/s

t' = time since start of recovery
t = time since start of pumping
R.W.L. = Recovery water level
S = Residual drawdown
SWL = Static Water Level

Table S3: *Recovery Tests of Borehole (BH 4) in granite gneiss of Ilorin metropolis*

t' (min)	R.W.L (m)	S' (RWL-SWL) (m)	t (490 + t') (min)	t/t'	t' (min)	RWL (m)	S' (RWL-SWL) (m)	t (490 + t') (min)	t/t'
1	10.265	5.265	491	491.00	85	7.865	2.865	575	6.76
2	10.124	5.124	492	246.00	90	7.767	2.767	580	6.44
3	9.989	4.989	493	164.33	100	7.713	2.713	590	5.90
4	9.864	4.864	494	123.50	110	7.664	2.664	600	5.45
5	9.741	4.741	495	99.00	120	7.608	2.608	610	5.08
6	9.627	4.627	496	82.66	130	7.552	2.552	620	4.76
7	9.524	4.524	497	71.00	140	7.499	2.499	630	4.50
8	9.423	4.423	498	62.25	150	7.445	2.445	640	4.26
9	9.324	4.324	499	55.44	160	7.387	2.387	650	4.06
10	9.225	4.225	500	50.00	170	7.331	2.331	660	3.88
12	9.138	4.138	502	41.83	180	7.272	2.272	670	3.72
14	9.053	4.053	504	36.00	190	7.218	2.218	680	3.57
16	8.971	3.971	506	31.62	200	7.160	2.160	690	3.45
18	8.895	3.895	508	28.22	210	7.101	2.101	700	3.33
20	8.819	3.819	510	25.50	230	6.501	1.501	720	3.13
22	8.749	3.749	512	25.27	250	6.438	1.438	740	2.96
24	8.680	3.680	514	21.41	270	6.376	1.376	760	2.81
26	8.612	3.612	516	19.84	290	6.317	1.317	780	2.68
28	8.545	3.545	518	18.50	310	6.259	1.259	800	2.58
30	8.450	3.450	520	17.33	330	6.201	1.201	820	2.48
35	8.416	3.416	525	15.00	350	6.144	1.144	840	2.40
40	8.451	3.451	530	13.25	370	6.088	1.088	860	2.32
45	8.288	3.288	535	11.88	390	6.032	1.032	880	2.25
50	8.228	3.228	540	10.80	410	5.906	0.906	900	2.19
55	8.170	3.170	545	9.90	430	5.905	0.905	920	2.13
60	8.113	3.113	550	9.16	450	5.904	0.904	940	2.08
65	8.057	3.057	555	8.53	470	5.904	0.904	960	2.04
70	8.022	3.022	560	8.00	490	5.904	0.904	980	2.00
75	7.969	2.969	565	7.53					
80	7.919	2.919	570	7.13					

SWL = 5.00 m
Time of pumping = 490 min
Borehole location: Tanke
Average pumping rate (*Q*) = 2.23 l/s
SWL = Static Water Level

t/ = time since start of recovery
t = time since start of pumping
R.W.L. = Recovery water level
S = Residual drawdown

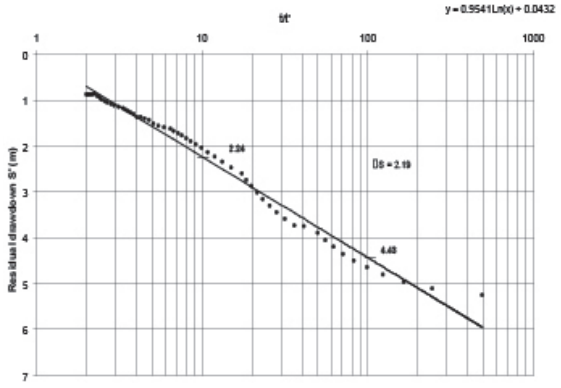

Figure S3: *Recovery Test curve of Borehole (BH 29) in granite gneiss of Ilorin metropolis.*

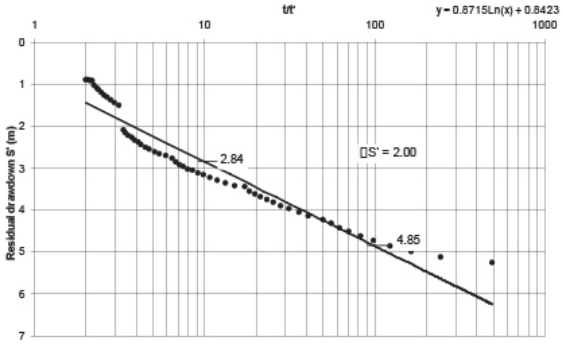

Figure S4: *Recovery Test Curve of Borehole (BH 4) in granite gneiss of Ilorin metropolis.*

Table S4: *Pumping Test of Borehole (BH 10) and (BH 24) in migmatite of Ilorin metropolis*

Time (min)	Water level (Draw- down, S) (m)	Time (min)	Water level (Draw- down, S) (m)	Time (min)	Water level (Draw- down, S) (m)	Time (min)	Water level (Draw- down, S) (m)
1	5.105	85	7.621	1	5.095	85	7.950
2	5.165	90	7.690	2	5.145	90	8.020
3	5.210	100	7.790	3	5.185	100	8.167
4	5.273	110	7.910	4	5.295	110	8.284
5	5.381	120	8001	5	5.390	120	8.385
6	5.422	130	8.118	6	5.484	130	8.740
7	5.480	140	8.201	7	5.567	140	8.594
8	5.595	150	8.299	8	5.561	150	8.692
9	5.677	160	8.430	9	5.725	160	8.790
10	5.725	170	8.510	10	5.789	170	8.881
12	5.790	180	8.624	12	5.894	180	8.950
14	5.881	190	8.711	14	5.993	190	9.015
16	5.964	200	8.815	16	6.110	200	9.115
18	6.125	210	8.920	18	6.215	210	9.192
20	6.190	230	9.014	20	6.321	230	9.324
22	6.273	250	9.105	22	6.435	250	9.444
24	6.344	270	9.210	24	6.522	270	9.524
26	6.405	290	9.333	26	6.616	290	9.651
28	6.499	310	9.416	28	6.701	310	9.765
30	6.536	330	9.504	30	6.775	330	9.850
35	6.666	350	9.619	35	6.872	350	9.949
40	6.774	370	9.705	40	6.984	370	10.023
45	6.872	390	9.800	45	7.101	390	10.101
50	6.980	410	9.910	50	7.233	410	10.210
55	7.025	430	10.002	55	7.334	430	10.314
60	7.192	450	10.092	60	7.448	450	10.420
65	7.283	470	10.172	65	7.535	470	10.500
70	7.394	490	10.255	70	7.621	490	10.587
75	7.430			75	7.704		
80	7.515			80	7.892		

Location: Borehole (BH 10) Olohunsogo
SWL (Static Water Level) = 5 900 m
Average Pumping rate (*Q*) = 1.62 1/s
Time of pumping = 490 min
Type of Pump: 1 HP Submersible

Location: Borehole (BH 24) Akerebiata
SWL (Static Water Level) = 5 800 m
Average Pumping rate (*Q*) = 1.731/s
Time of pumping = 490 min
Type of Pump: 1 HP Submersible

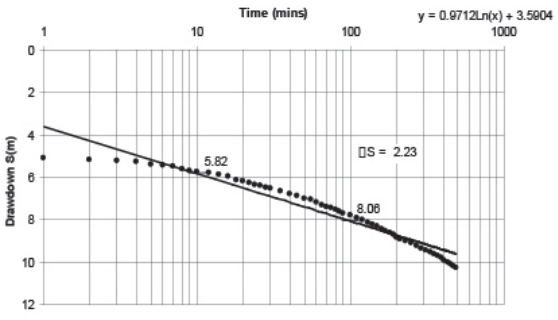

Figure S5: *Pumping Test Curve of Borehole (BH 10) in migmatite of Ilorin metropolis.*

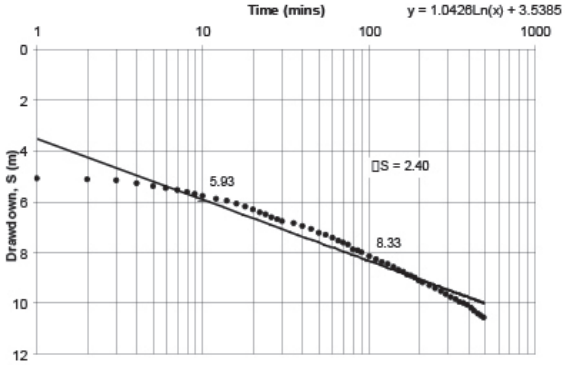

Figure S6: *Pumping Test Curve of Borehole (BH 24) in migmatite with overburden aquifer in Ilorin metropolis.*

Table S5: *Recovery Tests of Borehole (BH 10) in migmatite of Ilorin metropolis*

t' (min)	*R.W.L* (m)	S' *(RWL-SWL)* (m)	t (490 + t') (min)	t/t'	t' (min)	*RWL* (m)	S' *(RWL-SWL)* (m)	t (490 + t') (min)	t/t'
1	10.102	4.202	491	491.00	85	7.555	1.655	575	6.76
2	9.949	4.049	492	246.00	90	7.513	1.613	580	6.44
3	9.799	3.899	493	164.33	100	7.468	1.568	590	5.90
4	9.648	3.748	494	123.50	110	7.422	1.522	600	5.45
5	9.496	3.596	495	99.00	120	7.378	1.478	610	5.08
6	9.346	3.446	496	82.66	130	7.333	1.433	620	4.76
7	9.196	3.296	497	71.00	140	7.291	1.391	630	4.50
8	9.047	3.147	498	62.25	150	7.246	1.346	640	4.26
9	8.898	2.998	499	55.44	160	7.200	1.300	650	4.06
10	8.750	2.850	500	50.00	170	7.155	1.255	660	3.88
12	8.644	2.744	502	41.83	180	7.109	1.209	670	3.72
14	8.540	2.640	504	36.00	190	7.066	1.166	680	3.57
16	8.450	2.550	506	31.62	200	7.002	1.122	690	3.45
18	8.370	2.470	508	28.22	210	6.917	1.077	700	3.33
20	8.300	2.400	510	25.50	230	6.927	1.027	720	3.13
22	8.250	2.350	512	25.27	250	6.874	0.974	740	2.96
24	8.199	2.299	514	21.41	270	6.770	0.870	760	2.81
26	8.150	2.250	516	19.84	290	6.720	0.820	780	2.68
28	8.102	2.202	518	18.50	310	6.663	0.763	800	2.58
30	8.053	2.153	520	17.33	330	6.662	0.762	820	2.48
35	8.010	2.110	525	15.00	350	6.662	0.762	840	2.40
40	7.964	2.064	530	13.25	370	6.661	0.761	860	2.32
45	7.918	2.018	535	11.88	390	6.661	0.761	880	2.25
50	7.814	1.914	540	10.80	410	6.660	0.760	900	2.19
55	7.829	1.929	545	9.90	430	6.660	0.760	920	2.13
60	7.779	1.879	550	9.16	450	6.660	0.760	940	2.08
65	7.734	1.834	555	8.53	470	6.660	0.760	960	2.04
70	7.686	1.786	560	8.00	490	6.660	0.760	980	2.00
75	7.642	1.742	565	7.53					
80	7.598	1.698	570	7.13					

SWL = 5.00 m
Time of pumping = 490 min
Borehole location: Olohunsogo
Average pumping rate (*Q*) = 1.62 l/s

t' = time since start of recovery
t = time since start of pumping
R.W.L. = Recovery water level
SWL= Static Water Level
S' = Residual drawdown

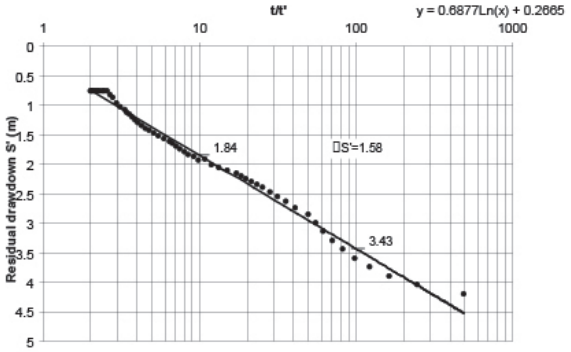

Figure S7: *Recovery Test curve of Borehole (BH 10) in migmatite of Ilorin metropolis.*

Table S6: *Recovery Tests of Borehole (BH 24) in migmatite of Ilorin metropolis*

t' (min)	*R.W.L* (m)	S' *(RWL-SWL)* (m)	t (490 + t') (min)	t/t'	t' (min)	*RWL* (m)	S' *(RWL-SWL)* (m)	t (490 + t') (min)	t/t'
1	10.442	4.642	491	491.00	85	7.401	1.601	575	6.76
2	10.297	4.498	492	246.00	90	7.361	1.651	580	6.44
3	10.154	4.354	493	164.33	100	7.316	1.516	590	5.90
4	10.009	4.209	494	123.50	110	7.269	1.469	600	5.45
5	9.866	4.966	495	99.00	120	7.224	1.424	610	5.08
6	9.726	3.926	496	82.66	130	7.180	1.380	620	4.76
7	9.583	3.783	497	71.00	140	7.140	1.340	630	4.50
8	9.439	3.639	498	62.25	150	7.100	1.300	640	4.26
9	9.299	3.499	499	55.44	160	7.060	1.260	650	4.06
10	9.158	3.358	500	50.00	170	7.019	1.219	660	3.88
12	9.123	3.323	502	41.83	180	6.978	1.178	670	3.72
14	8.987	3.187	504	36.00	190	6.938	1.138	680	3.57
16	8.855	3.055	506	31.62	200	6.893	1.093	690	3.45
18	8.725	2.925	508	28.22	210	6.858	1.058	700	3.33
20	8.594	2.794	510	25.50	230	6.822	1.022	720	3.13
22	8.461	2.661	512	25.27	250	6.790	0.990	740	2.96
24	8.338	2.538	514	21.41	270	6.757	0.957	760	2.81
26	8.228	2.428	516	19.84	290	6.718	0.918	780	2.68
28	8.128	2.328	518	18.50	310	6.683	0.883	800	2.58
30	8.038	2.238	520	17.33	330	6.651	0.851	820	2.48
35	7.958	2.158	525	15.00	350	6.615	0.815	840	2.40
40	7.881	2.081	530	13.25	370	6.580	0.780	860	2.32
45	7.826	2.026	535	11.88	390	6.550	0.750	880	2.25
50	7.766	1.966	540	10.80	410	6.549	0.749	900	2.19
55	7.711	1.911	545	9.90	430	6.548	0.749	920	2.13
60	7.668	1.868	550	9.16	450	6.548	0.748	940	2.08
65	7.601	1.801	555	8.53	470	6.548	0.748	960	2.04
70	7.560	1.760	560	8.00	490	6.548	0.748	980	2.00
75	7.507	1.707	565	7.53					
80	7.453	1.653	570	7.13					

SWL = 5 800 m
Time of pumping = 490 min
Borehole location: Akerebiata
Average pumping rate (*Q*) = 1.73 l/s
SWL= Static Water Level

t' = time since start of recovery
t = time since start of pumping
R.W.L. = Recovery water level
S = Residual drawdown

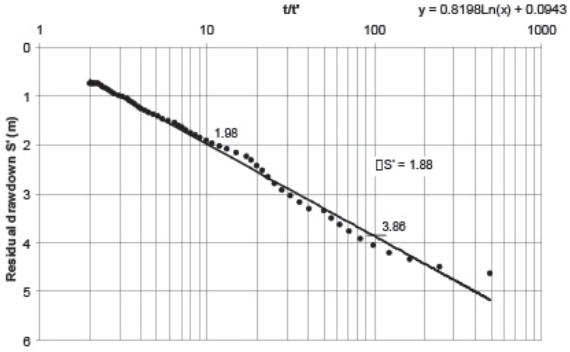

Figure S8: *Recovery Test Curve of Borehole (BH 24) in migmatite of Ilorin metropolis.*

Table S7: *Pumping Test of Borehole (BH 12) in quartzite of Ilorin metropolis*

Time (min)	Water level (Draw- down, S) (m)	Time (min)	Water level (Draw- down, S) (m)
1	4.396	85	7.105
2	4.455	90	7.185
3	4.536	100	7.295
4	4.625	110	7.395
5	4.741	120	7.523
6	4.850	130	7.595
7	5.018	140	7.747
8	5.057	150	7.762
9	5.125	160	7.815
10	5.295	170	7.892
12	5.360	180	7.978
14	5.450	190	8.058
16	5.550	200	8.128
18	5.601	210	8.237
20	5.715	230	8.304
22	5.830	250	8.423
24	5.924	270	8.507
26	5.997	290	8.589
28	6.095	310	8.684
30	6.185	330	8.790
35	6.290	350	8.890
40	6.375	370	8.995
45	6.447	390	9.081
50	6.455	410	9.163
55	6.570	430	9.230
60	6.690	450	9.302
65	6.763	470	9.385
70	6.814	490	9.471
75	6.950		
80	7.015		

Location: Borehole (BH 12) Gaa-Akanbi
SWL (Static Water Level) = 4.30 m
Average Pumping Rate (*Q*) = 2.23 1/s
Pumping Duration: 490 min
Type of Pump = 1 HP Submersible (Grundfos)

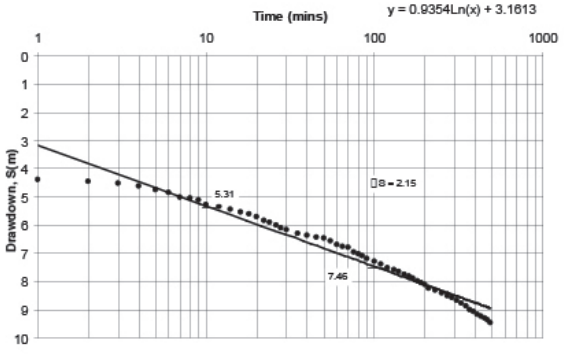

Figure S9: *Pumping Test Curve of Borehole (BH 12) in quartzites of Ilorin metropolis*

Table S8: *Recovery Tests of Borehole (BH 12) in quartzites of Ilorin metropol*

t' (min)	R.W.L (m)	S' (RWL-SWL) (m)	t (490 + t') (min)	t/t'	t' (min)	RWL (m)	S' (RWL-SWL) (m)	t (490 + t') (min)	t/t'
1	9.321	5.021	491	491.00	85	6.353	2.053	575	6.76
2	9.170	4.870	492	246.00	90	6.294	1.994	580	6.44
3	9.022	4.722	493	164.33	100	6.241	1.941	590	5.90
4	8.873	4.573	494	123.50	110	6.157	1.857	600	5.45
5	8.728	4.428	495	99.00	120	6.137	1.837	610	5.08
6	8.582	4.282	496	82.66	130	6.092	1.792	620	4.76
7	8.297	4.137	497	71.00	140	6.048	1.748	630	4.50
8	8.162	3.997	498	62.25	150	6.003	1.703	640	4.26
9	8.027	3.862	499	55.44	160	5.961	1.661	650	4.06
10	7.897	3.727	500	50.00	170	5.918	1.618	660	3.88
12	7.897	3.597	502	41.83	180	5.873	1.573	670	3.72
14	7.768	3.468	504	36.00	190	5.829	1.529	680	3.57
16	7.648	3.348	506	31.62	200	5.786	1.486	690	3.45
18	7.527	3.227	508	28.22	210	5.745	1.445	700	3.33
20	7.427	3.127	510	25.50	230	5.705	1.405	720	3.13
22	7.332	3.032	512	25.27	250	5.664	1.364	740	2.96
24	7.239	2.939	514	21.41	270	5.621	1.321	760	2.81
26	7.149	2.849	516	19.84	290	5.577	1.277	780	2.68
28	7.064	2.764	518	18.50	310	5.532	1.232	800	2.58
30	6.981	2.681	520	17.33	330	5.482	1.182	820	2.48
35	6.911	2.611	525	15.00	350	5.432	1.132	840	2.40
40	6.851	2.551	530	13.25	370	5.376	1.076	860	2.32
45	6.786	2.486	535	11.88	390	5.326	1.026	880	2.25
50	6.724	2.424	540	10.80	410	5.277	0.977	900	2.19
55	6.673	2.373	545	9.90	430	5.246	0.946	920	2.13
60	6.623	2.323	550	9.16	450	5.245	0.945	940	2.08
65	6.571	2.271	555	8.53	470	5.245	0.945	960	2.04
70	6.517	2.217	560	8.00	490	5.245	0.945	980	2.00
75	6.465	2.165	565	7.53					
80	6.405	2.109	570	7.13					

SWL = 4 300 m
Time of pumping = 490 min
Borehole location: Akerebiata
Average pumping rate (*Q*) = 2.23 l/s
SWL = Static Water Level

t' = time since start of recovery
t = time since start of pumping
R.W.L. = Recovery water level
S'= Residual drawdown

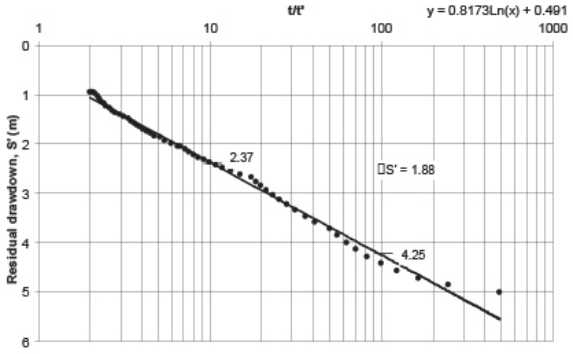

Figure S10: *Recovery Test Curve of Borehole (BH 12) in quartzites of Ilorin metropolis.*

Professional paper

Received: May 20, 2014
Accepted: August 5, 2014

About basalt production and ways to improve basalt product quality

Izkoriščanje bazalta in možnosti izboljšanja kakovosti bazaltnih proizvodov

Soyib Abdurakhmanovich Abdurakhmanov[1], Rashidova Ra'no[1], Mamatkarimova Barno Khabibullayevna[1], Sattarov Laziz Khalmuradovich[2,*]

[1]Navoi State Mining Institute, South street 27-a, 210100 Navoi City, Uzbekistan

[2]Karshi Engineering Economics Institute, Mustakillik Street 225, 180100, Karshi City, Kashkadarya region, Uzbekistan

*Corresponding author. E-mail: lbo_bosh@mail.ru

Abstract

In this article the current state of production and processing of basalts in Uzbekistan, the quality of the products and condition of basalt processing train of machines of industries are analyzed.

The reasons of low production level and basaltic rock processing, including low production potential of train of machines of basalt processing plants and insignificant choice, and ill-quality of products are identified.

Ways to increase the volume of basaltic rock production and product quality through cleaning the rock from sludge, hydroxide, salts and ashes (further sludge) are proposed. Opportunities of expansion of the range of the products by typification and application of new technologies on basalt processing are discussed.

Key words: basaltic rock, production, processing, product quality, product range, basalt clearance

Izvleček

V tem članku se analizira sedanje stanje proizvodnje in predelave bazaltov v Uzbekistanu, kakovost proizvedenih bazaltnih izdelkov in tudi palete bazaltnih proizvodov, izdelanih v podjetjih za predelavo bazalta v republiki Uzbekistan. Ugotovljeno je, da je razlog za nizko stopnjo proizvodnje in predelave naravnega bazalta v nepomembnem gospodarskem področju in slabi kakovosti izdelkov.

Podani so načini povečanja obsega proizvodnje naravnega bazalta in izboljšanje kakovosti proizvedenega bazalta z izpiranjem gline.

Ključne besede: naravni bazalt, proizvodnja, predelava, kakovost izdelkov, paleta izdelkov, bogatenje naravnega bazalta

Introduction

The need of a national economy of the Republic of Uzbekistan for materials from local raw materials, to a large extent, is defined by broad use of composite and fire-resistant materials based on glass-like, carbon and ceramic substances, and other substitutes. However, not all above-mentioned materials are made in our republic, but products from them are widely used in household appliances, car manufacturing, aircraft construction, industry, etc. In this regard, in the XX century scientists of a number of the countries have offered a material, received from the mountain rock – basalt, environmentally friendly and harmless for health. Successes achieved by scientists and specialists of Russia, Germany, USA, Japan, India, China and some other countries long ago and successfully put into practice the use of basalt. Nowadays the opportunity of obtaining various types of valuable materials that are of huge use for mankind is not a secret [1–3].

Uzbekistan is one of the leading countries of the world with rich natural basalt resources. There are more than ten non-governmental basalt processing organizations in Uzbekistan; however 2 or 3 of them work continuously. Therefore, volume of basalt processing in Uzbekistan is about 25–30 t/d [1].

It is necessary to note that basalt processing plants of Uzbekistan, mainly, specialize on the production of basalt-fibrous materials which are used as heat insulation material. These plants lack good technical equipment and effective methods of basalt production. As a rule, time consuming methods of basalt mining that at the same time incur big expenses are used, and in practical terms, technological solutions directed to increase the product quality are not applied, which hinders the expansion of basalt products' choice.

Currently, country's need for heat-insulating fibers is completely met. Requirements put before this materials mostly include quality such as fire resistance and fire safety, temperature stability, water resistance and acidity, absence of gas emission when heated, low density and durability in the conditions of variable thermal and climatic loads, etc. don't conform to modern standards.

Field of application of the basalt products in the world market extends very intensively. Day after day there are new basalt products like basalt plates and mats, pipes and rebar, cardboards and sound absorbers, reinforcing and composite materials, metal substitutes and balls, and so forth. However, as it was noted above, the power of the existing enterprises on the basalt processing don't meet the requirements of domestic market.

Thus, significance of a problem of basalt mining increase and quality improvement is due to growth of needs for basalt production and steady demand for it, not only in our Republic, but also in the international market. That's why, efficiency of using rich basalt mines of Uzbekistan through increasing basalt rock mining, quality improvement and expansion of basalt products' choice, development of new currency-saving methods of basalt processing are now mostly important requirements. These will improve the quality of rocks' processing, facilitate the economic development of basalt processing plants of the Republic and create additional workplaces.

Materials and methods

Basalt winning

In Uzbekistan's nature, mainly surficial deposits of basalt rocks are observed; average diameter of each is about 250–300 mm. [1, 4]. Therefore, basalts are mined only opencast with the usage of baby blasting workings. After this, rocks are sent to plants' location wherein basalts are bucked to necessary fraction size.

Analysis of basalt winning processes in "Gavasay", "Asmansay" and "Aydarkul" shows that all basalt processing plants are located at some distance from the deposit. In some cases, this distance is about 700 km and more which in fact increase the cost for transportation of the raw material and influence on the net price of finished product. Share of other vehicles and other mining and processing equipment is not big. It is possible to note following reasons for such situation:

— frequent use of manual skills for unloading or loading works;

— use of technical means with a low productivity;
— use of non-standard melting or other equipment;
— small investments to the growth of productivity of basalt processing enterprises;
— small experience and absence of highly qualified specialists.

Frequent use of manual skills for unloading or loading works, application of nonconventional stripping methods are explained by plant management with low cost, the low power of the enterprise, shortage of means, semi-automated or automated loading and discharging equipment. In turn, application of non-standard melting ovens or other equipment, hindering the growth of enterprise's development is explained by the high cost of equipment of good quality, its delivery and assembly, and also low-level of investments in this area.

Researches showed that none of the advertising companies carried out an advertisement of domestic manufacturers-producers for the last 10–15 years. Building a basalt processing enterprise next to basaltic deposit is an actually costly process. Delivery of fuel and energy resources to mountainside and to area, and back to enterprise's location is not effective option for the solution of this question.

At the same time, development of the winning and production volume on basalt processing is impossible without the development of powerful train of machines on loading-unloading basaltic products. Basalt processing enterprises due to lack of financial resources so far cannot solve this problem. That's why, optimum alternative solution here is the use of modern methods of basalt winning, transportation and processing.

Considering the abovementioned, we propose following solution to be applied in the basalt production:

— to build basalt processing plants next to basaltic deposits;
— to find alternative production solutions to increase the domestic basalt winning;
— to use modern basalt processing methods;
— to apply new technologies, including initial rock processing on the deposit;
— to apply methods that provide the quality improvement of the raw material and eventually the final product which, in turn, will be cheaper in net price.

Quality improvement of basaltic rock

At the research, we have identified that after crushing, basaltic rocks are subject to melting process. Currently, plants are not designed to clean or sort the basaltic rocks.

The analysis of technological processes in this area shows that basaltic product manufacturers in our country think that sorting is not a necessary process as crumbles after crushing into particles are sent to melting furnace, and as a result they get low-quality basalt fibrous-heat insulating material. Such factor as: grain size and rock form; dust-like and cledgy particles in basaltic content; availability of hazardous rocks; availability of detrimental impurities in basaltic content; radioactivity and salinity of basalts, their typification and properties are not considered.

Absence in technical literature is revealed of data on influence of slimes on the quality of the basaltic fibrous materials that can cause early corrosion of insulated object. Producers of basalt products consider that the absorptivity of a basaltic crumbles doesn't influence on its further processing; the raw material doesn't deteriorate, and not influenced by an atmospheric precipitation. As a result basalt crumbles are often stored even in the open air. There is also no proof that the remained salts on heat-insulating basaltic-fibrous materials do not cause early corrosion of insulated object. At the same time, it is established that basalt fibrous materials intensively absorb water, crude air and become wet in hostile environment [4].

While studying basaltic-fibrous heat-insulating materials, after their use for several years, we have identified the corrosion on the surface of pipes. This phenomenon can be explained by the fact that basaltic rocks have been processed without cleaning the slimes from its content.

Corrosion can be observed both underground pipes and ground pipes. The cause can be explained by the high water absorption of basaltic-fibrous materials and the availability of salt in the wool content.

As a rule, availability of slimes in basalts can be explained by the salinity of soil in basaltic deposits and rocks. According to the data, salinity of irrigated lands in our Republic is high, and this includes lands where big basaltic deposits are located. For example, average salinity of lands in Namangan region ("Gavasay" deposit location) reaches up to 28 %, Jizzakh region ("Asmansay" deposit) – 85.4 % and Navoi region ("Aydarkul" deposit) – 92.9 % [5–7].

Figure 1*: Typical corrosion in long-term use of basaltic-fibrous materials for insulation.*

Influence of salts on the quality, working capacity and durability of basaltic heat-insulating materials are studied through observing the pipelines in Navoi region where basaltic-fibrous heat-insulating materials of various diameter, produced by local manufacturers. Data and results of observation are given in Table 1.
Big corrosion layer is observed on the surface of pipes which were traditionally wrapped around by basaltic heat-insulating, thickness of which is 50–80 mm. Also, we have revealed that corrosion layer under basaltic heat-insulating material with 100 mm reached 0.5 mm.
Study and analysis of the consequence of using heat-insulating materials, obtained from not refined basalts showed that they are inclined to corrosion. We also revealed that heat-insulating materials together with slimes salts like NaCl, KCl and Cacl. Such mixtures while remained in basaltic fibers easily cooperate with environment and with water space. High water absorption of absorption cotton causes corrosion. This, in turn, decreases the terms of using final product and object where they are used which provides early loss of useful properties of basaltic fibers and cause destruction of the equipment as well.
For final assessment of the rock quality, we studied the condition of basalts through experimental way. For this purpose, we selected rocks at random from "Gavasay", "Asmansay" and "Aydarkul" with weight 200 kg from each. Samples of rocks were divided into two parts – 100 kg each. In the first part – 100 kg was put into sluicing process for cleaning the rocks from slimes.

Table 1: *Study results of pipes surface corrosion resistance.*

№	Thickness of basaltic heat-insulating material, [mm]	Relative degree of humidity of adjacent regions, 68–90 %		
		Corrosion layer thickness, after 5 years, [mm]	Corrosion layer thickness, after 8 years, [mm]	Corrosion layer thickness, after 10 years, [mm]
1	50	0.33	0.87	1.3
2	80	0.19	0.41	0.92
3	100	0.11	0.27	0.51

Table 2: *Study results on the identification of corrosion time of metals while using "basaltic fiber", obtained from various basalt deposits*

№	Name of indicators	Deposits		
		"Gavasay"	"Asmansay"	"Aydarkul"
1	Corrosion starting time on pipes (basalt without refining), year	6–8	5–6	2–4
2	Corrosion starting time on pipes (basalt after refining), year	12	10–12	10–12
3	Corrosion starting time on the surface of working parts of equipment, year	5	3	1
4	Salinity level of basalt deposit soil, %	28	85.4	92.9
5	Corrosion starting time on the surface of working parts of equipment, year	12	12	12

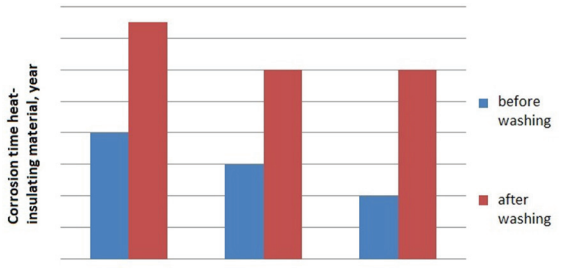

Figure 2: *Histogram of objects' usage period when basalt fiber is used as heat-insulating material before and after washing-out the basaltic rocks: 1 – indicators of basaltic deposits in "Gavasay"; 2 – indicators of basaltic deposits in "Asmansay"; and 3 – indicators of basaltic deposits in "Aydarkul".*

First, we processed not-refined basalts and then refined basalt rocks underwent the experiment. Later, we wrapped pipes with obtained heat-insulating materials and observed. Experiment took 12 years – until the first appearance of corrosion layer on pipes. Study results are given in Table 2.

We found out that more slimes were removed from "Aydarkul" deposit rocks. Long-term use of materials was observed in basalts obtained from "Gavasay" deposit. Results are given in histogram in figure 2. Histogram shows that the earliest corrosion can be observed in object where fibers obtained from "Aydarkul" are used, that is maximum after 4 years and "Asmansay" – after 6 years. Results showed that if basalts rocks are refined and washed, then the appearance of corrosion can be prolonged to average 3.5 times which proves the idea of efficiency of cleaning slimes from basaltic rocks.

Therefore, it is perspective to remove slimes from the surface of basalts by way of washing out with specialized equipment – wash trammel. Doing so, one can reach the decrease of time waste on the technological process. Such approach can be easily succeeded with the help of latticed wall of wash trammel which in this case plays a role as sieve, the size of which is matched to the size of basaltic rock particles simply.

After all, there is a practical interest in the quality indicators of basalts and their heat-insulating materials which prolonged the exploitation period of pipes to about 2 times (histogram, Figure 3)

It is established that quantity assessment of slime content in basaltic deposits of "Gavasay", "Asmansay" and "Aydarkul" is of high priority. Each tested 200 kg of basaltic

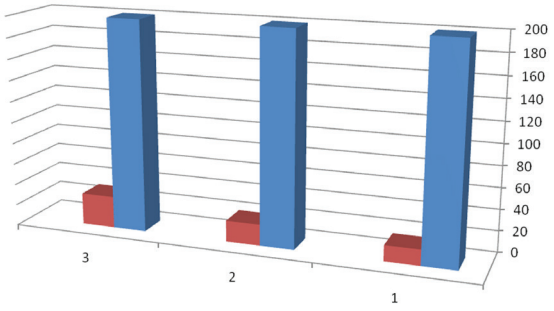

Figure 3: *Indicators of mechanical cleaning basalts in "Gavasay", "Asmansay" and "Aydarkul" basaltic deposits.*

rocks carry slimes, but in a different amount: "Gavasay" – 1 %, "Asmansay" – 1.5 % and rocks of "Aydarkul" – 2 %. In case is manufacturers want to get higher results, these indexes play very important role.

Analysis of the demand volume to the products of basalt processing plants shows that heat-insulating product from basalts are used in: energy industry, construction, road and automobile construction and so forth [2, 4]. At the same time, because of the difference of properties and material composition of basalts in various deposits, there is no opportunity for direct use of modern technologies in Uzbekistan. Therefore, one of the possible options of increasing the effectiveness of using basaltic raw material and organization of production of ecologically clean products it is necessary to develop rational technology of local basalt processing with the consideration of local deposits' soil salinity.

Altogether, new technologies of basaltic rock processing and new directions of using different products produced from basaltic rocks shows their infinite possibilities. Consequently, perspective direction of using basaltic primary resources of Uzbekistan and obtaining standard products are to conduct a thorough study of basalts and expand production potential of plants based on given parameters of properties, material composition and concentration of basalt mixtures. Doing so, to achieve the production of high-quality products of various purpose and saving currency means of the country.

Conclusion

Current status of mining and quality of basalt product in Uzbekistan are studied. As a result, we have established unprofitable use of basaltic primary resources, low quality of basalt products and limited variety of product. Additionally we have found that infinite opportunities of using local basaltic rocks.

It is also established that volume of basalt winning can be increased by following ways:

— improving train of machines based on the existing one;
— improving existing technologies on the basalt processing and modernization of present equipment;
— increasing the volume of production on the processing and production of basaltic products with the use of new technologies, based on the creation of administered production in total which paves an opportunity to sparingly and thinly spend energy resources and ease the zero-emission processing of basaltic rocks;

Expansion of product variety can be fulfilled though:

— basalt typification based on given parameters of properties, material composition and cleaning basaltic rocks from slimes;
— rock sorting on the processing stage which improves the useful properties of basalt products' durability;
— development of rational technologies on obtaining basaltic products in a wide array of choices and with given physical-chemical parameters and their application in the problem solving of different tasks;
— creation of new types of basaltic products with improved properties: fire-resistant, corrosion-resistant, dielectric permittivity, water-absorption and water-yielding capacity, acid-resistant, alkaline-resistant, porosity, thickness, solidity, and so on;
— development of new methodology and recommendations on the study and use of basaltic products for their practical application in the agriculture of Uzbekistan, countries of CIA, and particularly in enterprises of mining and smelting branch.

References

[1] Dodis, G. M., Kudinova, I. V. (2007): Structure melt from basaltofibrous rocks. *Bulletin KGNU*, Kyrgyzstan, pp. 2–14.

[2] Kurbanov, A. A., Abdurahmonov, S. A., Turaev, A. S. (2010): *Base of processing of basalts of KyzylKum.* The monography.publishing "Fan" AN RUz, 167 p.

[3] Lapinskaya, L. A., Proshljakov, B. K. (1974): *Bas of petrography*. Publishing house"Bowels", pp. 30–36.

[4] Kurbanova, A. (2009): *Specific of basalts featureof Kyzyl Kum*. The onography; publishing. "Fan" RUz., 160 p.

[5] Luchinskiy, V. I. (1949): *Petrography.* M.: Gosgeolizdat, pp. 213–225.
[6] Dzhigaris D. D. &Mahova M. F. (2006*): Base of basalt production fibres and products*, 410 p.
[7] Safonova, I. JU. (2005): *Geodynamic of conditions formation vendpaleozoic basalts aleasiatic ocean from folded areas of mountain Altai and east Kazakhstan.* Novosibirsk.

Instructions to Authors
Navodila avtorjem

RMZ – MATERIALS & GEOENVIRONMENT (RMZ – Materiali in geookolje) is a periodical publication with four issues per year (established in 1952 and renamed to RMZ – M&G in 1998). The main topics are Mining and Geotechnology, Metallurgy and Materials, Geology and Geoenvironment.
RMZ – M&G publishes original scientific articles, review papers, preliminary notes and professional papers in English. Only professional papers will exceptionally be published in Slovene. In addition, evaluations of other publications (books, monographs, etc.), in memoriam, presentation of a scientific or a professional event, short communications, professional remarks and reviews published in RMZ – M&G can be written in English or Slovene. These contributions should be short and clear.
Authors are responsible for the originality of the presented data, ideas and conclusions, as well as for the correct citation of the data adopted from other sources. The publication in RMZ – M&G obligates the authors not to publish the article anywhere else in the same form.

RMZ – MATERIALS AND GEOENVIRONMENT (RMZ – Materiali in geookolje), kratica RMZ – M&G je revija (ustanovljena kot zbornik 1952 in preimenovana v revijo RMZ – M&G 1998), ki izhaja vsako leto v štirih zvezkih. V reviji objavljamo prispevke s področja rudarstva, geotehnologije, materialov, metalurgije, geologije in geookolja.
RMZ – M&G objavlja izvirne znanstvene, pregledne in strokovne članke ter predhodne objave samo v angleškem jeziku. Strokovni članki so lahko izjemoma napisani v slovenskem jeziku. Kot dodatek so zaželene recenzije drugih publikacij (knjig, monografij …), nekrologi In memoriam, predstavitve znanstvenih in strokovnih dogodkov, kratke objave in strokovne replike na članke, objavljene v RMZ – M&G v slovenskem ali angleškem jeziku. Prispevki naj bodo kratki in jasni.
Avtorji so odgovorni za izvirnost podatkov, idej in sklepov v predloženem prispevku oziroma za pravilno citiranje privzetih podatkov. Z objavo v RMZ – M&G se tudi obvežejo, da ne bodo nikjer drugje objavili enakega prispevka.

Specification of the Contributions

Optimal number of pages is 7 to 15; longer articles should be discussed with the Editor-in-Chief prior to submission. All contributions should be written using the ISO 80000.

- Original scientific papers represent unpublished results of original research.
- Review papers summarize previously published scientific, research and/or expertise articles on a new scientific level and can contain other cited sources which are not mainly the result of the author(s).
- Preliminary notes represent preliminary research findings, which should be published rapidly (up to 7 pages).
- Professional papers are the result of technological research achievements, application research results and information on achievements in practice and industry.

Vrste prispevkov

Optimalno število strani je 7–15, za daljše članke je potrebno soglasje glavnega urednika. Vsi prispevki naj bodo napisani v skladu z ISO 80000.

- Izvirni znanstveni članki opisujejo še neobjavljene rezultate lastnih raziskav.
- Pregledni članki povzemajo že objavljene znanstvene, raziskovalne ali strokovne dosežke na novem znanstvenem nivoju in lahko vsebujejo tudi druge (citirane) vire, ki niso večinsko rezultat dela avtorjev.
- Predhodna objava povzema izsledke raziskave, ki je v teku in zahteva hitro objavo obsega do sedem (7) strani.
- Strokovni članki vsebujejo rezultate tehnoloških dosežkov, razvojnih projektov in druge informacije iz prakse in industrije.

— Publication notes contain the author's opinion on newly published books, monographs, textbooks, etc. (up to 2 pages). A figure of the cover page is expected, as well as a short citation of basic data.
— In memoriam (up to 2 pages), a photo is expected.
— Discussion of papers (Comments) where only professional disagreements of the articles published in previous issues of RMZ – M&G can be discussed. Normally the source author(s) reply to the remarks in the same issue.
— Event notes in which descriptions of a scientific or a professional event are given (up to 2 pages).

Review Process

All manuscripts will be supervised shall undergo a review process. The reviewers evaluate the manuscripts and can ask the authors to change particular segments, and propose to the Editor-in-Chief the acceptability of the submitted articles. Authors are requested to identify three reviewers and may also exclude specific individuals from reviewing their manuscript. The Editor-in-Chief has the right to choose other reviewers. The name of the reviewer remains anonymous. The technical corrections will also be done and the authors can be asked to correct the missing items. The final decision on the publication of the manuscript is made by the Editor-in-Chief.

Form of the Manuscript

The contribution should be submitted via e-mail as well as on a USB flash drive or CD.
The original file of the Template is available on RMZ – Materials and Geoenvironment Home page address: **www.rmz-mg.com**.
The contribution should be submitted in Microsoft Word. The electronic version should be simple, without complex formatting, hyphenation, and underlining. For highlighting, only bold and italic types should be used.

Composition of the Manuscript

Title

The title of the article should be precise, informative and not longer that 100 characters. The author should also indicate the short version of the title. The title should be written in English as well as in Slovene.

— Recenzije publikacij zajemajo ocene novih knjig, monografij, učbenikov, razstav … (do dve (2) strani; zaželena slika naslovnice in kratka navedba osnovnih podatkov).
— In memoriam obsega do dve (2) strani, zaželena je slika.
— Strokovne pripombe na objavljene članke ne smejo presegati ene (1) strani in opozarjajo izključno na strokovne nedoslednosti objavljenih člankov v prejšnjih številkah RMZ – M&G. Praviloma že v isti številki avtorji prvotnega članka napišejo odgovor na pripombe.
— Poljudni članki, ki povzemajo znanstvene in strokovne dogodke zavzemajo do dve (2) strani.

Recenzentski postopek

Vsi prispevki bodo predloženi v recenzijo. Recenzent oceni primernost prispevka za objavo in lahko predlaga kot pogoj za objavo dopolnilo k prispevku. Recenzenta izbere uredništvo med strokovnjaki, ki so dejavni na sorodnih področjih, kot jih obravnava prispevek. Avtorji morajo predlagati tri recenzente. Pravico imajo predlagati ime recenzenta, za katerega ne želijo, da bi recenziral njihov prispevek. Uredništvo si pridržuje pravico, da izbere druge recenzente. Recenzent ostane anonimen. Prispevki bodo tudi tehnično ocenjeni in avtorji so dolžni popraviti pomanjkljivosti. Končno odločitev za objavo da glavni urednik.

Oblika prispevka

Prispevek lahko posredujte preko e-pošte ter na USB-mediju ali CD-ju.
Predloga za pisanje članka se nahaja na spletni strani: **www.rmz-mg.com**.
Besedilo naj bo podano v urejevalniku besedil Word. Digitalni zapis naj bo povsem enostaven, brez zapletenega oblikovanja, deljenja besed, podčrtavanja. Avtor naj označi le krepko in kurzivno poudarjanje.

Zgradba prispevka

Naslov

Naslov članka naj bo natančen in informativen in naj ne presega 100 znakov. Avtor naj navede tudi skrajšan naslov članka. Naslov članka je podan v angleškem in slovenskem jeziku.

Information on the Authors
Information on the authors should include the first and last name of the authors, the address of the institution and the e-mail address of the leading author.

Abstract
The abstract presenting the purpose of the article and the main results and conclusions should contain no more than 180 words. It should be written in Slovene and English.

Key words
A list of up to 5 key words (3 to 5) that will be useful for indexing or searching. They should be written in Slovene and English.

Introduction

Materials and methods

Results and discussion

Conclusions

Acknowledgements

References
The sources should be cited in the same order as they appear in the article. They should be numbered with numbers in square brackets. Sources should be cited according to the SIST ISO 690:1996 standards.

Monograph:
[1] Trček, B. (2001): *Solute transport monitoring in the unsaturated zone of the karst aquifer by natural tracers*. Ph. D. Thesis. Ljubljana: University of Ljubljana 2001; 125 p.

Journal article:
[2] Higashitani, K., Iseri, H., Okuhara, K., Hatade, S. (1995): Magnetic Effects on Zeta Potential and Diffusivity of Nonmagnetic Particles. *Journal of Colloid and Interface Science*, 172, pp. 383–388.

Electronic source:
CASREACT – Chemical reactions database [online]. Chemical Abstracts Service, 2000, renewed 2/15/2000 [cited 2/25/2000]. Available on: <http://www.cas.org/casreact.html>.

Podatki o avtorjih
Podatki o avtorjih naj vsebujejo imena in priimke avtorjev, naslov pripadajoče inštitucije ter elektronski naslov vodilnega avtorja.

Izvleček
Izvleček namena članka ter ključnih rezultatov z ugotovitvami naj obsega največ 180 besed. Izvleček je podan v angleškem in slovenskem jeziku.

Ključne besede
Seznam največ 5 ključnih besed (3–5) za pomoč pri indeksiranju ali iskanju. Ključne besede so podane v angleškem in slovenskem jeziku.

Uvod

Materiali in metode

Rezultati in razprava

Sklepi

Zahvala

Viri
Uporabljane literaturne vire navajajte po vrstnem redu, kot se pojavljajo v prispevku. Označite jih s številkami v oglatem oklepaju. Literatura naj se navaja v skladu s standardom SIST ISO 690:1996.

Monografija:
[1] Trček, B. (2001): *Solute transport monitoring in the unsaturated zone of the karst aquifer by natural tracers*. doktorska disertacija. Ljubljana: Univerza v Ljubljani 2001; 125 str.

Članek v reviji:
[2] Higashitani, K., Iseri, H., Okuhara, K., Hatade, S. (1995): Magnetic Effects on Zeta Potential and Diffusivity of Nonmagnetic Particles. *Journal of Colloid and Interface Science*, 172, str. 383–388.

Spletna stran:
CASREACT – Chemical reactions database [online]. Chemical Abstracts Service, 2000, obnovljeno 15. 2. 2000 [citirano 25. 2. 2000]. Dostopno na svetovnem spletu: <http://www.cas.org/casreact.html>.

Scientific articles, review papers, preliminary notes and professional papers are published in English. Only professional papers will exceptionally be published in Slovene.

Annexes

Annexes are images, spreadsheets, tables, and mathematical and chemical formulas.
Annexes should be included in the text at the appropriate place, and they should also be submitted as a separate document, i.e. separated from the text in the article.
Annexes should be originals, made in an electronic form (Microsoft Excel, Adobe Illustrator, Inkscape, AutoCad, etc.) and in .eps, .tif or .jpg format with a resolution of at least 300 dpi.
The width of the annex should be at least 152 mm. They should be named the same as in the article (Figure 1, Table 1).
The text in the annexes should be written in typeface Arial Regular (6 pt).
The title of the image (also schemes, charts and graphs) should be indicated in the description of the image.
When formatting spreadsheets and tables in text editors, tabs, and not spaces, should be used to separate columns. Each formula should have its number written in round brackets on its right side.
References of the annexes in the text should be as follows: "Figure 1…" and not "as shown below:". This is due to the fact that for technical reasons the annex cannot always be placed at the exact specific place in the article.

Manuscript Submission

Contributions should be sent to the following e-mail address: rmz-mg@ntf.uni-lj.si.

In case of submission on CD or USB flash drive, contributions can be sent by registered mail to the address of the editorial board:
RMZ – Materials and Geoenvironment, Aškerčeva 12, 1000 Ljubljana, Slovenia.

The contributions can also be handed in at the reception of the Faculty of Natural Sciences and Engineering (ground floor), Aškerčeva 12, 1000 Ljubljana, Slovenia with the heading "for RMZ – M&G".

Znanstveni, pregledni in strokovni članki ter predhodne objave se objavijo v angleškem jeziku. Izjemoma se strokovni članek objavi v slovenskem jeziku.

Priloge

K prilogam prištevamo slikovno gradivo, preglednice in tabele ter matematične in kemijske formule.
Priloge naj bodo vključene v besedilu, kjer se jim odredi okvirno mesto. Hkrati jih je potrebno priložiti tudi kot samostojno datoteko, ločeno od besedila v članku.
Priloge morajo biti izvirne, narejene v računalniški obliki (Microsoft Excel, Adobe Illustrator, Inkscape, AutoCad ...) in shranjene kot .eps, .tif ali .jpg v ločljivosti vsaj 300 dpi. Širina priloge naj bo najmanj 152 mm. Datoteke je potrebno poimenovati, tako kot so poimenovane v besedilu (Slika 1, Preglednica 1).
Za besedilo v prilogi naj bo uporabljena pisava Arial navadna različica (6 pt).
Naslov slikovnega gradiva, sem prištevamo tudi sheme, grafikone in diagrame, naj bo podan v opisu slike.
Pri urejevanju preglednic/tabel, v urejevalniku besedila, se za ločevanje stolpcev uporabijo tabulatorji in ne presledki.
Vsaka formula naj ima zaporedno številko zapisano v okroglem oklepaju na desni strani.
V besedilu se je potrebno sklicevati na prilogo na način: „Slika 1 ...", in ne „... kot je spodaj prikazano:" saj zaradi tehničnih razlogov priloge ni vedno mogoče postaviti na točno določeno mesto v članku.

Oddaja članka

Prispevke lahko pošljete po elektronski pošti na naslov rmz-mg@ntf.uni-lj.si.

V primeru oddaje prispevka na CD- ali USB-mediju le-te pošljite priporočeno na naslov uredništva:
RMZ – Materials and Geoenvironment, Aškerčeva 12, 1000 Ljubljana, Slovenija

ali jih oddajte na:
recepciji Naravoslovnotehniške fakultete (pritličje), Aškerčeva 12, 1000 Ljubljana, Slovenija s pripisom „za RMZ – M&G".

The electronic medium should clearly be marked with the name of the leading author, the beginning of the title and the date of the submission to the Editorial Office of RMZ – M&G.

Information on RMZ – M&G

— Editor-in-Chief
  Assoc. Prof. Dr. Peter Fajfar
  Telephone: +386 1 200 04 51
  E-mail address: peter.fajfar@omm.ntf.uni-lj.si

— Secretary
  Ines Langerholc, Bachelor in Business Administration
  Telephone: +386 1 470 46 08
  E-mail address: ines.langerholc@omm.ntf.uni-lj.si

These instructions are valid from July 2013.

Elektronski mediji morajo biti jasno označeni z imenom vsaj prvega avtorja, začetkom naslova in datumom izročitve uredništvu RMZ – M&G.

Informacije o RMZ – M&G

— urednik
  izr. prof. dr. Peter Fajfar
  Telefon: +386 1 200 04 51
  E-poštni naslov: peter.fajfar@omm.ntf.uni-lj.si

— tajnica
  Ines Langerholc, dipl. poslov. adm.
  Telefon: +386 1 470 46 08
  E-poštni naslov: ines.langerholc@omm.ntf.uni-lj.si

Navodila veljajo od julija 2013.

IRGO

Inženirska geologija
Hidrogeologija
Geomehanika
Projektiranje
Tehnologije za okolje
Svetovanje in nadzor

ISSN 1408-7073